Technische Universität München

Fakultät für Chemie

Design and Development of Microbial Platforms for Sustainable Oleochemicals and Biorefinery Applications

Samer Younes

Vollständiger Abdruck der von der Fakultät für Chemie der Technischen Universität München zur Erlangung des akademischen Grades eines

Doktors der Naturwissenschaften (Dr. rer. nat.)

genehmigten Dissertation.

Vorsitzender		Prof. Dr. Tom Nilges
Prüfer der Dissertation	1.	Prof. Dr. Thomas Brück
	2.	apl. Prof. Dr. Wolfgang Eisenreich
	3.	Prof. Dr. Kathrin Castiglione

Die Dissertation wurde am 06.10.2021 bei der Technischen Universität München eingereicht und durch die Fakultät für Chemie am 03.12.2021 angenommen.

Abstract

Due to increasing fossil-fuel prices and environmental concerns, biorefinery models that produce oleochemicals from renewable biomass (e.g., vegetable oils) have garnered great interest. However, deforestation and food security compromise the sustainability aspect of vegetable oils. The use of Single Cell Oils (SCOs) as platforms for oleochemicals production offer a potentially sustainable solution. Nevertheless, commercialization of SCOs-based processes remains hindered by its relatively high production cost and low overall yield. Hence, any significant improvement in raw materials cost and space-time yields is central to the accelerated industrial deployment of SCO-derived biorefineries.

In the first chapter, we opted for implementing a "zero-waste" strategy to address the cost of media and raw materials. Previous research has focused on valorization of lignocellulosic biomass (e.g., wheat straw, corncob), as a cheap carbon source for SCOs production. However, the recalcitrant lignin abundant in this biomass necessitates thermo-chemical pre-treatments. These harsh conditions produce inhibitory compounds that might hinder the fermentative growth of microorganisms. We thus investigated the use of marine biomass, seagrass and microalgae, as a lignin-free alternative. Seven beach-cast seagrass samples in addition to *Scenedesmus obtusiusculus* biomass were comprehensively analyzed. A single-step "green" enzymatic hydrolysis process was developed to efficiently release the monomeric sugars contained in these biomasses, bypassing the energy- and cost-intensive pre-treatment steps. The industrially-favorable oleaginous yeast *Cutaneotrichosporon oleaginosus* served as the platform for fermentative SCOs production. The resulting lipid yields were comparable to or exceeded those observed with expensive synthetic media. We thus provide a value-adding utilization of untapped resources, which might help in the commercialization of SCOs.

In the second chapter, we pursued microbial strain development for the enhanced production of high-value chemicals. 3-hydroxybutyrate (3HB) is the monomeric unit of polyhydroxybutyrate (PHB), a bio-derived, biocompatible, and biodegradable polymer. The recombinant microbial production of 3HB/PHB, although environmentally-friendly, still suffers from low yield and high costs. The central metabolite in the 3HB production pathway is acetyl-CoA, the derivative of coenzyme A (CoA). We thus attempted to increase CoA titers by upregulating pantothenate kinase (PanK), the rate-limiting step in CoA biosynthetic pathway. To this end, four PanK genes of different taxonomic origins (mammalian, fungal and bacterial) were individually evaluated in 3HB-producing *Escherichia coli* cells. In a bioreactor fermentation, strains expressing murine PanK1β resulted in a 41% increase in 3HB titers compared to the control strain. Overexpressing eukaryotic PanK constitutes a suitable strategy for increasing the cytosolic acetyl-CoA pool, the key building block of all oleochemicals.

Zusammenfassung

Aufgrund der steigenden Preise für fossile Brennstoffe und der drängenden Umweltfragen sind Bioraffineriemodelle, die Oleochemikalien aus erneuerbarer Biomasse (z. B. Pflanzenölen) herstellen, auf großes Interesse gestoßen. Die Abholzung der Wälder und die Ernährungssicherheit sind jedoch nicht zu vernachlässigende Argumente, die den Nachhaltigkeitsaspekt von Pflanzenölen beeinträchtigen. Die Verwendung von Single Cell Oils (SCOs) als Plattform für die Produktion von Oleochemikalien bietet daher eine potenziell nachhaltige Lösung. Dennoch wird die Kommerzialisierung von SCO-basierten Prozessen durch die hohen Produktionskosten und den geringen Gesamtertrag behindert. Daher ist jede signifikante Verbesserung der Rohstoffkosten sowie der Raum-Zeit-Ausbeute von zentraler Bedeutung für den beschleunigten industriellen Einsatz von SCO-basierten Bioraffinerien.

Im ersten Kapitel haben wir uns für die Umsetzung einer "Zero-Waste"-Strategie entschieden, um die Kosten für Medien und Rohstoffe zu senken. Frühere Forschungsarbeiten konzentrierten sich auf die Verwertung von lignozellulosehaltiger Biomasse (z. B. Weizenstroh, Maiskolben) als billige Kohlenstoffquelle für die Produktion von SCOs. Das in dieser Biomasse reichlich vorhandene , jedoch schwer zugängliche Lignin macht dabei thermochemische Vorbehandlungen erforderlich. Unter den dafür notwendigen, Diese harschen Bedingungen entstehen hemmende Verbindungen, die das Wachstum von Mikroorganismen während einer anschließenden Fermentation behindern könnten. Daher untersuchten wir die Verwendung von Meeresbiomasse, Seegras und Mikroalgen, als ligninfreie Alternative. Sieben Seegrasproben und die Biomasse von *Scenedesmus obtusiusculus* wurden umfassend analysiert. Darauf aufbauend wurde ein einstufiges, "grünes" enzymatisches Hydrolyseverfahren entwickelt, um die, in diesen Biomassen enthaltenen, monomeren Zucker effizient freizusetzen, wobei die energie- und kostenintensiven Vorbehandlungsschritte umgangen werden. Die industriell nutzbare, ölhaltige Hefe Cutaneotrichosporon oleaginosus diente hierfür als Plattform für die fermentative SCO-Produktion. Die daraus resultierenden Lipidausbeuten waren vergleichbar mit denen, die mit teuren, synthetischen Medien beobachtet wurden, oder übertrafen diese sogar. Wir bieten damit eine wertschöpfende Nutzung ungenutzter Ressourcen, die bei der Kommerzialisierung von SCOs helfen könnte.

Im zweiten Kapitel haben wir die Entwicklung mikrobieller Stämme für die verbesserte Produktion hochwertiger Chemikalien verfolgt. 3-Hydroxybutyrat (3HB) ist die monomere Einheit von Polyhydroxybutyrat (PHB), einem biobasiertem, biokompatiblen und biologisch abbaubaren Polymer.

Die rekombinante mikrobielle Produktion von 3HB/PHB ist zwar umweltfreundlich, zeichnet sich jedoch durch geringe Ausbeuten und hohe Kosten aus. Der zentrale Metabolit im 3HB-Produktionsweg ist Acetyl-CoA, das Derivat des Coenzyms A (CoA). Wir versuchten daher, die CoA-Titer durch die Hochregulierung der Pantothenatkinase (PanK), dem ratenlimitierenden Schritt im CoA-Biosyntheseweg, zu erhöhen. Zu diesem Zweck wurden vier PanK-Gene unterschiedlicher taxonomischer Herkunft (Säugetier-, Pilz- und Bakterienzellen) einzeln in 3HB-produzierenden Escherichia coli-Zellen untersucht. In einer Bioreaktor-Fermentation führten Stämme, die das murine PanK1β exprimierten, zu einem 41%igen Anstieg der 3HB-Titer im Vergleich zum Kontrollstamm. Die Überexpression von eukaryotischem PanK stellt somit eine geeignete Strategie dar, um den cytosolischen Acetyl-CoA-Pool, als wichtigsten Baustein aller Oleochemikalien, zu erhöhen.

Acknowledgements

First and foremost, I would like to acknowledge my indebtedness and render my warmest thanks to my advisor, Professor Dr. Thomas Brück, who gave me the opportunity to pursue my doctoral degree in his research group. Your friendly guidance, expert advice and continued motivation have been invaluable throughout all stages of this work. Being part of your research team provided an optimal environment to grow as a scientist. Your mentorship continues to help me advance my career.

I would like to extend my sincere thanks to Prof. Dr. Tom Nilges, Prof. Dr. Wolfgang Eisenreich and Prof. Dr. Rainer Buchholz for their evaluation of my dissertation work.

I would also like to thank the group leaders of the WSSB team Dr. Farah Qoura, Dr. Daniel Garbe, and Dr. Norbert Mehlmer for their professional feedback and friendly support throughout the entirety of my doctoral studies. A special thanks to Dr. Norbert Mehlmer, for lending me his scientific expertise and intuition, which helped in the successful resolution of my experiments. Furthermore, I would like to thank Ms. Martina Haack, Ms. Guelnaz Celik and Ms. Veronika Redai for their valuable analytical and technical support.

I would like to thank my brilliant friends and colleagues, Dania, Elias, Jan, Max, Wolfgang, Marion, Felix B., Tobias, Markus, Wojtech, Dirk, Mahmoud, Kati, Johannes, Matthias, Tom, Zora, Pariya, Felix M., Michael, Nate, Kevin, Niko, Philipp, Selina, Petra, Sophia, Meli, Manfred, Nadim. You made this journey a memorable experience.

Finally, to my family Sarkis, Mary, Ramy, and Tony, my BIGGEST supporters, I am forever indebted to you. It is your unconditional love and constant support that raise me up whenever I get weary, and encourage me to explore new paths in life. For this, I dedicate this milestone to you.

Table of Contents

1. Introduction

1.1 Background

Currently, the majority of energy and industrially-produced chemicals are derived from finite fossil fuel reserves. The world's societies and global commercial markets are dependent on this depleting resource for the production of approximately 80% of its energy and 90% of its chemicals [1]. With a burgeoning industrialization and ever-growing world population, the thirst for these commodities is increasing exponentially, augmenting the dependance on petroleum-based fuels [2]. The large-scale production and use of this non-renewable energy source have led to various environmental and economical consequences. Since the Industrial Revolution, the anthropogenic emissions of CO_2 and other greenhouse gases (GHGs) have been considered as the main driver of global warming and climate change [3]. Energy supply and energy security have been affected by the recent pandemic, ongoing geopolitical turmoil, and fluctuations in the price of crude oil and natural gas (driven by rising demand and tight supply, natural gas price in Europe smashed historic high with a 441.3% increase from last year) [4] . These fossil-fuels attributed issues have led to the development and implementation of renewable energy alternatives such as wind, solar, hydrogen, bioenergy and bio-based commodities [5]. The "2030 Agenda for Sustainable Development" adopted by the United Nations in 2015, established the 17 Sustainable Development Goals (SDGs) as a road map to attain a "more sustainable society" by 2030, focusing on ecological, economical, and social factors [6]. The shift from petroleum to renewable alternatives would allow the transition from a society with waste generating, linear production routes to one with cyclic valorization, biorefinery and bioeconomy concepts [7-9].

1.2 Biorefinery

The UN SDGs framework pushes the industry to adopt a biorefinery model, which could bring about sustainable growth along with environmental advantages. The concept of biorefinery, depicted in **Fig. 1,** evolved towards the end of the twentieth century and became one of research cornerstones in the last decade [10,11]. It adopts a petrochemical refinery scheme (feedstock — raw oil — multiple products), to a sustainable biomass-based scheme [12]. In a biorefinery, renewable biomass feedstock - rather than fossil fuels feedstock - is processed and fractionated via various methods to generate a multitude of products (both platform and end use), such as oleochemicals, biofuels, biomaterials, biomolecules and bio-actives (e.g., polyphenols, carotenoids, vitamins, omega-3 fatty acids) [13,14].

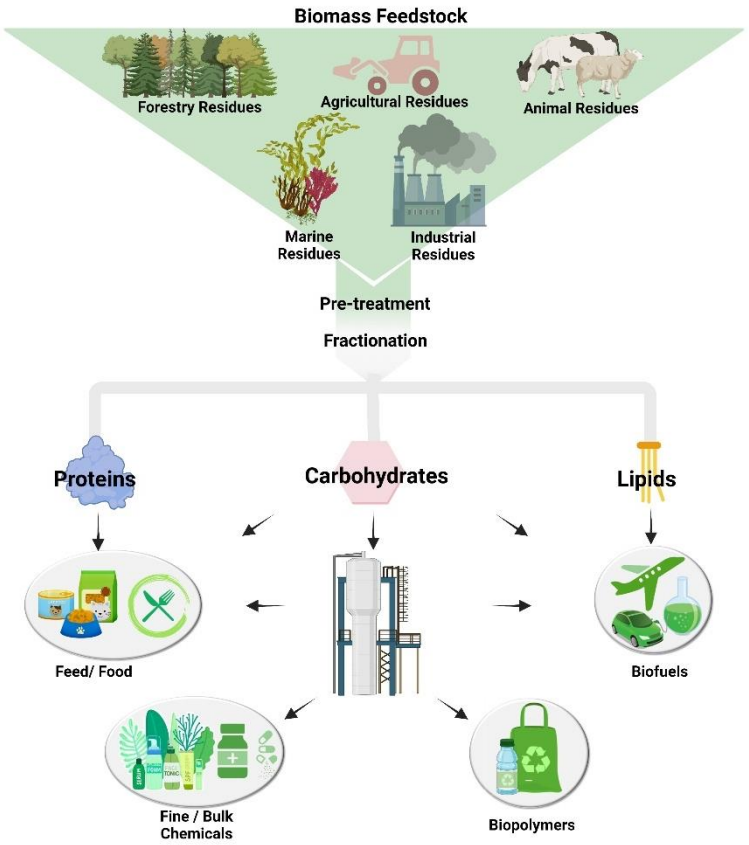

Fig. 1 The biorefinery Concept, adopted from Maity et al. [15].

The International Energy Agency (IEA) categorizes biorefineries based on feedstocks, biorefinery platform, products, and processes [16]. Process-based classification encompasses the following four groups: 1) Mechanical/Physical such as pre-treatment, grinding, pressing, fragmentation and distillation, which lead to size reduction or separation of the biomass individual components without affecting its chemical composition, 2) Biochemical processes carried out by enzymes or microorganisms, including fermentation, polymerization, anaerobic digestion, 3) Chemical processes such as hydrolysis, synthesis, hydrogenation, oxidation, and 4) Thermochemical processes, where biomass is subjected to high temperature and/or pressure, such as gasification, hydrothermal upgrading, and pyrolysis [16].

1.3 Oleochemicals

Oleochemicals are a large group of chemical compounds derived mainly from the breakdown of triacylglycerols (TAGs) found in animal or vegetable fats and oils, into glycerol and their respective free fatty acids (FFAs) [17,18]. Following further modifications at the carboxyl group, FFAs can yield fatty alcohols, fatty amines, fatty acids esters (FAEs) and fatty acid methyl esters (FAMEs), together, along

with glycerol, are termed basic oleochemicals [19,20]. The general classification of oleochemicals is carried out according to chain length, the terminal reductive state (e.g., acid, ester, aldehyde, alkane, alcohol, olefine), and any modifications to the aliphatic lead carbon chain (e.g., branching, unsaturation, hydroxyl-group) [21]. The value, applications and end-use of individual oleochemical are determined by its chemical features. For instance, soaps have historically been derived from long-chain fatty acids (C-16-C18), while medium-chain FAs (C8-C12) are precursors to lubricants and polymers, and have been utilized as herbicides [22,23]. FAMES and fatty acid ethyl-esters (FAEEs) are the major constituents of commercial Biodiesel [24]. Branching of the chain, to generate fatty acid branched-chain esters (FABCEs), improved the physical properties of the fuel, reduced its crystallization temperature, and allowed its use in cold climates [25-27]. Moreover, FAMEs and FAEEs have applications in the flavors and fragrances industries Fatty acids alcohols (FAOH) are building blocks for detergents, lubricants and surfactants, and have medicinal and personal care applications [28]. Long-chain alkanes and alkenes can serve as “green” or “drop-in” biofuels, which are substantially similar and completely interchangeable substitutes for conventional petroleum-derived hydrocarbons (gasoline, jet fuel, diesel). Drop-in biofuels are not associated with some of the drawbacks of FAMES (e.g., oxygen functional groups), which make the former more compatible with existing engines and distribution infrastructure [29-31]. Very-long-chain oleochemicals (> C20) such as fatty alcohols (e.g., 1- docosanol) and fatty waxes (e.g., Jojoba oil), have a wide range of applications from lubricants and coatings to cosmetics and pharmaceuticals [32-38].

As the oleochemicals demand increases, so does production of vegetable oils – the major feedstock for their production. Palm, soybean, rapeseed, and sunflower oils are among the popular crops, with the first two contributing to 65% of global production of plant oils [21,39]. In the last decade the demand for plant and animal-based lipids for generation of bioenergy and sustainable oleochemicals increased by approximately 65%. World production of vegetable oils increased over 20% between 2013 and 2019, and of the 200 million metric tons (MMT) produced in 2019, more than 20% were used as feedstock for oleochemicals production [18,19]. Although it enjoys sustainability and renewability, this traditional production route suffers from various environmental and economic drawbacks. Plant-derived oleochemicals are associated with deforestation, destruction of ecosystems and an overall carbon footprint [40,41]. Most crucially, competition for arable land and the use of edible crops for generation of oleochemicals jeopardize food security [41,42]. To meet the current annual global demand of biodiesel, more than double of the currently arable land would be required to grow crops that are explicitly grown for fuel production. Oleochemical production via microbes offer an attractive alternative route, free of these limitations [43].

1.4 Single cell oils (SCOs)

Lipids are building blocks of all living cells, which functions include signaling, and acting as structural components of cell membranes. They are an effective form of energy storage with a high energy value of about 39 kJ/g (9 kcal/g) [44]. Certain microbial species can accumulate intracellularly in excess of 20% ($g.g^{-1}$) lipids of their dry cell weight (DCW). These are termed oleaginous microorganisms and the stored lipids are known as single cell oils (SCOs) [7,45]. In eukaryotes (algae, yeast and fungi), SCOs are present predominately as triacylglycerols (TAGs) [46,47]. Only few prokaryotic species can accumulate lipids, which are stored mainly as polyhydroxyalkanoates (PHAs) and polyhydroxybutyrates (PHBs), rather than TAGs [48,49]. The process of lipid accumulation in oleaginous microorganisms is an adaptive response to conditions of physiological stress, such as nutrient limiting conditions [50]. If the cultivation medium is sufficiently abundant in essential nutrients, uninhibited cellular growth and division ensue. When cells run out of a key nutrient, usually nitrogen, they stop proliferating as nitrogen is essential for the biosynthesis of proteins and nucleic acids [51]. In oleaginous microorganisms, excess carbon substrate continues to be assimilated by the cells and converted into TAGs, PHAs or PHBs, where they serve as the main energy and carbon storage [52]. Under high carbon-to-nitrogen (C:N) ratio, oleaginous yeasts such as *Rhodosporidium toruloides*, *Yarrowia lipolytica* and *Cutaneotrichosporon oleaginosus* can accumulate more than 70% ($g.g^{-1}$ DCW) of lipids, while the non-oleaginous yeasts *Saccharomyces cerevisiae* and *Torulaspora delbrueckii* only accumulate 5–10% ($g.g^{-1}$ DCW) [53,54].

Driven by the various disadvantages of crude oil and the highly controversial "food-vs-fuel" debate regarding plant-derived oils, single cell oils (SCOs) have recently garnered attention as an intriguing platform for oleochemicals production [55,56]. The use of microorganisms as production platform for oleochemicals and high-value compounds offer various advantages over plant-based platforms: 1) higher renewability and sustainability levels, 2) no requirement for arable land or fresh water for irrigation, 3) no deforestation practices 4) usage of waste biomass as feedstock, 5) independence from seasonal, climatic or geographical constraints, 6) faster growth cycles, 7) higher lipid productivities per land area, 8) smaller carbon footprint, 9) ease of modification to generate tailored products, and 10) no competition with food security [43,57,58]. SCOs have generated further industrial interest due to the similarities between compositions of microbial oil and their vegetable counterparts [59]. The degree of saturation of FA determines the physiochemical properties of biofuels (e.g., biodiesel) derived from the respective oil; these include Iodine Value (IV), Cetane Number (CN), Higher Heating Value (HHV), Kinematic Viscosity (KV) and Density [58,60]. Oleic (C18:1), palmitic (C16:0), and stearic (C18:0), in addition to linoleic (C18:2) and palmitoleic (C16:1) represent the major fatty acids found in palm, rapeseed and sunflower oils - a profile suitable for production of oleochemicals such as biodiesel [61,62].

Although the composition of SCOs is species-dependent and can be influenced by various nutritional (e.g., substrate and media components) and physical (e.g., temperature, oxygen, light) parameters, various oleaginous microorganisms (mainly microalgae and yeast species) share the dominant fatty acids profiles of plant oils (**Table 1**) [63,64].

Table 1. Lipid contents and Fatty acid profiles of vegetable oils and oleaginous microorganisms, expressed in terms of mass, as a fraction of dry cell weight (% $g.g^{-1}$) [43,65-68].

Origin	Lipid content (% $g.g^{-1}$)	Fatty acid composition (% $g.g^{-1}$)					
		C16:0	C16:1	C18:0	C18:1	C18:2	C18:3
Oilseed							
Peanut	50	11	0	2	48	32	-
Rapeseed	45	4	-	2	62	22	10
Sunflower	45	7	-	5	19	68	1
Soybean	20	11	-	4	24	54	7
Tree fruits and kernels							
Coconut	50	9	-	3	6	2	-
Olive	48	13	1	3	71	10	1
Palm	50	44	-	4	38	10	1
Palm kernel	-	8	-	3	15	2	-
Yeast							
Cryptococcus curvatus	60	12	1	3	73	12	-
Cutaneotrichosporon oleaginosus	75	32	-	8	57	8	-
Lipomyces starkeyi	63	34	6	5	51	3	-
Rhodosporidium toruloides	66	18	3	3	66	-	-
Rhodotorula glutinis	72	37	1	3	47	8	-
Yarrowia lipolytica	48	11	6	1	28	51	-
Fungi							
Mortierella isabellina	50	29	-	3	55	3	3
Mucor circinelloides	25	22	-	5	38	10	15
Rhizopus arrhizus	57	18	-	6	22	10	12
Aspergillus terreus	-	23	-	-	14	40	-
Microalgae							
Chlorella sp.	32	19	11	1	9	14	16
Chlorella zofingiensis	32	23	2	2	36	18	8
Nannochloropsis sp.	-	26	24	3	28	4	-
Scenedesmus obliquus	28	16	3	4	50	8	-
Bacteria							
Rhodococcus opacus	56	-	19	74	-	-	-

1.5 Eukaryotic platforms

1.5.1 Microalgae and Fungi

For years, microalgae have been exploited as a source for value-added products, with numerous commercial applications that include enhancing the nutritional value of food and animal feed, as well as being incorporated into cosmetics and personal care products [69]. Recently, oleaginous microalgae, including *Scenedesmus*, *Chlamydomonas*, *Chlorella* and *Nannochloropsis* species, have been considered as a promising source for SCOs production [69]. Owing to their efficient photosynthesis capabilities, the reduced needs for growth area compared to terrestrial plants, and their ability to channel the majority of their energy into cell division (high density biomass generation), and a favorable fatty acids profile, oleaginous microalgae have been implemented as platforms in third generation biorefineries and oleochemical production. They can utilize both inorganic and organic carbon sources through four different cultivation methods (i.e., autotrophic, mixotrophic, heterotrophic, and photoheterotrophic) [70,71]. Although several species, such as *Aspergillus terreus*, *Claviceps purpurea*, *Tolyposporium*, *Mortierella alpina* and *Mortierella isabellina*, can accumulate high lipid contents, most fungi are explored mainly for the production of specialty lipids, such as docosahexaeneoic acid (DHA; C22:6), gamma-linolenic acid (GLA; C18:3), eicosapentaenoic acid (EPA; C20:5) and arachidonic acid (ARA; C20:4). These fatty acids are of nutritional and pharmaceutical significance [43,72]. *M. alpina* in particular been used to commercially produce ARA-rich oil for infant formula applications since the late 1980s [73].

1.5.2 Yeast

Oleaginous yeasts, including species of the genera *Candida*, *Rhodosporidium, Yarrowia*, *Cryptococcus*, *Rhodotorula*, *Lipomyces*, and *Trichosporon*, and *Cutaneotrichosporon* can accumulate lipids up to 80% $g.g^{-1}$ of their dry cell weight [74]. Recent studies showcase oleaginous yeasts as particularly suitable for SCOs production and subsequent oleochemical and biorefinery applications [75]. These strains possess certain key criteria that give them distinctive advantage over both microalgae and fungi, such as: ease of cultivation, robustness, tolerance towards fermentation inhibitors, high cell densities growth along with high lipid content, amenability to genetic modulation and the ability to uptake various carbon sources (e.g., glucose, xylose, glycerol, starch, acetate) products [76]. Oleaginous yeasts can produce SCOs heterotrophically from a variety of low-cost feedstocks such as agricultural residues, food waste streams and industrial co-products [77].

Cutaneotrichosporon oleaginosus (ATCC 20509), was first isolated by Moon et al., in 1978 from factory drain samples of the Iowa State University Dairy Farm [78]. In addition to the broad spectrum of

monomeric sugars (pentoses and hexoses), *C. oleaginosus* can readily metabolize glycerol, N-acetylglucosamine, volatile fatty acids, ethanol and 4-hydroxymethylfurfural [79,80]. This yeast displays favorable characteristics, such as tolerance to fermentation inhibitors, fast growth rates, high lipid yields (up to 85% $g.g^{-1}$), and most importantly an industrially relevant fatty acid profile, with palmitic, stearic and oleic acid as the dominant FAs [7,54]. In our recent work, the determined physiochemical properties of the SCO from *C. oleaginosus* were found to be positioned within the limits specified by internationally accepted biofuel standards (US biodiesel ASTM D6751 and EU biodiesel standard EN 14214) [58]. The yeast has been the focus of ongoing research ranging from model-based culture media optimization, tailored fatty acid profiles, waste valorization and cyclic biorefinery approach, high-throughput optimization (strain development and process monitoring), in addition to techno-economic sustainability studies [7,8,57,58,81-83].

1.5.3 Biochemistry of SCOs accumulation in oleaginous yeasts

In *de novo* synthesis, fatty acids are produced by the cells, which are then integrated into the lipid storage biosynthetic pathway. Lipid accumulation starts when the carbon source is in excess and one of the growth nutrients (usually nitrogen) is kept limited [84]. Upon nitrogen starvation, the change in carbon flux is initiated with the activation of nitrogen-scavenging enzyme AMP deaminase (AMPD). This enzyme catalyzes the deamination of adenosine monophosphate (AMP) to inosine monophosphate (IMP), freeing ammonia (NH3), which can be utilized by the cell as a nitrogen source [85]. The decrease in intracellular AMP concentrations results in inhibition of isocitrate dehydrogenase (ICDH), the enzyme responsible for the conversion of isocitrate to oxoglutarate within the TCA cycle of the mitochondria. This inhibition causes accumulation of citrate, which is then transported to the cytosol, where ATP citrate lyase (ACL) converts it into acetyl-CoA and oxaloacetate [84]. The cytosolic acetyl-CoA is irreversibly converted into malonyl-CoA by acetyl-CoA carboxylase (ACC). Malonyl-CoA binds the acyl-carrier protein (ACP) of the fatty acid synthase (FAS) complex. A repeated series of condensation, reduction and dehydration reactions leads to the elongation of the fatty acid chain, two carbons at a time, consuming two NADPH molecules per cycle. In most oleaginous yeasts, malic enzyme (ME) is the sole source of reducing power required by the FAS complex; ME converts malate to pyruvate via NADPH release [85]. The FAS complex releases fatty acids of C16:0 or C18:0 chain lengths. These can be further modified by elongases and desaturases to make longer chains or desaturated chains (e.g. C16:1 or C18:2) [86]. Fatty acids are then assembled into TAGs by esterification to a glycerol-3-phosphate backbone within the Kennedy pathway. TAGs assembly ultimately results in the formation of lipid droplets, budding from the surface of the endoplasmic reticulum ER (**Fig. 2**) [84].

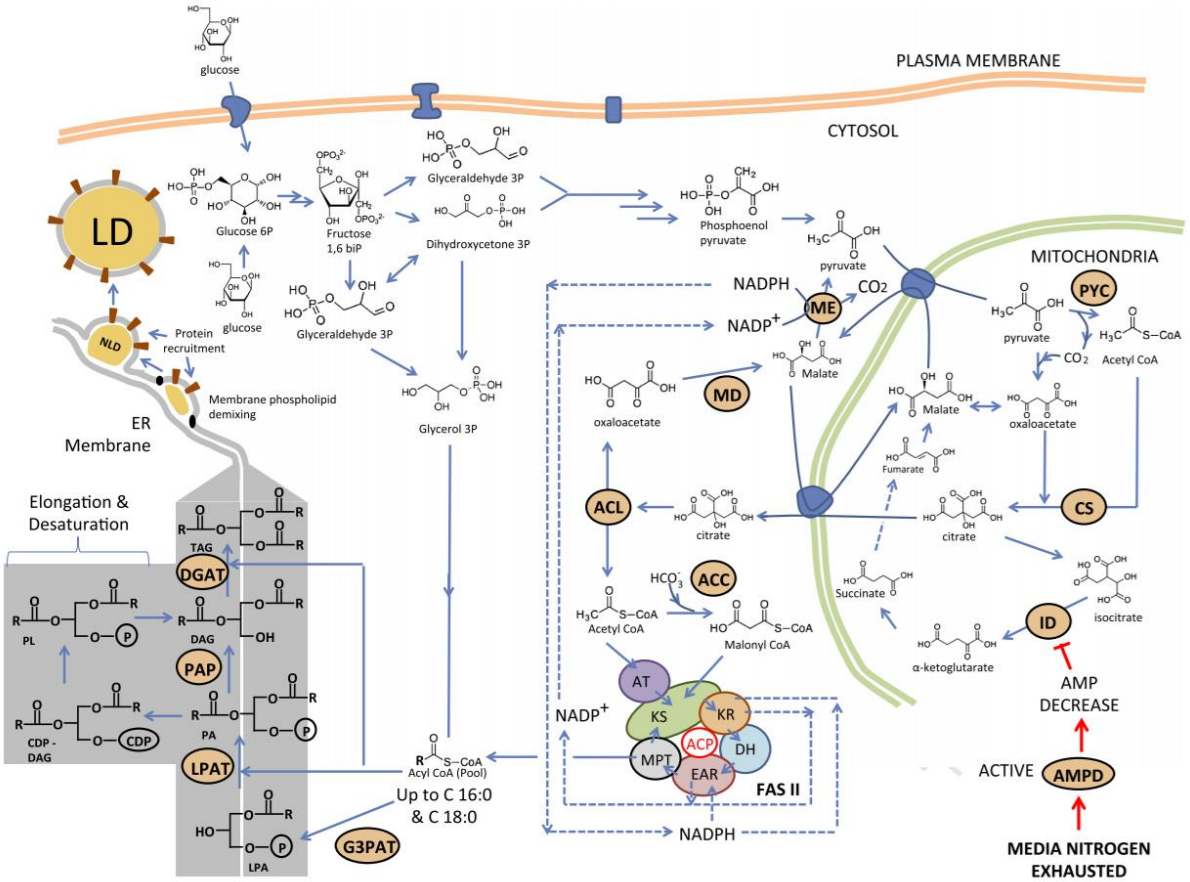

Fig. 2 Biochemistry of triacylglycerols (TAGs) accumulation in oleaginous yeast via *de novo* synthesis, obtained from Sitepu et al. [87].

1.6 Prokaryotic platforms

As stated previously, several prokaryotic species can accumulate lipids in the form of polyhydroxyalkanoates, which are solid biopolymers with equivalent physicochemical characteristics to petroleum-based polyesters [88]. PHAs are a family of bacterially synthesized biopolyesters possessing advantageous characteristics over petroleum-derived plastics: They are biodegradable, biocompatible and bioresorbable [89]. Poly-(R)-3-hydroxybutyrate (PHB) was the first and best studied PHA member, with well over 150 different PHA monomers units described to date. PHAs and PHBs have found applications in the packaging (e.g., films, boxes, coating, fibers foam materials) transportation (biofuel), as well as medical (e.g. implants) industries [90]. Non-conventional bacteria, such as *Halomonas boliviensisis*, *Ralstonia eutropha*, and *Bacillus megaterium* naturally produce PHB as response to as nutrient limiting conditions, which links PHB biosynthesis to that of SCO's [91]. In the halophile *H. boliviensisis*, three enzymes are involved in the metabolism of PHB: (1) acetoacetyl-CoA thiolase (*phbA*) which catalyzes condensation of two acetyl-CoA molecules into acetoacetyl-CoA, (2)

acetoacetyl-CoA reductase (*phbB*), which reduces acetoacetyl-CoA to 3-hydroxybutyrate-CoA, and (3) PHB synthase (*phbC*), that polymerizes the 3HB monomer units into PHB [92].

However, PHA- and PHB-derived biopolymers suffer from several drawbacks, including stiffness, brittleness, and high melting point of 175 °C (near degradation point) [93]. The hydroxy-monomers, supplied via native cell metabolism, are typically 3-hydroxyalkanoates (3HA) and 3-hydroxybutyrate (3HB). These molecules are almost entirely in R- configuration due to the stereo-specificity of enzymes involved in PHA/PHB biosynthesis [94]. The high stereoregularity makes the polyesters optically active, and result in high crystalline [93,95]. In the last decades, process development and metabolic engineering approaches have been employed to develop recombinant production strains (e.g. *Escherichia coli*) with improved overall titers, and enhanced PHB thermal and mechanical properties [96].

1.7 Challenges for microbial-based oleochemicals/biorefineries

To date, SCOs has been successfully commercialized only for specialty oils used in the food and supplement industries [97]. The economical competitiveness of SCOs as platforms for oleochemicals and bioenergy production remains hindered by its relatively high production cost and low yield [98]. Currently, plant-derived biodiesel is roughly five times cheaper than its microbial-derived counterpart, which is selling at around 4.5 €/L [87]. The key issues to overcome in biological systems are the cost of substrates and productivity ceiling, the latter predetermined by the genetic constitution of the specific strain [99]. Media and raw materials account for about 10-50% of total production costs in the specialty sector (e.g., antibiotics, vitamins, supplements), and about 50-90% of the total production cost in the commodity sector (oleochemicals) [100]. The theoretical yield of SCOs from glucose is 0.32 $g.g^{-1}$, however, the practical yield is only about $g.g^{-1}$, as substantial amounts of the carbon source are directed towards the production of biomass and other metabolites [101]. To overcome these impediments, researchers opt for utilizing “zero-cost” waste and by-product streams as carbon source, and seek development of robust and high-yielding microbial strains.

1.8 Strategies for improving commercial viability of SCOs biorefineries

1.8.1 Valorization of waste biomass

Lignocellulosic biomass, such as wheat straw, corn stover, corn cob, sugar can bagasse, rice straw, and soybean hull, represents a cheap, abundant, carbon-neutral, and renewable resource for the production of SCOs and oleochemicals. Valorization of this waste biomass has been employed as a viable alternative for expensive substrates (e.g., pure glucose), lowering the costs of the overall bioprocesses [102]. However, the heterogeneous composition of cellulose, hemicellulose and lignin in

lignocellulosic biomass has limited its broad implementation in industrial scale. These limitations include: 1) limited ability to control C/N ratio, 2) limited sugar concentrations (100 $g.L^{-1}$), and 3) the presence of sugar mixtures (diauxic growth effects) [101]. However, the most prominent technical roadblock is the pre-treatment step. To depolymerize the recalcitrant lignin and hydrolyze the hemicellulose and cellulose fractions into usable sugars, harsh pre-treatment conditions are required. Chemical, thermo-chemical and chemo-enzymatic hydrolysis have been previously employed to hydrolyze and liquefy the biomass [103]. These harsh conditions can produce inhibitory compounds such as furfural, 5-hydroxymethylfurfural, vanillin, acetic acid, and formic acid, that might hinder or completely abolish the growth of microorganisms. Furfural was found to elongate the lag-phase; while benzoic acid reduced growth rate and biomass yield [104]. Thus, complex detoxification step would be necessary prior to the fermentation, ensuing additional costs and tarnishing the eco-friendly aspect of the biofuel production process [105].

Recently, marine biomass (seagrass and microalgae) has been investigated as potential carbon sources for biorefinery applications [106]. Both resources offer several advantageous characteristics over other lignocellulosic biomass, mainly the lack of recalcitrant lignin, bypassing the need for harsh pre-treatment and detoxification steps [107]. Seagrass biomass represent an untapped carbon source for fermentative SCOs production. Regarded as nuisance, especially in resorts and touristic destinations, beach-cast seagrass deposits can be valorized without affecting the sensitive marine environment [108]. Although several microalgae have been employed for the photosynthetic conversion of atmospheric CO_2 to lipids, production yields remain shy compared to oleaginous yeast species [57]. Furthermore, following lipid extraction, the residual biomass is discarded and does not contribute to the overall process economy. In that respect, the residual biomass, often rich in fermentable sugars, can be redirected as feedstock for oleaginous yeast cultivation [109].

1.8.2 Strain development

A century of innovation and discovery have brought about wealth of genome sequences, understanding of the underling mechanisms and metabolic pathways, development of synthetic biology tools for engineering genomes (homologous recombination, TALENS, CRISPR), analytical methods for identifying enhanced strains, systems biology models for predicting cellular phenotypes, and protein design/evolution [44]. These advancements allowed to circumvent natural barriers, and transformed engineered microorganisms into interactive blueprint for tailored products. Strain enhancement of microorganisms has been employed for numerous industrial applications, including bioenergy production, bioremediation, biorefinery, and biopharmaceuticals [110,111].

Metabolic engineering strategies that redirect the carbon flux toward SCOs production allowed for improved yields and volumetric productivities. Approaches include: 1) increasing the cytosolic acetyl-CoA pool for de novo FA synthesis, 2) enhancing the activity of FA synthesis (push mechanisms), 3) up-regulating end-product formation (pull mechanisms) or 4) inhibiting competing pathways [112]. Acetyl-CoA is the key building block of all oleochemicals, and a central metabolite involved in numerous biosynthetic pathways and biochemical systems [113]. These include the oxidation of fatty acids, carbohydrates, pyruvate, lactate, ketone bodies and amino acids. The synthesis of acetyl-CoA is highly regulated and competes with production of several fermentation byproducts (e.g. acetate, ethanol, lactate) [114]. Strategies implemented to increase the acetyl-CoA pool in prokaryotic and eukaryotic microorganisms have been previously reported [115].

2. Materials and Methods

2.1 Strains and plasmids

2.1.1 Seagrass strains

Seagrass samples of diverse conditions - fresh and aged – were collected from the Baltic Sea (2 samples; Hohenkirchen and Greifswald), Mediterranean Sea (2 samples; Malta), Caribbean Sea (1 sample; Isla de Mujeres, Mexico), Great Australian Bight (1 sample; Beachport, South Australia) and North Atlantic Ocean (1 sample; Bahamas) in the summer season of 2013 and 2014. Triplicate samples were washed thoroughly to remove contaminants (accumulated salt, sand), then dried and grounded using a planetary ball mill (Fritsch, Germany) to 0.5 mm thickness.

2.1.2 Algal strain

Scenedesmus obtusiusculus (A189) residues were obtained from Pharmaceutical Biology Group, Ernst Moritz Arndt University (EMAU), Griefswald, Germany.

2.1.3 Yeast strains

Cutaneotrichosporon oleaginosus ATCC 20509, *Cryptococcus curvatus* (CBS 5324) and *Rhodosporidium toruloides* (NP11) were obtained from the culture collection of Werner Siemens Chair of Synthetic Biotechnology (WSSB), Technical University of Munich (TUM), Munich. Yeast strains were maintained on YPD (yeast extract peptone dextrose) agar plates (20 $g.L^{-1}$ agar, 20 $g.L^{-1}$ glucose, 20 $g.L^{-1}$ peptone/tryptone and 10 $g.L^{-1}$ yeast extract).

2.1.4 Bacterial strains and plasmids

E. coli strains and their corresponding plasmids utilized in the course of this work are listed in **Table 2**. Cells were stored in glycerol stocks at -80°C and plasmids were stored at -20 °C. The *E. coli* DH5α strains was used for cloning and amplification procedures. *E. coli* BL21 (DE3) strains was used for expression and 3HB production.

Table 2. Bacterial strains and plasmids

Strains	Description	References
E. coli BL21 (DE3)	Expression host, F− ompT gal dcm hsdSB (rB− mB−) λ(DE3)	NEB
E. coli HB-1	*E. coli* BL21 (DE3)- pJBGT3RX	This study
E. coli HB-2	*E. coli* BL21 (DE3)- pJBGT3RX- pet28	This study
E. coli HB-3	*E. coli* BL21 (DE3)- pJBGT3RX- pETpanKI	This study
E. coli HB-4	*E. coli* BL21 (DE3)- pJBGT3RX- pETpanKII	This study
E. coli HB-5	*E. coli* BL21 (DE3)- pJBGT3RX- pETpanK1β	This study
E. coli HB-6	*E. coli* BL21 (DE3)- pJBGT3RX- pETpanKIII	This study

A low-copy plasmid pJBGT3RX harboring β-ketothiolase (t3), an acetoacetyl-CoA reductase (rx) and a chloramphenicol resistance gene was gratefully provided by Prof. Gen Larsson from KTH Royal Institute of Technology in Sweden. This plasmid was transformed into *E. coli* BL21 cells and the resulting strain producing 3HB is henceforth termed HB-1.

To increase the intracellular CoA/acetyl-CoA pool, plasmid pET28a (Novagen/Merk Millipore), which harbors a kanamycin resistance gene, was used to express 4 variants of pantothenate kinase (PanK) in HB-1. DNA sequences of *Aspergillus nidulans* PanKII (accession: AF098669.1), *Mus musculus* panK1β (accession: NM_023792.2) and *Bacillus subtilis* PanKIII (accession: 936960) were obtained from NCBI database (https://www.ncbi.nlm.nih.gov). The mature sequences were codon optimized for *E. coli* expression and chemically synthesized by Eurofins Scientific (https://eurofinsgenomics.eu/). In addition, *E. coli* panKI was also assessed. All panK genes were amplified by PCR with complementary tails to the NcoI and HindIII restriction sites and later cloned into the multiple cloning site (MCS) of an empty pET28a plasmid. PanK cloning was confirmed by sequencing (https://eurofinsgenomics.eu/). Primers were also synthesized by Eurofins Scientific. Strain HB-2 harbors pJBGT3RX and empty pET28a plasmids. In addition to t3 and rx genes, strains HB-3 to HB-6 also express *E. coli* panKI, *A. nidulans* panKII, *M. musculus* panK1β and *B. subtilis* panKIII, respectively.

2.2 Pretreatment and hydrolysate preparation

2.2.1 Seagrass hydrolysate

Enzymatic hydrolysis of seagrass samples was conducted in a 2 L glass bottles holding 1 L acetate buffer solution (50.0 mm, pH 5.0) and 60.0 g of biomass. Enzymatic Reactions were initiated by adding enzyme solutions of Cellic CTec 2 (Novozymes, Denmark), Cellic HTec (Novozymes, Denmark), Pectinex (Novozymes, Denmark), and Novozymes 188 (Novozymes, Denmark) and incubating the mixture at 50°C and 400 rpm, using magnetic stirrer. Buffer and enzymes were sterile-filtered prior to hydrolysis. Additionally, two controls, each consisting of either the substrate or the enzyme solution were prepared in 50 mL falcon tubes containing 25.0 mL of acetate buffer solution (50.0 mm, pH 5.0) and 500.0 mg of biomass. After 72 hours, the solutions were centrifuged (30 min, 8000 g), and cross-filtered using 10 kDa membrane made from regenerated cellulose. The parameters of the cross-filtration were accordingly: inlet pressure (P1) of 2 bar, repentant pressure (P2) of 0.3–0.5 bar, the permeate was open to atmospheric pressure, the flow rates of repentant and permeate were 2 $L.min^{-1}$ and 0.1 $L.min^{-1}$, respectively, and 0.2 mm filter capsules were installed at the outlet. Biological triplicates of the seagrass hydrolysate were prepared.

2.2.2 Algal hydrolysate

Enzymatic hydrolysis of *Scenedesmus obtusiusculus* dry biomass was conducted in a 2 L glass bottles holding 1 L acetate buffer solution (50.0 mm, pH 5.0) and 50.0 g of biomass. Enzymatic Reactions were initiated by adding enzyme solutions of Cellic CTec 2 (Novozymes, Denmark), Cellic HTec2 (Novozymes, Denmark), Pectinex (Novozymes, Denmark), and Fungamyl (Novozymes, Denmark) and incubating the mixture at 50° C and 400 rpm, using a magnetic stirrer. Buffer and enzymes were sterile-filtered prior to hydrolysis. After 72 hours, the solutions were centrifuged (30 min, 8000 g), and cross-filtered using 10 kDa membrane made from regenerated cellulose. The parameters of the cross-filtration were accordingly: inlet pressure (P1) of 2 bar, repentant pressure (P2) of 0.3–0.5 bar, the permeate was open to atmospheric pressure, the flow rates of repentant and permeate were 2 $L.min^{-1}$ and 0.1 $L.min^{-1}$, respectively, and 0.2 mm filter capsules were installed at the outlet. Biological triplicates of *Scenedesmus* hydrolysate (SH) were prepared.

2.3 Strain maintenance, inoculum preparation and culture conditions

2.3.1 Lipid Production

Strain maintenance and inoculum preparation

Yeast strains were maintained on yeast peptone dextrose (YPD) agar (20 $g.L^{-1}$ glucose, 20 $g.L^{-1}$, tryptone/peptone; Carl Roth, Germany, 10 $g.L^{-1}$ yeast extract; Applichem, Germany, 20 $g.L^{-1}$ agar) at 4 °C for short-term storage.

For inoculum preparation, a single colony of *C. oleaginosus* was inoculated in a 125 mL Erlenmeyer flask holding 50 mL YPD liquid medium (20 $g.L^{-1}$ glucose, 20 $g.L^{-1}$, tryptone/peptone; Carl Roth, Germany, 10 $g.L^{-1}$ yeast extract; Applichem, Germany) for 24 h at 28° C and 120 rpm in a rotary incubator. Yeast cells were then centrifuged and washed with PBS buffer (8 $g.L^{-1}$ NaCl, 0.2 $g.L^{-1}$ KCl, 1.44 $g.L^{-1}$ Na2HPO4, 0.24 $g.L^{-1}$ KH2PO4; pH 7.4).

Shake flask experiments

To assess the fermentative potential of *C. oleaginosus* grown on seagrass hydrolysate, lipid accumulation was induced by subsequent inoculation in a 1 L Erlenmeyer flasks holding 300 mL of seagrass hydrolysate (enzymatic variants). Shake flasks were supplemented with an aeration system, supplying the cultures with 0.2 $L.min^{-1}$ pre-filtered air. A technical draw for aerated flasks is available in the Supporting Information (**Fig. 3)**. Additionally, nitrogen-limited medium (MNM; 30 $g.L^{-1}$ glucose, 1.5 $g.L^{-1}$ yeast extract, 0.5 $g.L^{-1}$ NH_4Cl, 7.0 $g.L^{-1}$ KH_2PO_4, 5.0 $g.L^{-1}$ $Na_2HPO_4 \cdot 12H_2O$, 1.5 $g.L^{-1}$ $MgSO_4 \cdot 7H_2O$,

0.08 g.L^{-1} $FeCl_3 \cdot 6H_2O$, 0.01 g.L^{-1} $ZnSO_4 \cdot 7H_2O$, 0.1 g.L^{-1} $CaCl_2 \cdot 2H_2O$, 0.1 mg.L^{-1} $MnSO_4 \cdot 5H_2O$, 0.1 mg.L^{-1} $CuSO_4 \cdot 5H_2O$, 0.1 mg.L^{-1} $Co(NO_3)_2 \cdot 6H_2O$; pH 5.5) as previously described by Suutari *et al.* was used as a positive control [116]. With a starting optical density of 0.1, measured at 600 nm, fermentation was sustained for 5 days at 28°C in a rotary incubator at 120 rpm. Biological cultures of the oleaginous yeasts were carried out in triplicates.

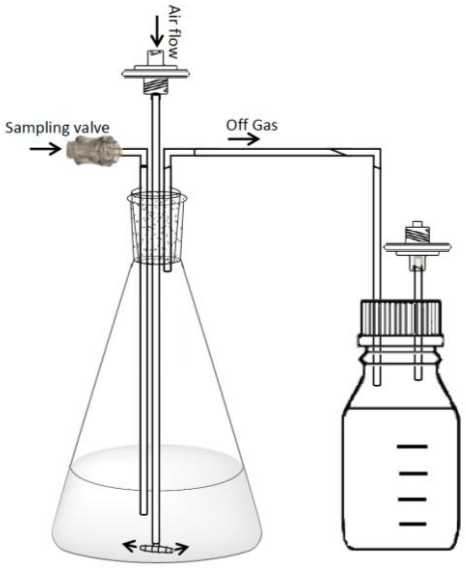

Fig. 3 The aeration system design aimed at supplying yeast cultures with 0.2 L/min pre-filtered air.

To assess the fermentative potential of *C. oleaginosus, C. curvatus and R. toruloides* when grown on SH, lipid accumulation was induced by subsequent inoculation in a 250 mL baffled flasks holding 50 mL of SH (enzymatic variants) lacking any additives or carbon supplementation. Additionally, nitrogen-limited medium (MNM) as previously described by Suutari *et al.* was used as a positive control [116]. With a starting optical density of 0.5, measured at 600 nm, fermentation was sustained for 4 days at 28°C in a rotary incubator at 120 rpm. Biological cultures of the oleaginous yeasts were carried out in triplicates.

Fed-batch Fermentation

Fed-batch cultivation of *C. oleaginosus* was performed in a 2 L bioreactor (INFORS HT system, Switzerland) with a working volume of 1 L of seagrass hydrolysate, prepared from *P. oceanica* (120 g) as described in **Section 2.2.1: Seagrass hydrolysate**. A volume of 1 L of the hydrolysate served as the main fermentation medium, having a carbon to nitrogen ratio of 52. Another 1 L of the hydrolysate was concentrated 10 times using a rotary evaporator and served as feed for the bioreactor. For inoculation, 10% of the seed culture was transferred to the bioreactor. Fermentation was maintained

for 6 days at a temperature of 28°C, a pH of 6.5 ±0.2 using 1 M aqueous NaOH, 0.01% (v/v) of antifoam agent 204 (Sigma Aldrich, Germany), stirring of 200-400 rpm and automatically-regulated aeration (1.0-2.0 normal liters per minute of air) to maintain a minimal dissolved oxygen of 50%. Substrate feed was initiated within the first 24 hours of fermentation and samples were taken every 24 h for to determine optical density, DCW, and lipid content.

2.3.2 3HB Production

Strain maintenance and inoculum preparation

Bacterial strains were maintained on YPD agar at 4 °C for short-term storage. For inoculum preparation, a single colony of *E. coli* (HB1 to HB-6) was inoculated in a 125 mL Erlenmeyer flask holding 50 mL YPD liquid medium for 24 h at 28°C and 120 rpm in a rotary incubator. Cultures were then centrifuged and washed with PBS buffer.

Shake flask experiments

To assess 3HB production by *E. coli,* HB1 to HB-6 strains were cultivated in sterile baffled 500 mL shake flasks holding 50 mL of Minimal M9 media (1 $g.L^{-1}$ NH_4Cl, 0.5 $g.L^{-1}$ NaCl, 3 $g.L^{-1}$ KH_2PO_4, 6 $g.L^{-1}$ Na_2HPO_4, 0.493 $g.L^{-1}$ $MgSO_4 \cdot 7H_2O$, 0.011 $g.L^{-1}$ $CaCl_2$, 0.42 $g.L^{-1}$ $FeCl_3$- $6 \cdot H_2O$ supplemented with 0.4% glucose; pH of 6.9). Culture media was additionally supplemented with antibiotics (Kanamycin and/or Chloramphenicol). Pantothenate (pantothenic acid), the substrate for the pantothenate kinase, was also added to an initial concentration of 5 mM. When the optical density of the cultures reached 0.6, 3HB production was induced with the addition of 150 µM isopropyl-β-D-1-thiogalactopyranoside (IPTG). Cultivation was carried out at 37°C and 120 rpm.

Fed-batch Fermentation

Fed-batch cultivation of *E. coli* HB-5 was performed in a 1.3 L DASGIP® parallel bioreactor (Eppendorf AG, Germany) with a working volume of 1 L of modified M9 media (8 $g.L^{-1}$ NH_4Cl, 13.3 $g.L^{-1}$ KH_2PO_4, 1.24 $g.L^{-1}$ $MgSO_4 \cdot 7H_2O$, 0.42 $g.L^{-1}$ $FeCl_3 \cdot 6H_2O$, 40 $g.L^{-1}$). Initial concentration of 5 mM Pantothenate was also added to the culture medium. The feed consisted of 500 $g.L^{-1}$ glucose, 20 g $L^{-}1$ $MgSO_4 \cdot 7H2O$, 2 $mg.L^{-1}$ thiamine–HCl, 16 mL and 100× trace elements solution (5 g,L^{-1} EDTA; 0.83 $g.L^{-1}$ $FeCl_3 \cdot 6H_2O$; 84 mg,L^{-1} $ZnCl_2$, 13 mg,L^{-1} CuCl2–$\cdot 2H_2O$, 10 mg,L^{-1} $CoCl_2 \cdot 2H_2O$, 10 $mg.L^{-1}$ H_3BO_3, and 1.6 $mg.L^{-1}$ $MnCl_2 \cdot 4H_2O$) (pH = 7.0). Fermenters were inoculated with an optical density of 0.1. Fermentation was maintained at a temperature of 37°C, a controlled pH of 7.0 using 6 M aqueous NaOH, 0.01% (v/v) of antifoam agent 204 (Sigma Aldrich, Germany), initial stirring of 200 rpm and automatically-regulated

aeration (2.0 volumes of air per volume of medium per min -vvm) to maintain a minimal dissolved oxygen of 30%. A pH value shift above 7.05 initiated a feed shot of 40 mL. Upon nitrogen limitation, 3HB production was induced with 150 µM IPTG. Upon ammonium depletion, as indicated by dissolved oxygen tension (DOT) increase, 7 g L^{-1} of NH_4Cl was added to allow for high cell density. Samples were taken at different intervals to determine the optical density, DCW, and 3HB titers.

2.4 Analytics

2.4.1 Biomass analysis

Seagrass and algal strains

Water content of algal biomass was determined following the milling and drying of the algal samples at 60 °C overnight. The standard Kjeldahl procedure was utilized to determine the number of proteins in the seagrass and algal biomass and monitor nitrogen depletion throughout the yeast fermentation on seagrass [117]. Briefly, Dry 2 g of biomass was digested (InKjel M, behr Labor technik GmbH-Germany) and distilled (Vapodest 10, Gerhardt- Germany). Ash content of SH was determined by following the AOAC procedure [118]. Biological replicates ensured reproducible measurements. The ash profile of the seagrass hydrolysate was determined as described in **section 2.4.4: Electron microscopy and EDX**. Total carbohydrate concentration in SH was determined by the thymol-sulfuric acid method [119]. Lipid content of the SH was measured gravimetrically as described in **section 2.4.6: Lipid analysis: Gravimetric analysis**.

Yeast strains

A volume of 2 mL of each yeast cultures grown on SH was transferred in to pre-weighed 2 mL Eppendorf tubes. The tubes were weighed again the following centrifugation (14,000 g, 5 min), washing and drying at 60 °C overnight. Measurements were recorded in triplicates and calculated by subtracting the weight of the sample tubes from their respective pre-weights. DCW of yeast cultures grown on seagrass was processed by lyophilization for 2 days at -80 °C and 0.04 mbar (Christ alpha 2–4 LD plus).

Biomass accumulation was also monitored offline by measuring the optical density at 600 nm. Samples were withdrawn and diluted to an estimated OD_{600} of 0.1-0.4 and measurements were recorded using a spectrophotometer GENESYS ™ 10S UV/ VIS spectrophotometer (Thermo Fisher Scientific, Germany) was utilized and 1 mL cuvettes.

2.4.2 Hydrolysate analysis

A sexokinase assay kit (Megazyme-Ireland), was used to measure the glucose concentration of each sample at 340 nm, repeated four times. For the standard curve, five calibration points were measured at concentrations: 0.5, 1.0, 2.0, 3.0, and 4.0 gL^{-1}. The final sugar analysis was performed by using HPLC as described in **section 2.4.5: Sugar Analysis**.

2.4.3 Sequencing for the phylogenic tree construction

The innuPREP Plant DNA Kit (Analytik Jena, Germany) was used to isolate the genomic DNA from seagrass samples. DNA extracts were run on a 1% agarose gel (100 mA, 120 V, 10 min). A gel area corresponding to 8000–10000 kilobase (kb) size was cut and DNA was purified with innuPREP DOUBELEpure Kit (Analytik Jena, Germany). Two sets of primers were used for the amplification of the 18S rRNA region (~ 950 bp). The first set EukA (5'-AACCTGGTTGATCCTGCCAGT-3') and EukB (5'-TGATCCTTCTGCAGGTTCACCTAC-3') [120]. Primers ITS1 (5'-TCCGTAGGTGAACCTGCGG-3') and NL4 (5'-GGTCCGTGTTTCA AGACGG-3') bind to entire intervening ITS1, 5.8S, ITS2 rRNA, and the D1/D2 domain (a portion of the 26S rRNA gene) [121].

2.4.4 Electron microscopy and EDX

The ash profile of seagrass biomass was determined using Scanning Electron Microscopy (SEM) with energy-dispersive X-ray (EDX) analysis. SEM was performed using a JSM 7500F scanning electron microscope (JEOL, Japan) with an accelerating voltage of 1, 2, or 5 kV and a secondary electron detector. Ash samples were mounted on a carbon film and prepared for analysis. EDX analysis was performed on multiple areas (100X100 mm^2) in backscattered electron (BSE) mode. The elemental composition of the ash was calculated from the average value.

2.4.5 Sugar analysis

Sugar composition of the seagrass and algal hydrolysates was analyzed by an Agilent 1100 series HPLC equipped with a Refractive Index (RI) detector (Shodex, RI101) and an Ultraviolet Index (Sedere-France, Sedex 75). Following cross-filtration, 5 µL of the hydrolysates was injected for a separation run lasting 30 min. The seagrass hydrolysate sugars were separated by two methods. In the first, a Rezex ROA-Organic Acid column (Aminex HPX 87H) was used with the eluent (5.0 mm H_2SO_4) at a flow rate of 0.5 $mL.min^{-1}$. The column and detector temperature was set to 70 °C and 40 °C, respectively. In the second method, also adopted for SH, sugars were separated using an Aminex HPX-87P column (8% crosslinked resin, lead ionic, Bio-Rad) with an isocratic mobile phase of double distilled water at a flow rate of 0.6 and 0.4 $mL.min^{-1}$, for seagrass hydrolysate and SH respectively. The column and detector

temperature was set to 70 °C and 50°C, respectively. The RI signal of the samples were aligned with that of internal standard curves.

2.4.6 Lipid Analysis

Gravimetric Analysis

The lipid content of the prepared SH and yeast cultures was quantified by the Bligh–Dyer method [122]. Briefly, triplicate volumes of 15 mL were washed and homogenized using a high-pressure Emulsiflex C3 homogenizer (Avestin, Canada) at a sample port pressure of 1200 bar and a chamber pressure of 8 bar. A volume of 6 mL of Folch's reagent (2:1 chloroform: methanol) was added to the homogenate and shaken at 120 rpm and room temperature overnight [123]. Subsequently, 1.2 mL of 0.9% NaCl were added to aid in phase separation. The chloroform layer was aspirated using a syringe and added to pre-weighed glass vessels. The folch extraction was repeated 3 times. The chloroform was fully evaporated under a nitrogen stream and the glass vials were weighed again. The extracted lipid measurements were used to calculate the lipid weight and the lipid content as percent of the yeast DCW.

Nile Red Analysis

Relative quantitation of the intracellular lipid content of yeast strains was carried out according to a modified protocol of Nile Red analysis established by Sitepu et al. [124]. Briefly, triplicates of yeast cultures were serially diluted to ensure an optical density below one. A volume of 225 µL was subsequently transferred to a black Nunc™ F96 MicroWell™ Polystyrene Plate (Thermo Scientific Waltham, MA, USA). These plates ensure minimal fluorescence background and stray light. The addition of 50 µL of DMSO was followed by a 5 min incubation. Initial absorbance readings were recorded at 600 nm for growth monitoring and background fluorescence measurements were recorded using an EnSpire 2 microplate reader from Perkin Elmer (Waltham, MA, USA). Nile red (9-diethylamino-5H-benzo [alpha] phenoxazine-5-one; Sigma-Aldrich, Germany) was added to a final working concentration (WC) of 5 $\mu g.mL^{-1}$ from a stock solution (60 µg/mL), prepared in DMSO. Stock and working solutions of Nile Red were stored in the dark to avoid photo-bleaching. Kinetic fluorescence measurements were recorded with an excitation wavelength of 530/25 nm; and an emission wavelength of 590/35 nm for 5 min with 30 s interval. Maximal Fluorescence Emission (MFE) values were determined and corrected for variation in cell density by dividing the fluorescence unit by background optical density values to obtain the lipid content (%).

Fatty acid profile

Yeast cultures were harvested, washed twice and lyophilized. Lipids extracts were extracted with the Folch method [123] and transestrified with methanol as described by Griffiths et al and developed by Gorner et al. [125,126]. Glyceryl trinonadecanoate (C19:0-TAG, 1.0 mg) was added to lipid extracts prior to the reaction as an internal standard. FAMEs were analyzed GC-2010 Plus Gas Chromatograph (Shimadzu, Japan) equipped with a Flame Ionization Detector (FID). A sample volume of 1 µL was applied via an AOC-20i Auto Injector (Shimadzu, Japan) onto a ZB-WAX column [30 m, 0.32 mm ID; 0.25 µm df; (Phenomenex, USA)]. The column was 30.0 m in length with an internal diameter of 0.32 mm and a film thickness of 0.25 mm. The initial column temperature was set at 150°C (maintained for 1 min). A temperature gradient was applied from 150°C to 240°C (5°C.min^{-1}), followed by 6 min maintenance at 240°C. Hydrogen was used as carrier gas at a flow rate of 3 mL.min^{-1} and constant flow compensation. Marine Oil FAME Mix (Restek, USA), which is composed of 20 fatty acids ranging in length from myristic acid (C14: 0) to nervonic acid (C24: 1), was used as a standard for retention time-based identification. Calculation of individual FAME concentrations was based on detected peak areas. Lauric acid (C12:0; Sigma-Aldrich, Germany) was used as an internal standard to determine the esterification efficiency.

2.4.7 3HB Quantitation

To quantify 3HB concentration of *E. coli* strains HB1-HB6 for shake flask experiments and fed-batch fermentation, 5ml of triplicate samples were withdrawn on regular intervals and centrifuged (2000g, 5min). The supernatant was then filtered (0.45 µm; VWR collection, Germany) and 3HB content was determined using the Megazyme D-3-Hydroxybutyric Acid Assay Kit (Cat No. K-HDBA; Megazyme, Germany).

3. Overview of Included Publications

3.1 A Seagrass-Based Biorefinery for Generation of Single-Cell Oils for Biofuel and Oleochemical Production

Mahmoud A. Masri, Samer Younes, Martina Haack, Farah Qoura, Norbert Mehlmer, and Thomas Brück

Published in: Energy Technology

Editor-in-Chief: John Uhlrich

Date of Publication: 27 September 2017

DOI: 10.1002/ente.201700604

3.1.1 Author Contributions

Conceptualization of the study and design of the methodological approach was jointly designed by all authors. Planning and execution of experiments was carried out by the author of this thesis, Samer Younes. Data validation was jointly carried out by all authors. Samer Younes and Mahmoud Masri prepared the original draft of the manuscript, which was jointly finalized and reviewed by all authors.

3.1.2 Summary I

Microbial oils, particularly derived from oleaginous yeasts, are a sustainable alternative to plant and animal-based lipids [125]. However, the economical applicability of these organisms is dependent on utilization of cost-efficient growth media, which could be realized with waste biomass hydrolysates (i.e., marine biomass residues, fishery waste, wheat straw hydrolysate) or other biotechnological waste streams [98]. Seagrass meadows are one of the most productive autotrophic ecosystems on earth. However, residual seagrass biomass in the order of 78 Mio tons per annum accumulate as waste on beaches and shores [108]. Due to the inappropriate C:N:P of seagrass biomass, only 19% of dead seagrass biomass is consumed by herbivores and heterotrophic microbes [126]. In this study, we thoroughly investigated and evaluated the biotechnological utilization of this underexploited resource (beach-cast seagrass biomass) as feedstock for microbial oil production.

Seven beach-cast samples of seagrass (*Zostera marina, Zostera noltii, Syringodium filiforme, Posidonia australis, Posidonia oceanica,* and *Thalassia testudinum*) were collected from marine ecosystems around the world. A combination of 18S rRNA phylogenetic, structural, and comprehensive biomass analyses of seagrass leaves were conducted. Single-step enzymatic hydrolysis was developed to efficiently release the monomeric sugars contained in seagrasses biomass without any thermo-chemical pre-treatment. A mixture of seagrass-specific hydrolases, including cellulolytic, hemicellulolytic, pectinolytic, laminarolytic enzymes and a β-glucosidase was formulated. The optimum activity was obtained at a commercially relevant concentration (1.5 % $g.g^{-1}$ of DCW), temperature of 50.0 °C, and pH 5.0 (50.0 mm, Sodium acetate) for 72 h. The resulting sugar rich hydrolysate, deficient in N and P (following ultrafiltration), was used as a sole fermentation medium for cultivation of the oleaginous yeast *Cutaneotrichosporon oleaginosus*. The hydrolysate of *P. oceanica* allowed for the highest lipid yields (6.8 $g.L^{-1}$), compared to the synthetic minimal medium (5.1 $g.L^{-1}$) in shake flasks studies. Subsequently, this hydrolysate was utilized as the sole fermentation medium in a 2L fed-batch bioreactor, where C. oleaginous accumulated 24.5 $g.L^{-1}$ of lipids (0.35 $g.L^{-1}h^{-1}$). The yeast fatty acid profile, analyzed by GC-FID, showed high percentage of C16:0, C18:0 and C18:1, suitable for subsequent high quality biodiesel production. Finally, cumulative data indicated

that, by exploiting only half of the global beach-cast seagrass, approximately 4 million tons of microbial oils could be generated.

To the best of our knowledge, utilization of beach-cast seagrass biomass as feedstock for single-cell oils (SCOs) production has not been previously considered. The resulting yeast biomass and lipid yields are comparable to or exceed those observed with well-optimized minimal nitrogen media. Moreover, in this study we only employed aged seagrass banquettes that are washed ashore. Thus, we provide a value-adding utilization of an untapped resource, without negatively impacting sensitive marine ecosystems. In this study, the techno-economic analysis showcased the commercial potential of this resource material for biodiesel generation. Beach cast seagrass biomass residues can serve as cheap, renewable and widely available feedstock for production of SCOs.

A Seagrass-Based Biorefinery for Generation of Single-Cell Oils for Biofuel and Oleochemical Production

Mahmoud A. Masri[+], Samer Younes[+], Martina Haack, Farah Qoura, Norbert Mehlmer,* and Thomas Brück*[a]

78 million tons of residual seagrass deposits accumulate annually on shorelines worldwide. These represent an untapped feedstock for fermentative single-cell oil production, targeted at biofuel and oleochemical generation, without affecting the sensitive marine environment or compromising food security. Seven beach-cast samples of seagrass (related to *Z. marina*, *Z. noltii*, *S. filiforme*, *P. australis*, *P. oceanic*, and *T. testudinum*) were collected from marine ecosystems around the world. A combination of 18S rRNA phylogenetic, structural, and comprehensive biomass analyses of seagrass leaves were applied. The carbohydrate content ranged from 73 to 81% ($w/^{d}w_{biomass}$). Single-step enzymatic hydrolysis was developed to efficiently release the monomeric sugars contained in seagrasses biomass without any pretreatment. *P. oceanica* hydrolysate allowed for higher lipid yields (6.8 $g L^{-1}$) compared to the synthetic minimal medium (5.1 $g L^{-1}$) in shake flasks, and was subsequently utilized as the sole fermentation medium for oleaginous yeast *T. oleaginosus* at a technical scale using a fed-batch bioreactor, which provided 24.5 $g L^{-1}$ lipids (0.35 $g L^{-1} h^{-1}$). Moreover, the sugar/lipid conversion ratio was 0.41 (w/w). Cumulative data indicates that by exploiting only half of the global beach-cast seagrass, approximately 4 million tons of microbial oils could be generated.

Introduction

The increasing use of plant-based lipids for sustainable energy and biofuels applications does compromise food security and results in reduced biodiversity.[1] Currently, more than two times the globally available arable land would be required to meet the global market demand of biodiesel.[2] Consequently, searching for alternative starting materials that offer renewability and sustainability is of vital importance.

Single-cell oil (SCO) production as a platform for biofuel production has been investigated with microorganisms encompassing *Aspergillus awamori*,[3] *Scenedesmus sp.*,[4] *Yarrowia lipolytica*,[5] *Cryptococcus sp.*,[6] and *Trichosporon oleaginosus*.[7] *T. oleaginosus* (ATCC 20509), a recently isolated oleaginous yeast,[8] is able to convert different monomeric carbon sources (C5 and C6 sugars), as well as complex waste feedstock materials, into triacylglycerol lipids stored in subcellular compartments,[9] with cellular lipid yields of up to 70% of the cell dry weight.[8] Palmitic acid, stearic acid, and oleic acid are the major fatty acids of the accumulated triglycerides. Moreover, the biodiesel B20 derivative from *T. oleaginosus* lipid has been shown to meet the ASTM certification.[7a] Therefore, the SCO fatty acid composition offers a potent alternative to vegetable oils, by alleviating competition with food resources. Nevertheless, feeding these oleaginous microorganisms with a suitable carbon source, which allows for cost-effective biodiesel production, remains a considerable challenge.

Marine biomass as a carbon source, accounts for up to 71% (w/w) of all biologically stored carbon globally.[10] At present, macroalgae and seagrass are the most abundant marine macrophytes available.[11] With relatively high photon conversion efficiency,[12] seagrass meadows are among the highest productivity ecosystems on earth. This productivity is estimated to be approximately 27.4 million tons per year of organic carbon (C_{org}).[13] Seasonally, detached seagrass-leaf material accumulates as banquettes on beaches and shorelines. This phenomenon is enhanced by the relatively low natural biodegradation rate ($\approx$19%) of this leafy biomass by herbivores and heterotrophs.[14] For instance, in the south coast of Australia (Beachport, South Australia), seagrass accumulated at a height of 1.5 m extending along the shoreline with a length in excess of 50 km (Figure S1, Supporting Information). Seagrass biomass contains an unfavorable C/N/P ratio of 474:24:1 which hampers its biological degeneration.[15] Factoring in that approximately 50% of the available seagrass biomass is degraded, buried on the ocean seabed, or

[a] M. A. Masri,[+] S. Younes,[+] M. Haack, Dr. F. Qoura, Dr. N. Mehlmer, Prof. Dr. T. Brück
Department of Chemistry—Professorship of Industrial Biocatalysis
Technical University of Munich (Germany)
E-mail: brueck@tum.de

[+] These authors contributed equally to this work.

Supporting information and the ORCID identification number(s) for the author(s) of this article can be found under: https://doi.org/10.1002/open.201700604.

consumed by herbivores, simple calculations indicate that 40 million tons of dry seagrass biomass remain available for biotechnological applications. To that end, efficient enzymatic hydrolysis of seagrass leaf microfibril could provide a sustainable stream of monomeric hexose and pentose sugars that could be used as a fermentation medium. In general, the resulting sugar-rich hydrolysate as well low nitrogen and phosphor content may actually be beneficial for cultivation of selected oleaginous yeasts, as these organisms initiate lipogenesis only when the nitrogen or phosphate concentration is low. However, according to published data, enzymatic hydrolysis and fermentation steps were successful only when pretreatment stages were used in advance. These pretreatment processes present additional costs and usually release inhibitory compounds that hinder the fermentation.[16]

Few studies have evaluated the utilization of fresh seagrasses biomass as a feedstock platform for the production of bioethanol.[17] In the available reports, the utilization of beach-cast seagrass residue has not been considered. To the best of our knowledge, the production of SCO by microbial fermentation on hydrolysates derived from beach-cast seagrass biomass has not been investigated.

The aim of this work was to investigate the feasibility of utilizing seagrass hydrolysate for the fermentation of oleaginous yeast with the focus on biodiesel production, in addition to other industrial applications.[9] Seven seagrass samples from six different seagrass eco-regions were collected, and a phylogenetic classification of each sample was established using ITS1 and 18s rRNA sequencing. To further elucidate the structure of the samples, electron microscopy analysis of the leaves was performed. Biomass analysis of each seagrass sample was also conducted in a detailed manner. Subsequently, an optimized enzyme system was devised that allowed efficient hydrolysis and liquefaction of the seagrass biomass without the need for chemical pretreatment. Without further nutrient addition, the resulting seagrass hydrolysate was utilized as the sole cultivation medium for the oleaginous yeast *Trichosporon oleaginosus*. Hydrolysates derived from aged-seagrass samples proved to be an excellent cultivation media, comparable to conventional defined synthetic media. Lipid production was scaled to fed-batch fermentation using the best performing seagrass hydrolysate to evaluate the potential for biodiesel generation. Finally, the fatty acid profile of the produced lipid was characterized to test its suitability for biodiesel production. This study demonstrated for the first time that residual seagrass biomass, accumulating in massive deposits on beaches and shorelines, can be applied as a new feedstock for the production of biogenetic fats and oils. With downstream processing, the resulting plant oil-like lipids could be upgraded by using well-known processes into high-value biokerosene, biodiesel, and biolubricants.[6,7,9]

Results and Discussion

Previous reports demonstrated that oleaginous yeasts such as *Yarrowia lipolytica* and *Lipomyces starkeyi* can produce lipids from sources such as pure glucose, xylose, and sucrose in batch fermenters.[18] Further studies investigated the use of renewable feedstocks such as glycerol and molasses as carbon sources for lipid accumulation in oleaginous yeasts.[18a] *Trichosporon oleaginosus* (ATCC 20509) has the capacity to metabolize a variety of carbon sources including hexoses and pentoses.[8] Under nitrogen- or phosphate-limiting conditions, this yeast can accumulate up to 70% of its dry weight as lipids, composed mainly of C_{16} and C_{18} fatty acids.[19]

Regarded as nuisance, especially in resorts and touristic destinations, beach-cast seagrass deposits are exclusively disposed of without valorization.[20] In this study, we have examined the value-added use of aged seagrass waste as a readily available, low-cost, raw feedstock for production of microbial lipids in *T. oleaginosus*. Nevertheless, neither a comprehensive biomass analysis nor an optimized enzymatic treatment system have yet been established.

Identification of seagrass samples

The different seagrass strains and their corresponding locations are shown in Table 1. These identified seagrasses are related to the four genera (out of eleven total known Genera) *Zostera*, *Syringodium*, *Posidonia*, and *Thalassia* sp., which cluster in the four seagrass families *Zosteraceae*, *Cymodoceaceae*, *Posidoniaceae*, and *Hydrocharitaceae*, respectively.

Table 1. Selected seagrass samples, locations, and identification based on ITS1 and 18S rRNA sequencing.

Strain	Location[a]
Z. marina (1)	Baltic Sea (Hohenkirchen)
S. filiforme	Caribbean Sea (Mexico)
P. australis	South Australia
T. testudinum	North Sea (Bahamas)
Z. marina (2)	Baltic Sea (Greifswald)
Z. noltii	Mediterranean Sea (Malta1)
P. oceanic	Mediterranean Sea (Malta2)

[a] GPS Data is given in the Supporting Information (Table S1).

In this study, the standard 18S sequence information was employed, for the first time for phylogenetic analysis of seagrass. The data was subsequently assembled to generate a maximum-likelihood phylogenetic tree (Figure S2). This tree identified two major groups: *Posidonia australis* is resolved in the smaller one, basal to the group containing *Zostera* spp., *Syringodium filiforme*, *Thalassia testudinum*, and *Posidonia oceanica*, all species with complex phyllotaxy. All sequences are available in the Supplementary Information.

The *Zostera* clade was resolved based solely on strain level (*Z. noltii* and *Z. marina*) and not into different geographically distinct groups. *Posidonia oceanica* and *Syringodium filiforme* are resolved in a third clade within two lineages of species and the forth clade harbored *Thalassia testudinum*.

Unexpectedly, *Posidonia oceanica* and *Posidonia australis* showed a considerable genetic divergence in the 18S rDNA-based phylogenetic tree. In contrast, previous reports apply-

ing an rbcL cladogram showed that these two *Posidonia* strains are closely related.[21] However, the present study is the first using conventional 18S rDNA sequences to assemble a phylogenetic relatedness of global seagrass populations. Consequently, more work should be conducted towards the choice of genetic markers that can be reproducibly used to construct the seagrass phylogeny, as it is predicted that 91% of the entire seagrass diversity is still unknown.[22] Possible candidates that could complement the current phylogenetic marker are phyB and the plastidial matK.[22]

Comprehensive biomass analysis

The overall biochemical composition of the seven seagrass samples is summarized in Table 2. As expected, all samples display a high carbohydrate content of 73–81% ($w/^{d}w_{biomass}$) of total dry weight. Interestingly, the protein content differs widely among the various seagrasses. *P. oceanica* and *T. testudinum* 5% ($w/^{d}w_{biomass}$) contained less protein than *Z. marina* (14% $w/^{d}w_{biomass}$, Baltic Sea, Hohenkirchen, Germany). Interestingly, the lipid content of 2–3% ($w/^{d}w_{biomass}$) was relatively low for all seagrass samples, except for *Z. noltii*, which showed a lipid content of 7% ($w/^{d}w_{biomass}$). The fatty acid analysis data for each lipid sample is reported in the Supporting Information (Table S2). Ash constituted 12–13% ($w/^{d}w_{biomass}$) of the dry weight for most seagrass samples. *Z. noltii* and *Z. marina* (Baltic Sea- Hohenkirchen, Germany) were the exception with lower-than-average ash contents of 7 and 10% ($w/^{d}w_{biomass}$), respectively. The subtle differences in the biochemical compositions of all seven examined seagrass strains may be attributed to different climate conditions, the composition of the ocean water, the time of the year, or the composition of marine sediments.

Table 2. Biochemical analysis of seagrass samples.

Seagrass	Content in seagrass [% ($w/^{d}w_{biomass}$)]			
	lipid	protein	sugar	ash
Z. marina (1)	2.6±0.13	13.4±0.13	73.4±1.17	10.6±0.94
S. filiforme	1.8±0.09	07.6±0.08	77.3±0.87	13.3±1.03
P. australis	2.1±0.19	07.5±0.06	78.7±1.17	11.7±0.04
T. testudinum	2.4±0.34	05.3±0.11	79.1±0.74	13.2±0.66
Z. marina (2)	3.0±0.25	10.4±0.11	73.3±0.57	13.3±0.03
Z. noltii	7.2±0.46	11.9±0.14	73.9±0.91	07.0±0.41
P. oceanica	2.3±0.41	05.1±0.06	80.8±0.57	11.8±0.68

Moreover, as most samples were collected as beach-cast residues, sun bleaching and exposure to the weather is an essential factor that will influence the biomass composition of all seagrass samples. The state of the biomass is also reflected by its color as in the case of the *Z. marina* sample, collected from the Baltic Sea- Hohenkirchen, which was fresh, relatively pure, and had a dark green color. Conversely, the second *Z. marina* sample collected from Baltic Sea, Greifswald was aged and characterized by a light-yellowish color.

Finally, biomass analysis showed water contents of the various seagrass samples ranging between 8 and 10% ($w/w_{biomass}$) (data not shown).

Carbohydrate compositional content

The biomass analysis indicates that conventional chemical biomass hydrolysis with single acid treatment will result in an underestimation of the actual sugar content.[23] Consequently, we have developed and optimized a combined approach involving both a chemical and an enzymatic biomass treatment, which improved the determination of the total and differential carbohydrate contents (optimization data is not shown). The results are presented in Table 3 as a percentage of the total dry biomass weight.

As expected, glucose is the dominant monomeric carbohydrate, most likely derived from cellulosic leaf fibers. Hence, glucose contributes approximately 67% ($w/^{d}w_{biomass}$) of the total biomass in *Z. noltii*, whereas it only accounts for about 40% ($w/^{d}w_{biomass}$) of *P. australis*. All seven strains contain various neutral pentose (rhamnose and xylose) and hexose (glucose and galactose) sugars as well as some sugar acids (glucuronic and galacturonic acid). Glucose is the dominant sugar in all samples, whereas all other sugar types have been detected at concentrations <10% ($w/^{d}w_{biomass}$). This data makes seagrass biomass a potentially suitable source for the fermentation of various microorganisms, as glucose is the preferred carbon source for a diverse array of pro- and eukaryotic microorganisms.

Chemical composition of biomass ash

Minerals contained in the ash are important for yeast fermentation as some trace elements play an essential role in

Table 3. Carbohydrate composition of collected seagrass samples.

Seagrass	Carbohydrate in seagrass [% ($w/^{d}w_{biomass}$)]				
	galacturonic acid	glucose	xylose, mannose, fructose	rhamnose	fucose
Z. marina(1)	6.46±0.26	58.13±0.11	4.27±0.16	3.82±0.39	0.99±0.06
S. filiforme	5.73±0.10	56.08±0.19	3.67±0.19	3.05±0.17	1.19±0.03
P. australis	5.18±0.15	51.53±0.15	7.31±0.51	7.79±0.07	1.31±0.05
T. testudinum	8.81±0.08	56.09±0.22	2.77±0.05	3.91±0.27	1.01±0.03
Z. marina(2)	6.54±0.12	54.06±0.01	3.87±0.16	5.54±0.13	1.12±0.01
Z. noltii	4.11±0.24	66.36±0.02	2.48±0.35	3.31±0.07	0.56±0.02
P. oceanica	6.61±0.10	55.99±0.17	3.67±0.09	7.17±0.12	1.23±0.02

lipid production.[24] At present, this is the first report on the ash composition from banquettes of various seagrass species.[25] Elemental analysis of ash from each seagrass sample was performed using SEM and energy-dispersive X-ray spectroscopy (EDX). The main inorganic elements constituting the ash structure are Ca and Mg, followed by smaller amounts of Al and S. The concentrations of these elements vary extensively between the seagrass species; this is largely dependent on the availability of nutrients in the specific marine ecosystem. Minute concentrations of Sr, W, Cr, and Mo were detected among the various samples. Interestingly, phosphate was completely absent from both *P. oceanica* and *T. testudinum*. The detailed elemental analysis is presented in Supporting Information (Table 4).

Structural analysis

For industrial applications, high biomass density offers an economical advantage concerning the cost of handling and transportation of the materials. To gain detailed insight into the seagrass structural characteristics, fiber location, and quantity, SEM was applied to examine cross sections of each type of seagrass leaf. As depicted, *Z. marina* leafs (Figure 1) are organized in closed cell structures located only at the outer surfaces of the leaf. They appear to reinforce a central hollow matrix, which leads to a low density of leaves. Conversely, a dense non-hollow structure is observed in *P. oceanica*, with fiber bundles interspersed within the leaf matrix (Figure 1). This observation might explain the fact that, throughout the handling of the seagrass samples, *P. oceanica* had the highest density, which presents it as the most advantageous material for processing and transportation.

Treatment of seagrass biomass

The production of biomass hydrolysates for microbial biofuel production can be conducted using complete chemical hydrolysis (H_2SO_4 or solid acid catalysts).[26] Moreover, mild chemical processing can be also implemented as pretreatment for subsequent enzymatic hydrolyses. However both methods often generate inhibitory substances, thereby necessitating a complex detoxification step preceding fermentation.[27] To circumvent these difficulties, a purely enzymatic-based approach was applied in the current study, which efficiently releases the carbohydrate monomers without any pretreatment. Sterilization of the various seagrass samples was performed in a laboratory-scale autoclave at 120 °C for 15 min. This step was performed to eliminate microbial contaminants that could be present within the seagrass residues. Sterilization opens up the cell wall to allow access for the hydrolytic enzymes; however, this step is not really considered as pretreatment (such as chemical pretreatment and hydrolysis of carbohydrates), as saccharification of hemicellulose and cellulose starts at temperatures above 150 °C.[16] Nitsos et al., (2012) implemented optimization procedures of hydrothermal pretreatment of lignocellulosic biomass with temperatures varying within 130–220 °C over 15–180 min,[28] which still generated—although to a lower extent—unwanted inhibitory chemicals. The main structural constituents of seagrass are cellulose and hemicellulose with no lignin present, alleviating the harsh pretreatment that lignocellulosic biomass would have required.

A mixture of seagrass-specific hydrolases, including cellulolytic, hemicellulolytic, pectinolytic, laminarolytic enzymes and a β-glucosidase, was formulated to provide an optimum hydrolase system. The corresponding activities were obtained from four commercial enzyme products: Cellic CTec 2 (C), Cellic HTec (H), Pectinex (P), and Novozymes 188 (B), which are all products of Novozymes. The optimization of the required enzymes system extended over 35 different enzyme mixtures at varied concentrations. Briefly, the optimization process was performed using *Z. marina* as a model substrate. Biomass-to-glucose conversion ratios from various mixtures of Cellic CTec 2 with Cellic HTec at a fixed total concentration of 1.0 % ($w/^{d}w_{biomass}$) are presented in Figure S3 (Supporting Information). The ratio ranges 2:3 and 1:4 (C/H w/w) showed the highest conversion ratios at 36.1 to 37.8 % ($w/^{d}w_{biomass}$), respectively. The ratio 1:4 (C/H w/w) was used at different concentrations starting from 0.2 to 2.0 % ($w/^{d}w_{biomass}$) (2–20 mg g^{-1} biomass). Addition of the β-glucosidase activity to the previous mix increased the glucose recovery from 37.8 to 47.5 % (Figure S4).

The optimum activity was obtained at a commercially relevant concentration (1.5 % $w/^{d}w_{biomass}$, 15 mg g^{-1} biomass), temperature of 50.0 °C, and pH 5.0 (50.0 mM, Sodium acetate) for 72 h. All seven seagrass samples were subjected to the

Table 4. Mineral composition of seagrass ash samples.

Seagrass	Elemental content [% ($w/^{d}w_{ash}$)]																
	O	Na	Mg	Al	Si	P	S	Cl	K	Ca	Mn	Fe	Cu	Sr	W	Cr	Mo
Z. marina (1)	67.4[a]	1.4	10.3	1.4	7.3	0.7	1.8	0.0	0.6	8.5	0.2	0.2	0.1	n.d.	n.d[b].	n.d.	n.d.
S. filiforme	65.8	n.d.	8.9	0.7	n.d.	0.9	6.1	n.d.	n.d.	17.2	n.d.	n.d.	n.d.	0.5	n.d.	n.d.	n.d.
P. australis	63.0	n.d.	9.8	1.1	0.1	0.3	1.5	n.d.	n.d.	23.7	n.d.	0.2	n.d.	n.d.	0.1	n.d.	n.d.
T. testudinum	73.1	n.d.	6.0	0.6	n.d.	n.d.	5.3	n.d.	n.d.	15.0	n.d.	n.d.	n.d.	n.d.	n.d.	n.d.	n.d.
Z. marina (2)	66.4	2.6	8.4	1.3	6.3	0.8	1.8	n.d.	2.1	9.1	0.5	0.3	0.3	n.d.	n.d.	0.0	n.d.
Z. noltii	65.0	2.3	10.6	1.3	2.6	3.2	1.3	0.5	0.5	11.9	0.1	0.2	0.1	n.d.	n.d.	n.d.	0.5
P. oceanica	69.3	n.d.	12.7	1.0	n.d.	n.d.	2.6	n.d.	n.d.	14.1	n.d.	n.d.	n.d.	0.3	n.d.	n.d.	n.d.

[a] Relative STDV for all given numbers is $\leq \pm 2$ %. [b] n.d.: Not detectable

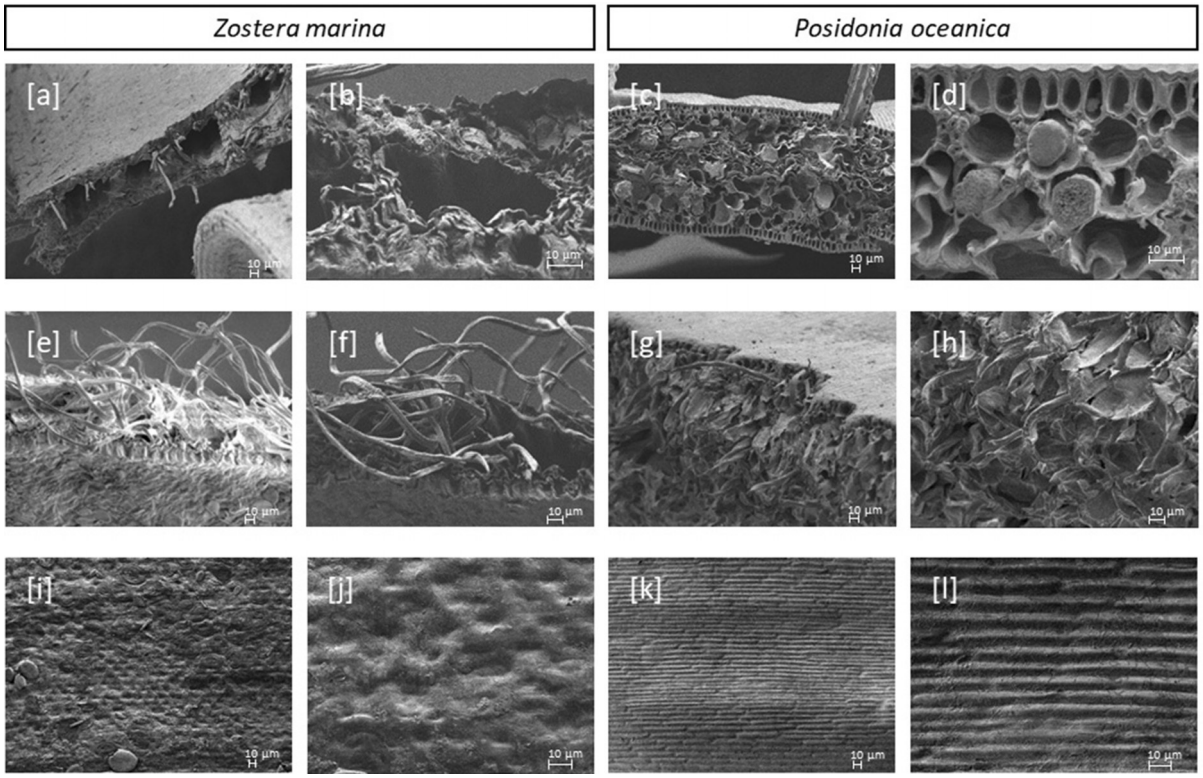

Figure 1. Electron microscopy image. Applied energy: 1.00 kV, LEI, detector: SEM/LM. *Zostera marina*: (A, B) show the leaf transverse section at 300 and 1500 times magnification, respectively, (C, D) show the leaf fibers at 430 and 600 times magnification, respectively and (E, F) show the surface of leaf at 300 and 1000 times magnification, respectively. *Posidonia oceanica*: (G, J) show the leaf transverse section at 300 and 1500 times magnification, respectively, (H, K) show the leaf fibers at 430 and 600 times magnification, respectively; and (I, L) show the surface of leaf at 300 and 1000 times magnification, respectively. Scale bars correspond to 10 µm.

same enzymatic treatment for three days. Glucose release as the controlling process indicator was monitored by HPLC (Figure 2). Hydrolysate from *Z. noltii* contained the highest amount of glucose with 32 $g L^{-1}$ followed by *P. oceanica* with almost 28.5 $g L^{-1}$. As expected, glucose was the major sugar in the hydrolysate. However, other monosaccharides have been generated as well. The sugar composition of the final hydrolysates is presented in Supporting Information (Table S3).

The remainder of the organic-bound nitrogen in the final hydrolysate (following 10 kDa cross filtration) was determined by using the Kjeldahl method. For all samples, the nitrogen content was measured in $g L^{-1}$ and a Kjeldahl nitrogen-to-protein conversion factor of 6.25 was used (Table 5). Consistent with the biomass analysis results prior to the cross filtration, *T. testudinum* and *P. oceanica* hydrolysates exhibited the lowest nitrogen contents with 0.6 and 0.5 $g L^{-1}$, respectively, whereas *Z. marina* (North Sea) hydrolysate contained the highest amount (3.5 $g L^{-1}$). It is also worth mentioning that the Kjeldahl method applied here measured the nitrogen bound in organic substances only (total Kjeldahl nitrogen was not determined). However, it is acceptable to consider that nitrogen as ammonia (NH_3) and ammonium (NH_4^+) are negligible and the total nitrogen in the hydrolysates was not appreciably underestimated. Factoring in glucose as the main carbon source, *T. testudinum* and *P. oceanica* hydrolysates hold the highest C/N ratios with approximate values of 48 and 52, respectively.

Utilization of hydrolysates as sole media for bio-oil production

The potential use of seagrass hydrolysate as sole carbon source for lipid production was evaluated. This assessment was conducted without any nutritional addition to the hydrolysate. The well-documented oleaginous yeast *Trichosporon oleaginosus* was cultivated in each of the seven hydrolysates. The resulting data are compared to the cultivation data obtained in nitrogen-limiting medium A, optimized to promote high lipid accumulation.[29] To evaluate the *T. oleaginosus* growth rate, the optical density (OD_{600}) was recorded every 24 h with an initial optical density of 0.5 (Figure 3). Cultures grown in *P. oceanica* hydrolysate as the sole cultivation medium, reached $OD_{600} = 45$ at day 5, which was faster than any other cultivation medium.[29] Most interestingly, no growth was observed in hydrolysates from *Z. noltii* and *Z. marina* (North Sea).

By contrast, *T. oleaginosus* grew very well in *Z. marina* hydrolysate from the Baltic Sea. This is due to the former hydrolysates originating from fresh seagrass samples, whereas the latter hydrolysates were all derived from aged seagrass samples that were previously exposed to sunlight.

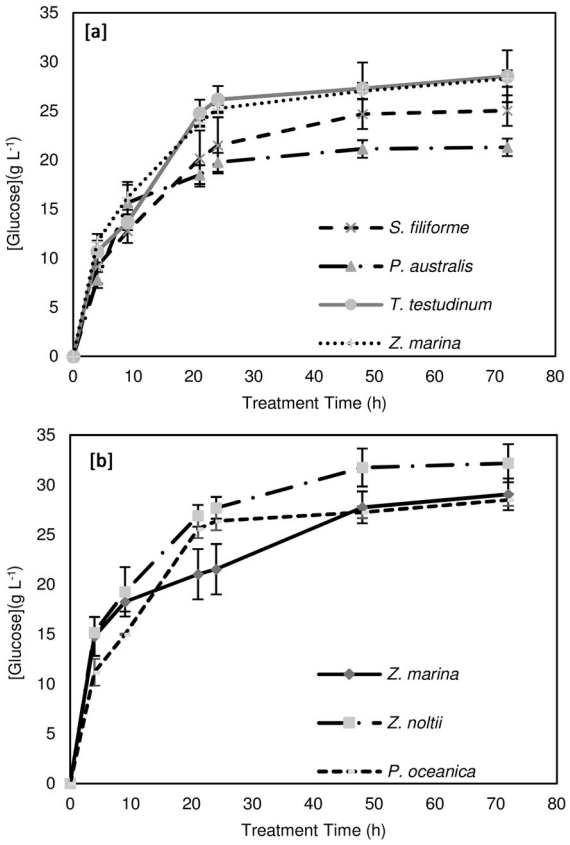

Figure 2. Time dependent release of glucose during enzymatic treatment of the seagrass samples. [a] *S. filiforme*, *P. australis*, *T. testudinum*, and *Z. marina* (2); [b] *Z. marina* (1), *Z. noltii* and *P. oceanica*.

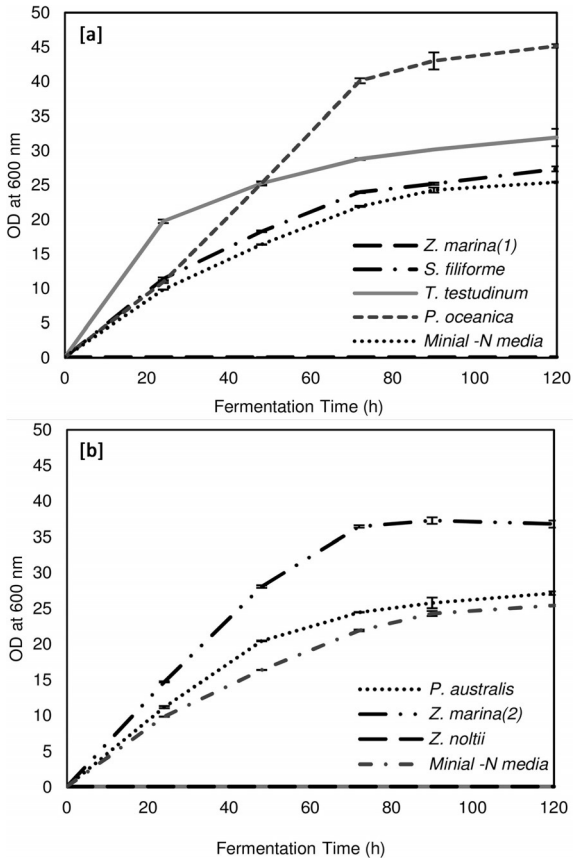

Figure 3. T. oleaginous growth by the time during shake flask fermentation using the seagrass hydrolysates as a sole medium. [a]: hydrolysate of *Z. marina* (1), *S. filiforme*, *T. testudinum* and *P. oceanica*; [b] hydrolysate of *Z. marina* (2), *Z. noltii* and *P. australis*.

Table 5. Kjeldahl nitrogen content in the hydrolysate after 10 kDa cross filtration.[a]

Hydrolysate	Protein content [% ($w/^{d}w$)]	Nitrogen content [% ($w/^{d}w$)]	[g L^{-1}]
Z. marina (1)	2.10	0.34	3.54
S. filiforme	0.43	0.07	0.72
P. australis	0.47	0.07	0.76
T. testudinum	0.38	0.06	0.59
Z. marina (2)	0.55	0.09	0.90
Z. noltii	1.60	0.26	2.56
P. oceanica	0.36	0.06	0.55

[a] All relative standard deviation are less than 5%.

Certain inhibitory compounds, including phenolic acids,[30] bacteriostatic agent,[31] and rosmarinic acid,[32] could be still present in fresh samples from *Z. noltii* and *Z. marina* (North Sea). Interestingly, yeast grown in *T. testudinum*, *Z. marina* (Baltic Sea), and *P. oceanica* reached OD_{600} values of 29, 39, and 40, respectively, in just 3 days, whereas *T. oleaginous* cultivated in medium A (Minimal-N medium) was only able to reach $OD_{600} = 15$ in the same time period. The presence of various nutrients and trace elements in the respective seagrass hydrolysates could account for this high growth rate.

Gravimetric analysis was performed to determine the total lipid content in *T. oleaginosus* after 5 days of fermentation (Figure 4). The yeast produced nearly 55% ($w/^{d}w_{biomass}$) lipids while growing in minimal-N medium. Amongst the seagrasses, *P. australis* and *S. filiforme* hydrolysates enabled the highest lipid accumulation of approximately 50% ($w/^{d}w_{biomass}$). *T. oleaginosus* cultivated in *P. oceanica* hydrolysate accumulated approximately 45% ($w/^{d}w_{biomass}$) lipid content.

These aforementioned results show the total lipid content (C) as percent of cell dry weight. Measuring lipid production (P)—expressed as grams per liter of culture—produced differing results (Figure 5). After 5 days fermentation, the lipid productivity of *T. oleaginosus* reached its peak of 6.8 g L^{-1} in *P. oceanica* hydrolysate. *T. testudinum* hydrolysate allowed for a 5.7 g L^{-1} lipid accumulation, whereas yeast grown in medium A produced roughly 5.1 g L^{-1} of SCO.

Lipid accumulation in oleaginous microorganisms is usually initiated upon nutrient deprivation (nitrogen, phosphate, or sulfur).[33] Minimal-N medium is known to induce lipid biosynthesis in *T. oleaginosus* as it contains low nitrogen content. Nitrogen-limitation is considered to be essential for induction of lipogenesis in oleaginous yeasts and other organisms. Consequently, it was implemented for large-scale (15-L stirred-tank) fed-batch fermentation and biofuel production in yeast.[34]

The results of biomass analysis of *P. oceanica* and *T. testudinum* may explain the high lipid accumulation in *T. oleagi-*

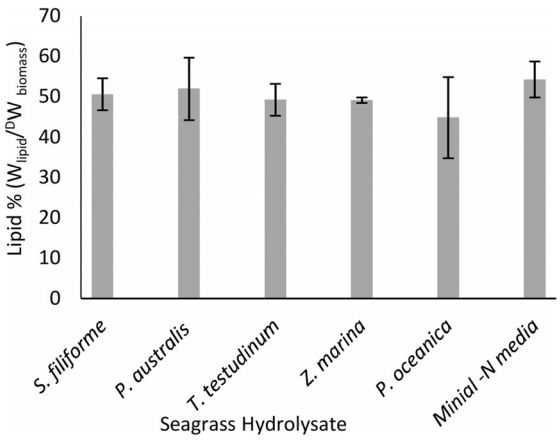

Figure 4. Lipid production of *T. oleaginous* cultivated in various seagrass hydrolysates after 5 days shake flask fermentation as percent dry weight% ($w_{lipid}/^{d}w_{biomass}$).

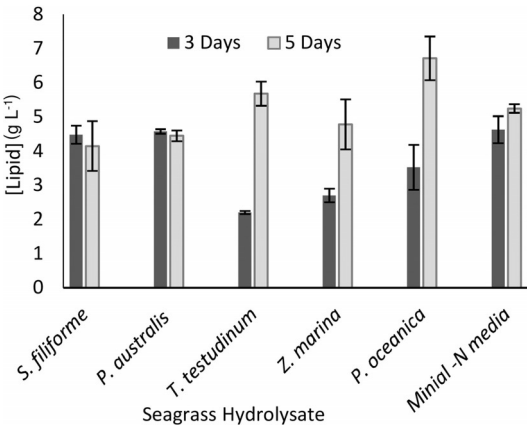

Figure 5. Lipid production of *T. oleaginous* cultivated in various seagrass hydrolysates after 3 and 5 days as lipid g L^{-1} culture.

nosus cultivated in their corresponding hydrolysates. Protein content in these two samples was the lowest amongst all seagrasses with only 5% ($w_{lipid}/^{d}w_{biomass}$) of total dry weight. Following 10 kDa cross-filtration, *P. oceanica* and *T. testudinum* hydrolysates contained the least amount of nitrogen and exhibited the highest C/N ratios (52 and 48 respectively) among all other samples. However, the C/N ratio of medium A is approximately 150; thus, other factors besides nitrogen-limitation may be driving the lipogenesis in *T. oleaginosus* grown in these two samples. In the ash analysis, phosphate from *P. oceanica* and *T. testudinum* strains was not detectable. The effect of phosphate limitation on the lipid production in yeast strains has been previously examined.[35] Exemplary, lipid accumulation in *Rhodosporidium toruloides* was directly associated with a high carbon/phosphorus (C/P) ratio, and it was maintained even in the presence of excess nitrogen.[36] *P. oceanica* and *T. testudinum* hydrolysates with both high C/N and high C/P ratios allowed for higher lipid accumulation compared to minimal-N medium exhibiting only nitrogen limitation. The deficiency of phosphate and exhaustion of nitrogen allowed rapid lipid accumulation from less than 2.4 g L^{-1} at day 3 (*T. testudinum* hydrolysate) to a maximum of 6.8 g L^{-1} at day 5 (*P. oceanica* hydrolysate). Furthermore, the relatively high nitrogen content in the hydrolysates compared to medium A allowed for higher yeast biomass production. Following 5 days culture, *T. oleaginosus* cultivated in *T. testudinum* and *P. oceanica* reached cell dry masses of approximatey 11.6 and 15.5 g L^{-1}, respectively. Conversely the yeast only achieved approximately 9.8 g L^{-1} of dry biomass when grown in medium A (Figure S5, Supporting Information). The Seagrass hydrolysates exhibited rather optimal C/N/P content, thereby allowing simultaneous high cell biomass and high lipid production. C/N and C/P ratios might not be the only reason behind the high lipid yields. Chemical nutrition and the presence of various trace elements in the hydrolysates could also explain the clear advantage over the synthetic medium A. Further investigation would help to elucidate the factors contributing to lipogenesis in *T. oleaginosus* grown in seagrass hydrolysates.

In this study, the hydrolysates from seagrass were used as the sole carbon source for yeast growth and lipid production in aerated shake flasks. Optimization of fermentation can help to enhance the obtained lipids yield. This is achieved by adding further nutrition to the media or using bioreactors.

Lipid production in fed-batch bioreactor

Based on the data from previous shake flask cultures, *P. oceanica* from Malta was chosen as biomass feedstock for fermentation at liter scale. *T. oleaginosus* was cultivated in controlled fed-batch with *P. oceanica* hydrolysate as the sole carbon source and without any nutrients addition. The hydrolysate contained 28.5 ± 0.59 g L^{-1} glucose and 5.53 ± 0.26 g L^{-1} pentose. 1 L of undiluted hydrolysate was employed as the main fermentation medium with another 100 mL of concentrated *P. oceanica* hydrolysate used as feed for the fermentation. The highest yeast dry cell weight (DCW) of approximately 42 g L^{-1} was obtained from 70 h batch culture (Figure 6). Lipid accumulation was initiated after 24 h upon depletion of nitrogen as nutrient. Yeast lipid content peaked at 54.4% ($w/^{d}w_{biomass}$) triglycerides (0.35 g L^{-1} h^{-1}) after 96 h of fermentation (Figure 7), with the total lipid concentration reaching 24.5 g L^{-1} of hydrolysate at the same time point (Figure 8).

Bioconversion of cellulosic biomass by microbial fermentation usually necessitates an acidic/alkaline thermochemical pretreatment step to facilitate the subsequent enzymatic hydrolysis of cellulose.[37] Lipid production from corn stover by the oleaginous yeast *Cryptococcus curvatus* required a pretreatment of the biomass with 0.5 M NaOH at 80 °C for 75 min.[38]

Moreover, pretreatment could generate substances that inhibit the enzymatic hydrolysis step and disrupt the microbial fermentation. Furfural was found to elongate the lag-phase, whereas benzoic acid negatively affected the microbial growth rate and biomass yield.[39] A complex chemical detoxification phase would be required, and all these extra steps present additional costs and diminish the eco-friendly aspect

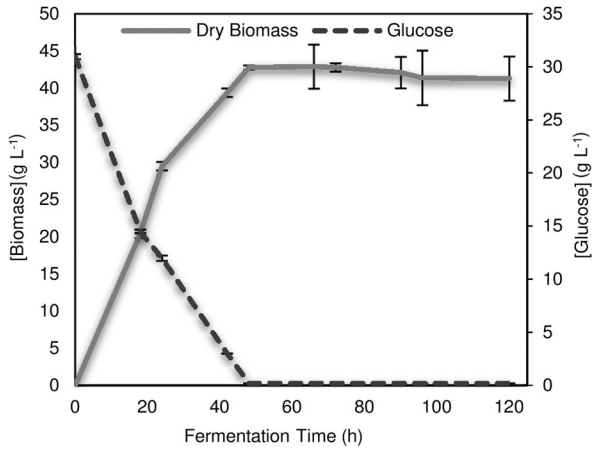

Figure 6. Increase of biomass and substrate consumption of *T. oleaginous* during fermentation time using *P. oceanica* hydrolysate in a 1 L stirred tank bioreactor.

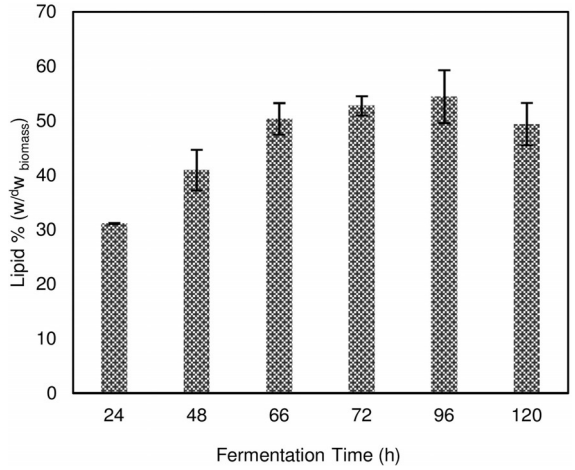

Figure 7. *T. oleaginous* fermentations on *P. oceanica* hydrolysate conducted in 1 L stirred tank bioreactors. Lipid yield expressed as percentage of the dry cell weight.

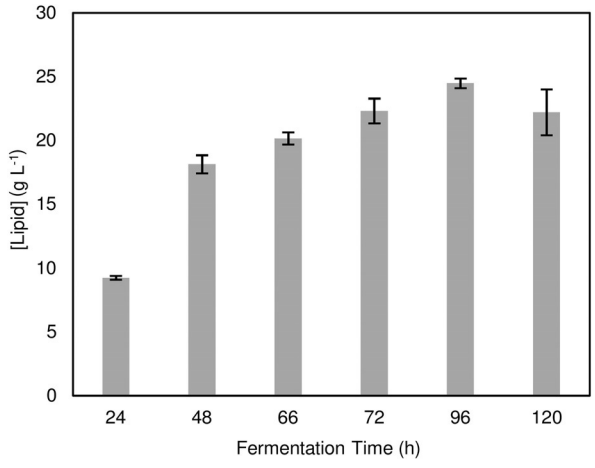

Figure 8. *T. oleaginous* fermentations on *P. oceanica* hydrolysate conducted in 1 L stirred tank bioreactors. Lipid productivity as g L^{-1}.

of the process. In our upscaling experiment, neither dilution nor detoxification of the hydrolysate medium was necessary given that no inhibitory effect on the yeast was detected. This fact highlights the importance of using a purely enzymatic-based hydrolysis approach, and the viability of seagrass biomass as feedstock for microbial oil production.

Following fermentation, seagrass biomass (120 g) was converted to 25 g of microbial lipids with a lipid coefficient of 208.4 mg g^{-1}. In comparison, Meo et al., 2017 used *T. oleaginosus* in a bioreactor to convert 250 g of microalgae biomass into 30 g of lipids with a lipid coefficient of only 120 mg g^{-1}. Furthermore, the researchers supplemented 126 g pure glucose as feed,[40] whereas in our experiment, seagrass hydrolysate was used as the sole carbon source for both the main and the feeding fermentation media. Additionally, the microalgae biomass was disrupted (to open the cell and facilitate the subsequent hydrolysis) with a high-pressure homogenizer—an energy consuming process—and required additional pretreatment. Therefore, our result demonstrate that seagrass is a superior feedstock compared to microalgae hydrolysate. Finally, the yeast fatty acid profile, measured by gas chromatography with flame ionization detection (GC–FID), shows high percentages of $C_{16:0}$, $C_{18:0}$, and $C_{18:1}$, which are suitable for subsequent high-quality biodiesel production (Table 6).

Table 6. Comparison of the *T. oleaginosus* fatty-acid profile cultivated in medium A and *P. oceanica* hydrolysate.

Media	Fatty acid content [% (*w*/*w*)]			
	$C_{16:0}$[a]	$C_{18:0}$	$C_{18:1}$	other
medium A	31.6[a]	9.5	51.0	7.9
P. oceanica	34.7	6.2	51.2	7.9

[a] Relative STDV for all given numbers is $\leq \pm 1\%$.

With no need for pretreatment or expensive additives, lack of environmental impact, and universal availability, seagrass biomass can be a cost-effective feedstock for microbial lipid production—a particularly valuable factor in advancing and achieving the sustainable production of biodiesel.

Material balance and techno-economic evaluation

Every 1 ton of seagrass could theoretically generate approximately 17 000 L of hydrolysate (60 g L^{-1}). After centrifugation and separation, 16 000 L of hydrolysate can be recovered, which contain an average of 0.510 ton of fermentable sugars (34 g L^{-1}). Moreover, the hydrolysate contains various organic materials, such as proteins, which represent nitrogen and carbon sources in addition to carbohydrates. To liquefy the seagrass, approximately 14 kg of enzyme and 83 kg of chemicals (buffer solution) are required per ton of seagrass feedstock. The hydrolysis step would generate 0.370 tons of solid residual biomass, which can be utilized in further applications such as animal feed or plant fertilizers. According to current results, 0.21 tons of oil can be produced.

In 2014, a techno-economic evaluation for microbial oil production estimated the costs to be \$5.5 kg^{-1}.[41] The study was based on pure glucose as feedstock with an annual production capacity of 10 000 tons of oil. To achieve targeted capacity, 12 fermenters each having a volume of 250 m^3, would be required, and these fermenters each would run 47 times per year. The total volume of culture media would amount to 140 850 m^3, with a total glucose content of 42 081 tons. In the reported evaluation, the glucose-to-SCO conversion yield was 0.23 $g\,g^{-1}$.[41]

Based on the current study, supplying the previous unit with seagrass hydrolysate as alternative and sole fermentation media requires two times a volume of 140 850 m^3 (first as main media and second as feeding after 10 times concentration). To produce the required volume, 18.78 tons of seagrass are required (0.06 ton m^{-3}). In addition, 12 vessels each with a volume of 250 m^3 would be necessary to run about 104 times per year. Taking into consideration that each run requires approximately 7 h loading and 70 h operation, the total process time would be 7500 hours per year.

Following hydrolysis, a solid/liquid disk separator should be installed in combination with a hydrolysate concentration unit. Furthermore, sterilization of raw materials is always required prior to hydrolysis. As the techno-economic evaluation has already included the sterilization step, it would be redundant to re-include it in the hydrolysate production process.

The installed equipment costs, fixed capital investment (FCI) calculations, operations (C_{OL}) costs, and utility costs (C_{UT}) of the previously mentioned process steps can be estimated using a similar unit equivalent to the study from Koutinas et al.[41] Hence, the costs of the bioreactor (R-101), solid/liquid disk separator (VE-101), filtration (D-201), and condenser (V-202) can be used to estimate the cost of the hydrolysate manufacturing process.[41] Additionally, heating units (E-101 and E-102)[41] will be included. Overall aforementioned items and their respective costs are listed in Tables 7 and 8.

Table 7. Cost of raw materials of the hydrolysate production.

Material	Unit costs	Amount per Year [ton]	Cost per Year [\$]
seagrass	\$1 ton^{-1}	18 779	\$18 779
enzyme	\$10 kg^{-1}	262.9	\$2 629 000
chemical	\$1.5 kg^{-1}	524.2	\$7 863 000
total			**\$10 510 779**

Finally the estimated annual cost of hydrolysate manufacture (COM) can be calculated by applying the Turton equation:[42]

$$COM = 0.28FCI + 2.73C_{OL} + 1.23(C_{RM} + C_{UT} + C_{WT})$$

Therefore, the COM of hydrolysate will be \$34.38 million to generate 281 690 m^3 hydrolysate, which corresponds to \$0.112 per liter.

Based on the calculation following Koutinas et al., after replacing the glucose with seagrass hydrolysate, the cost of microbial oil from seagrass hydrolysate is estimated to be \$7.3 kg^{-1}. It is worth mentioning that the glucose-to-SCO conversion yield was 0.23 $g\,g^{-1}$,[34,41] whereas the seagrass biomass and the contained sugar-to-SCO conversion yields were 0.21 and 0.41 $g\,g^{-1}$, respectively.

Contrary to plant-derived oil, microbial oil production is not affected by seasonal or climate changes. Moreover, microbial oil (MO) production does not affect agricultural activity and food security. However, due to the low biomass production costs, vegetable oil costs are lower than MO ranging between 1.1 and \$2.1 kg^{-1} for soybean and peanut oil, respectively.[41] Despite the availability of cheap raw materials, the challenge of SCOs production remains in the hydrolysis and biomass formation steps, which represent a significant part of the overall process costs.

Discussion

Seasonally, piles of seagrass residues accumulate on beaches and shores all over the globe. In excess of 80% of this biomass is not degraded biologically. This undesirable "waste" is constantly being removed or buried, especially in touristic destinations. In this work, we assessed the application of this waste material as a feedstock for SCO and subsequent biofuel/biolubricant production. This assessment presents seagrass biomass as a new starting material for biodiesel production, alternative to edible plant-based lipids.

Electron microscopy and comprehensive biomass analysis were performed on the various seagrass samples. The acquired data facilitated the optimization of enzymatic hydrolysis and offered insights regarding the hydrolysate compositions, trace elements content, and C/N/P ratios. An enzymatic-based hydrolysis method was optimized that efficiently released the carbohydrate monomers and allowed the production of seagrass hydrolysate without the need for energy-intensive thermochemical pretreatment. This single-step method prevented the generation of inhibitory compounds

Table 8. FCI cost, operational cost, and utility cost of the hydrolysate production

Category	Description	Cost per year [M\$]
FCI cost	sum of (R-101, VE-101, D-201 V-202 E-101 and E-102) × 1.2[41]	54.6
operational cost (C_{OL})	sum of worker count x4.5 = 20	0.50
utility cost (C_{UT})	sum of (R-101, VE-101, D-201 V-202 E-101 and E-102)[41]	3.912
material cost (C_{RM})	from Table 7	10.5

that normally required complex detoxification steps prior to fermentation. This approach is both cost-effective and eco-friendly.

Low density and high moisture content in feedstock materials are the main limitations for energy-efficient biomass-based processes, generating increased transport and operational costs.[16] Biomass analysis of the collected samples showed low water content. Furthermore, structural analysis, in particular that of *P. oceanica*, revealed a dense (non-hollow) structure. Seagrass biomass, exhibiting high density and minimal water content, is an advantageous raw material for cost-effective industrial applications. However, the biomass composition of seagrass might vary depending on the environment (location) and time of harvest. Furthermore, not all seagrass species offer the same industrial advantages as *P. oceanica*.

Previous reports used pure sucrose,[7a] synthetic media,[43] pre-treated secondary wastewater sludge,[7b] and pre-treated microalgae hydrolysate fed with pure glucose[40] as cultivation media for oily yeasts. Conversely, *T. oleaginosus* was successfully cultivated in all hydrolysates of aged-seagrass as the sole carbon source, without expensive additives such as yeast extract and biotin. *T. oleaginosus* cultivated in *P. oceanica* hydrolysate in a bioreactor accumulated a substantial amount of lipids ($\approx$25 g L^{-1}). The produced lipid, mainly in the form of triglycerides, is a preferred feedstock for chemo-catalytic conversion into green jet fuels,[44] thermochemical (pyrolysis) conversion into biogas and biosolids,[45] and ultrasonic cavitation to make clean biodiesel.[46] McCurdy et al., showed that lipids from *T. oleaginosus* can be converted into biodiesel with a recovery of 98.9%. Furthermore, flash point, viscosity, sulfur content, and acid number of the corresponding B20 meet the ASTM requirement and it is comparable to Soybean B20.[7a]

Based on the data presented in this study, 120 g of seagrass could be converted fermentatively to 25.0 g of lipids. Accordingly, by exploiting only half of the available residual seagrass biomass from around the globe, approximately 3.915 million tons of triglyceride-type lipids could theoretically be produced (with a process efficiency 85%). Enzymatic transesterification of these lipids with methanol or ethanol would yield 6.24 million tons (5.6 billion liters) of B100 biodiesel and 0.48 million tons glycerol [based on a conversion factor of 80% (*w*/*w*)]. Interestingly, this potential biodiesel yield from seagrass residues is comparable to the entire B100 production of USA in 2015 (4.8 billion liters),[1] which adds up to 26% of the global B100 production volume (21.6 billion liters) in that same year.[47] Moreover, the USA predominantly (53%) generated this B100 production volume through conversion of edible oils, such as corn and soybean oil.[1] The generation of these edible oil feedstocks required approximately 6.4 and 11.8 million hectares of agricultural land, respectively, for corn and soybean cultivation.[1,48]

The use of seagrass residues for the production of equivalent volumes of B100 biodiesel would not affect any agricultural activity or have any effect on sensitive marine ecosystems. Therefore, seagrass biomass would represent a real sustainable alternative to the application of edible plant oils particularly. However, despite its many industrial advantages, the use of seagrass as feedstock for SCO production might suffer from logistical drawbacks, such as collection and transportation of feedstocks from around the globe. The use of seagrass residue for renewable fuel production would require a significant alteration in the production logistics of the centralized processing of biofuels. As seagrasses are available only at scattered locations, which commonly are not close to human populations, its effective utilization as a biofuels feedstock would argue for a small decentralized production network. It is conceivable, that small, decentralized fermentation/chemical upgrading units could be installed at seagrass collection sites, which would convert only the relevant biomass amounts locally available. The resulting biofuel volumes could either be collected and then brought to centralized logistic hubs, or more preferably be utilized by nearby human settlements or industrial facilities that require a self-sustaining energy source. This study offers fundamental knowledge that can be used in future work to optimize oil production in large-scale bioreactors, investigate mechanisms of substrate-to-lipid conversion, and further assess the economics of biofuel and biodiesel production before commercialization of this technology.

Conclusions

Produced from readily available beach-cast waste materials, this simplified enzyme-treated seagrass media, provides a potential route to cost-effective sustainable bioenergy/biofuel production. Out of seven samples of seagrasses, *P. oceanica* (Mediterranean Sea) displays the best lipid productivity exceeding the well-optimized minimal nitrogen media. Generally, marine biomass does not affect terrestrial agricultural activity. Moreover, in this study we only employ aged seagrass banquettes that are washed ashore and do not affect the marine ecosystem. Therefore, the process presented in this study offers a biorefinery model for sustainable generation of microbial lipids with no impact on agricultural security or sensitive marine ecosystems.

Experimental Section

Samples

Fresh and aged seagrass samples were collected during the summer seasons of 2013 and 2014 from six different locations worldwide: two samples from the Baltic Sea (Hohenkirchen and Greifswald), two from the Mediterranean Sea (Malta), one in the Caribbean Sea (Isla de Mujeres, Mexico), one from the Great Australian Bight (Beachport, South Australia), and one sample from the North Atlantic Ocean (Bahamas). The samples were washed thoroughly to remove accumulated salt, sand and contaminants, dried, and ground down to $\leq$0.5 mm thickness using a planetary ball mill (Fritsch, Germany). For reproducibility purposes, all experiments and analyses were conducted in triplicate.

Sequence determination, phylogeny

Genomic DNA was isolated from seagrass samples using the innuPREP Plant DNA Kit (Analytik Jena, Germany). Extracted DNA was then run on 1% agarose gel (100 mA, 120 V) for 10 min. A gel area corresponding to 8000–10 000 kilobase (kb) size was cut. DNA was purified from the cut gel using innuPREP DOUBELEpure Kit (Analytik Jena, Germany). Two sets of primers were used for DNA amplification from all samples. The first set EukA (5′- AACCTGGTTGATCCTGCCAGT-3′) and EukB (5′-TGATCCTTCTGCAGGTTCACCTAC-3′) amplify the entire 18S rRNA region (almost 950 bp).[49] Primers ITS1 (5′-TCCGTAGGTGAACCTGCGG-3′) and NL4 (5′-GGTCCGTGTTTCA AGACGG-3′)[50] bind to entire intervening ITS1, 5.8S, ITS2 rRNA, and the D1/D2 domain (a portion of the 26S rRNA gene).

Biomass analysis

HPLC analysis

Sugar composition was analyzed by an Agilent 1100 series HPLC with a Refractive Index (RI) detector (Shodex, RI101) and Ultraviolet Index (Sedere-France, Sedex 75). The sugars were separated by using two different methods. In the first, a Rezex ROA-Organic Acid column (Aminex HPX 87H) was used with the eluent (5.0 mM H_2SO_4) at a flow rate of 0.5 mL min^{-1}. The column heater was set at 70 °C, and the detector was set at 40 °C. In the second method, sugars were separated using an Aminex HPX-87P column. An isocratic mobile phase of double distilled H_2O was pumped at a rate of 0.6 mL min^{-1}. The column temperature was 70 °C with the detector set at 50 °C.

GC–FID analysis

Lipids were extracted according to the Folch procedure.[51] The fatty acids were converted into fatty acid methyl esters (FAMEs) as described in Griffiths et al.[52] Glyceryl trinonadecanoate ($C_{19:0}$-TAG, 1.00 mg) was added prior to the reaction as an internal standard. FAMEs was analysed using GC–FID [Zebron Capillary GC column (Phenomenex, Germany)]. The column was 30.0 m in length with an internal diameter of 0.32 mm and a film thickness of 0.25 μm. The column operated at a temperature of 150 °C for 1 min before increasing to 240 °C at a rate of 5 °C min^{-1}. The injector injected a sample amount of 1.0 μL at a temperature of 240 °C with a split ratio of 10 and hydrogen was used as the carrier gas at a flow rate of 3 mL min^{-1}.Before injection, FAME ($C_{12:0}$) was added to the samples as an internal standard for quantitation.

Electron microscope and EDX

Scanning electron microscopy (SEM) was performed using a JSM-7500F scanning electron microscope (JEOL, Japan) with an accelerating voltage of 1, 2, or 5 kV and a secondary electron detector.

The ash profile was determined using SEM with energy-dispersive X-ray (EDX) analysis. Ash samples were mounted on a carbon film and prepped for analysis. EDX analysis was performed on multiple areas (100 × 100 μm^2) in backscattered electron (BSE) mode for each ash sample. The average value was calculated to obtain the elemental composition of the ash.

Kjeldahl analysis

The protein amount was determined using the standard operating procedure by Kjeldahl et al. Dry seagrass biomass (2.00 g) was digested (InKjel M, behr Labor technik GmbH-Germany) and distilled (Vapodest 10, Gerhardt- Germany).

Seagrass treatment

Enzymatic hydrolysis of each of the seagrass samples was conducted using 2 L glass bottles (Schott) containing 1.0 L of acetate buffer solution (50.0 mM, pH 5.0) and 60.0 g of biomass. Reactions were initiated by adding an enzyme solution and incubating at 50 °C while stirring at 400 rpm using magnetic stirrer for 72 h. The used enzymes include Cellic CTec 2 (Novozymes- Denmark), Cellic HTec (Novozymes- Denmark), Pectinex (Novozymes- Denmark), and Novozymes 188 (Novozymes- Denmark). In parallel, two controls were included: control one contained a substrate without the enzyme solution and control two contained an enzyme solution without a substrate. The controls were conducted in 50 mL falcon tubes containing 25.0 mL of acetate buffer solution (50.0 mM, pH 5.0) and 500.0 mg of biomass.

Hydrolysate preparation

The samples were then centrifuged for 30 min at 8000 g, followed by cross-filtration (10 kDa membrane made from regenerated cellulose was used with the following parameters: inlet pressure (P1) 2 bar, repentant pressure (P2) 0.3–0.5 bar, and the permeate was open to atmospheric pressure. The flow rates of repentant and permeate were approximately 2 L min^{-1} and 0.1 L min^{-1}, respectively. 0.2 μm filter capsules were installed at the outlet to sterilize the resulted hydrolysate). A sexokinase assay kit (Megazyme- Ireland), was used to measure the glucose concentration of each sample at 340 nm, repeated four times. For the standard curve, five calibration points were measured at concentrations: 0.5, 1.0, 2.0, 3.0, and 4.0 g L^{-1}. The final sugar analysis was performed by using HPLC as described above. A subsample from each hydrolysate was analyzed to detect reduced nitrogen using the Kjeldahl method.

Utilization of hydrolysates as sole medium for bio-oil production

For observation of its growth rate and lipid accumulation, the yeast *Trichosporon oleaginosus* (ATCC 20509) was cultivated in 1 L Erlenmeyer flasks containing 300 mL of the different enzymatic hydrolysates. The flasks were supplemented with an aeration system supplying the cultures with 0.2 L min^{-1} pre-filtered air. Nitrogen-limited medium (medium A) as previously described,[53] was used as a positive control. With an initial seeding $OD6_{00} = 0.5$, all cultures were incubated in a rotary shaker at 120 rpm at 28 °C for 5 days. OD_{600} was measured every day, and liquid cultures were divided for subsequent gravimetric analysis. A technical draw for aerated flasks is available in the Supporting Information (Figure S6).

Lipid at fed-batch bioreactor

Dried grinded *P. oceanica* (120 g) was subjected to enzymatic hydrolysis followed by 10 kDa cross-filtration (as previously described) generating 2 L of hydrolysate. For fed-batch cultivation, 1 L served as the main fermentation medium and the remaining

1 L was concentrated 10 times by using a rotary evaporator and used as feed for the bioreactor. *T. oleaginosus* was cultured in the seed medium YPD (10 g L^{-1} yeast extract, 20 g L^{-1} peptone, and 20 g L^{-1} glucose) at 28 °C and 120 rpm for 24 h. 10 % of the culture was inoculated into the seagrass hydrolysate. Fed-Batch cultivation of *T. oleaginosus* was performed in a 2 L bioreactor (INFORS HT system, Switzerland) with a working volume of 1 L in *P. oceanica* hydrolysate with an approximate C/N ratio of 52. The temperature was maintained at 28 °C, and the pH of the bioreactor was adjusted to pH 6.5 ± 0.2 with 1 M NaOH by the system. Stirring (200–400 rpm) and aeration (1.0–2.0 normal liters per minute of air) were regulated automatically to maintain the dissolved oxygen at above 50 %. Foam was prevented by the addition of 0.01 % (*v*/*v*) of an antifoam agent (Antifoam 204, Sigma Aldrich). Substrate feeding was initiated at day 1. Samples were withdrawn manually at 24 h intervals for 6 days, and were used for subsequent determination of OD_{600}, the dry cell weight, and lipid content.

Dry biomass determination/ gravimetric analysis lipids

Dry biomass was processed by lyophilization for 2 days at −80 °C and 0.04 mbar (Christ alpha 2–4 LD plus). Gravimetric quantification of the lipid was performed using the Bligh–Dyer method.[54] Briefly, a high-pressure homogenizer (Avestin emulsiflex C3) was used followed by three times solvent extraction using Folch solution.

Fatty acid profile

GC–FID, see the procedure as described above.

Acknowledgements

M.M., F.Q., and T.B. acknowledge financial support by the German Federal Ministry of Education and Research for supporting the "LIPOMAR" (grant number: 031A261) and "Advanced Biomass Value" (grant number: 03SF0446A) projects. Information concerning the Advanced biomass projects can be obtained at: http://www.ibbnetzwerk-gmbh.com/de/service/pressebereich/pm-06052013-advanced-biomass-value/. S.Y., N.M., and T.B. also acknowledge financial support for the project "Resource efficient production processes for polyhydroxybutyrate based biopolymers" of the Bavarian State Ministry for Environment and Consumer Protection (StMUV, grant number TLKO1U-69045).

Conflict of interest

The authors declare no conflict of interest.

Keywords: bioenergy · biofuels · enzymatic treatment · fermentation · seagrass

[1] U.S.E.I. Administration, U.S. Energy Information Administration, **2016**.
[2] V. H. Smith, B. S. Sturm, S. A. Billings, *Trends Ecol. Evol.* **2010**, *25*, 301–309.
[3] G. V. Subhash, S. V. Mohan, *Fuel* **2014**, *116*, 509–515.
[4] a) L. Chng, K. Lee, D. Chan; b) A. Guldhe, B. Singh, I. Rawat, K. Ramluckan, F. Bux, *Fuel* **2014**, *128*, 46–52.
[5] Y. A. Tsigie, L. H. Huynh, P. L. T. Nguyen, Y.-H. Ju, *Fuel Process. Technol.* **2013**, *115*, 50–56.
[6] Y.-H. Chang, K.-S. Chang, C.-L. Hsu, L.-T. Chuang, C.-Y. Chen, F.-Y. Huang, H.-D. Jang, *Fuel* **2013**, *105*, 711–717.
[7] a) A. T. McCurdy, A. J. Higham, M. R. Morgan, J. C. Quinn, L. C. Seefeldt, *Fuel* **2014**, *137*, 269–276; b) X. Zhang, S. Yan, R. D. Tyagi, R. Y. Surampalli, J. R. Valéro, *Fuel* **2014**, *134*, 274–282.
[8] P. Gujjari, S.-O. Suh, K. Coumes, J. J. Zhou, *Mycologia* **2011**, *103*, 1110–1118.
[9] a) P. Akhtar, J. Gray, A. Asghar, *J. Food Lipids* **1998**, *5*, 283–297; b) P. Meesters, G. Huijberts, G. Eggink, *Appl. Microbiol. Biotechnol.* **1996**, *45*, 575–579; c) Y. Liang, T. Tang, T. Siddaramu, R. Choudhary, A. L. Umagiliyage, *Renewable Energy* **2012**, *40*, 130–136.
[10] I. K. Chung, J. Beardall, S. Mehta, D. Sahoo, S. Stojkovic, *J. Appl. Phycol.* **2011**, *23*, 877–886.
[11] S. Beer, E. Koch, *Mar. Ecol. Prog. Ser.* **1996**, *141*, 199–204.
[12] B. Subhadra, M. Edwards, *Energy Policy* **2010**, *38*, 4897–4902.
[13] J. W. Fourqurean, C. M. Duarte, H. Kennedy, N. Marbà, M. Holmer, M. A. Mateo, E. T. Apostolaki, G. A. Kendrick, D. Krause-Jensen, K. J. McGlathery, *Nat. Geosci.* **2012**, *5*, 505–509.
[14] J. Cebrián, C. M. Duarte, N. Marbà, *J. Exp. Mar. Biol. Ecol.* **1996**, *204*, 103–111.
[15] S. Enríquez, C. M. Duarte, K. Sand-Jensen, *Oecologia* **1993**, *94*, 457–471.
[16] M. H. L. Silveira, A. R. C. Morais, A. M. D. C. Lopes, D. N. Olekszyszen, R. Bogel-Łukasik, J. Andreaus, L. P. Ramos, *ChemSusChem* **2015**, *8*, 3366–3390.
[17] a) M. Uchida, T. Miyoshi, M. Kaneniwa, K. Ishihara, Y. Nakashimada, N. Urano, *J. Biosci. Bioeng.* **2014**, *118*, 646–650; b) M. Pilavtepe, M. S. Celiktas, S. Sargin, O. Yesil-Celiktas, *Ind. Crops Prod.* **2013**, *51*, 348–354.
[18] a) M. Rakicka, Z. Lazar, T. Dulermo, P. Fickers, J. M. Nicaud, *Biotechnol. Biofuels* **2015**, *8*, 1; b) R. Wang, J. Wang, R. Xu, Z. Fang, A. Liu, *BioResources* **2014**, *9*, 7027–7040.
[19] R. Kourist, F. Bracharz, J. Lorenzen, O. N. Kracht, M. Chovatia, C. Daum, S. Deshpande, A. Lipzen, M. Nolan, R. A. Ohm, *mBio* **2015**, *6*, e00918-15.
[20] a) E. P. Green, F. T. Short, *World atlas of seagrasses*, University of California Press, **2003**; b) G. De Falco, S. Simeone, M. Baroli, *J. Coastal Res.* **2008**, *24*, 69–75.
[21] a) D. H. Les, M. A. Cleland, M. Waycott, *Syst. Bot.* **1997**, *22*, 443–463; b) Y. Kato, K. Aioi, Y. Omori, N. Takahata, Y. Satta, *Genes Genet. Syst.* **2003**, *78*, 329–342.
[22] B. H. Daru, K. Yessoufou in *DNA Barcoding in Marine Perspectives*, Springer, Switzerland, **2016**, pp. 313–330.
[23] D. W. Templeton, M. Quinn, S. Van Wychen, D. Hyman, L. M. Laurens, *J. Chromatogr. A* **2012**, *1270*, 225–234.
[24] J. M. Ageitos, J. A. Vallejo, P. Veiga-Crespo, T. G. Villa, *Appl. Microbiol. Biotechnol.* **2011**, *90*, 1219–1227.
[25] a) M. Yamamuro, A. Chirapart, *J. Oceanogr.* **2005**, *61*, 183–186; b) J. L. Siegal-Willott, K. Harr, L.-A. C. Hayek, K. C. Scott, T. Gerlach, P. Sirois, M. Reuter, D. W. Crewz, R. C. Hill, *J. Zoo Wildlife Med.* **2010**, *41*, 594–602; c) G. Brudecki, R. Farzanah, I. Cybulska, J. E. Schmidt, M. H. Thomsen, *Energy Procedia* **2015**, *75*, 760–766.
[26] a) Y. A. Tsigie, C.-Y. Wang, N. S. Kasim, Q.-D. Diem, L.-H. Huynh, Q.-P. Ho, C.-T. Truong, Y.-H. Ju, *BioMed Res. Int.* **2012**, *2012*, 378384; b) S. Morales-delaRosa, J. M. Campos-Martin, J. L. Fierro, *Cellulose* **2014**, *21*, 2397–2407.
[27] H. Huang, X. Guo, D. Li, M. Liu, J. Wu, H. Ren, *Bioresour. Technol.* **2011**, *102*, 7486–7493.
[28] C. K. Nitsos, K. A. Matis, K. S. Triantafyllidis, *ChemSusChem* **2013**, *6*, 110–122.
[29] L. Yong-Hong, L. Bo, Z. Zong-Bao, B. Feng-Wu, *Chin. J. Biotechnol.* **2006**, *22*, 650–656.
[30] P. Davies, C. Morvan, O. Sire, C. Baley, *J. Mater. Sci.* **2007**, *42*, 4850–4857.
[31] Y. Liu, G. Jiang, Z. Wu, *J. Ocean Univ. China* **2010**, *9*, 68–70.

[32] J. Wang, X. Pan, Y. Han, D. Guo, Q. Guo, R. Li, *Mar. Drugs* **2012**, *10*, 2729–2740.
[33] S. Papanikolaou, G. Aggelis, *Eur. J. Lipid Sci. Technol.* **2011**, *113*, 1031–1051.
[34] Y. Li, Z. K. Zhao, F. Bai, *Enzyme Microb. Technol.* **2007**, *41*, 312–317.
[35] G. Zhang, W. T. French, R. E. Hernandez, J. Hall, D. Sparks, W. E. Holmes, *J. Chem. Technol. Biotechnol.* **2011**, *86*, 642–650.
[36] S. Wu, C. Hu, G. Jin, X. Zhao, Z. K. Zhao, *Bioresour.Technol.* **2010**, *101*, 6124–6129.
[37] L. J. Jönsson, B. Alriksson, N.-O. Nilvebrant, *Biotechnol. Biofuels* **2013**, *6*, 16.
[38] Z. Gong, H. Shen, X. Yang, Q. Wang, H. Xie, Z. K. Zhao, *Biotechnol. Biofuels* **2014**, *7*, 158.
[39] Y. Zha, B. Muilwijk, L. Coulier, P. J. Punt, *J. Bioprocess. Biotech.* **2012**, *2*, 112–122.
[40] A. Meo, X. L. Priebe, D. Weuster-Botz, *J. Biotechnol.* **2017**, *241*, 1–10.
[41] A. A. Koutinas, A. Chatzifragkou, N. Kopsahelis, S. Papanikolaou, I. K. Kookos, *Fuel* **2014**, *116*, 566–577.
[42] R. Turton, R. C. Bailie, W. B. Whiting, J. A. Shaeiwitz, *Analysis, synthesis and design of chemical processes*, Pearson Education, **2008**.
[43] Y. Wei, V. Siewers, J. Nielsen, *Appl. Microbiol. Biotechnol.* **2017**, *101*, 3577–3585.
[44] C. Zhao, T. Brück, J. A. Lercher, *Green Chem.* **2013**, *15*, 1720–1739.
[45] N. Muradov, A. Gujar, J. Baik, T. Ali, *Fuel Process. Technol.* **2015**, *140*, 236–244.
[46] S. Asif, L. F. Chuah, J. J. Klemeš, M. Ahmad, M. M. Akbar, K. T. Lee, A. Fatima, *J. Cleaner Prod.* **2017**, *161*, 1360–1373.
[47] S. GmbH, https://www.statista.com, **2016**.
[48] T. J. t. F. Project, **2016**.
[49] B. Díez, C. Pedrós-Alió, R. Massana, *Appl. Environ. Microbiol.* **2001**, *67*, 2932–2941.
[50] C. Kurtzman, C. Robnett, *J. Clin. Microbiol.* **1997**, *35*, 1216–1223.
[51] J. Folch, M. Lees, G. S. Stanley, *J. Biol. Chem.* **1957**, *226*, 497–509.
[52] M. Griffiths, R. Van Hille, S. Harrison, *Lipids* **2010**, *45*, 1053–1060.
[53] M. Suutari, P. Priha, S. Laakso, *J. Am. Oil Chem. Soc.* **1993**, *70*, 891–894.
[54] E. G. Bligh, W. J. Dyer, *Can. J. Biochem. Physiol.* **1959**, *37*, 911–917.

Manuscript received: August 23, 2017
Revised manuscript received: September 24, 2017
Accepted manuscript online: September 27, 2017
Version of record online: December 11, 2017

3.2 Microbial lipid production by oleaginous yeasts grown on *Scenedesmus obtusiusculus* microalgae biomass hydrolysate

Samer Younes, Felix Bracharz, Dania Awad, Farah Qoura, Norbert Mehlmer & Thomas Brueck

Published in: Bioprocess and Biosystems Engineering

Editor-in-Chief: Dirk Weuster-Botz

Date of Publication: 28 April 2020

DOI: 10.1007/s00449-020-02354-0

3.2.1 Author Contributions

Conceptualization of the study and design of the methodological approach was jointly designed by all authors. Planning and execution of experiments was carried out by the author of this thesis, Samer Younes and Felix Bracharz. Data validation was jointly carried out by all authors. Samer Younes prepared the original draft of the manuscript, which was jointly finalized and reviewed by all authors.

3.2.2 Summary II

Plant-derived biofuels and oleochemicals are currently regarded as one of the most viable options for reducing fossil-fuel dependency. However, the use of arable lands and valuable resources (e.g., fresh water) for vegetable-oil production, impacts agricultural activity, increases deforestation practices and jeopardizes food security [7]. Single cell oils (SCOs), accumulated by oleaginous microorganisms (e.g., microalgae, yeast), offer a potential sustainable alternative, that does not carry environmental, societal or economical disadvantages [56]. The utilization of "zero cost" waste biomass hydrolysates as feedstock could reduce the overall costs of microbial-derived oleochemicals [81]. Compared to terrestrial crops (e.g., palm, rapeseed) biomass generation from microalgae has high space and time yields. Every year, around 280 tons/ha of algae dry biomass are produced globally, with only 3.9 tons/ha of forest biomass [127]. Recent studies focused on utilizing this biomass residue for the renewable production of oil, food and feed [128].

In this study, we explored the valorization of *Scenedesmus obtusiusculus* A189 biomass as feedstock for yeast oil production. This freshwater green microalgae is characterized by fast growth rate and high lipid accumulation potential [107]. Biomass analysis of *S. obtusiusculus* revealed high inherent carbohydrate content and lack of recalcitrant lignin, consistent with published studies [129]. Accordingly, we developed and optimized a single-step "green" enzymatic hydrolysis process that allowed efficient saccharification of microalgae biomass, without thermo-chemical pre-treatment steps. Mixtures of cellulase, hemicellulolase, pectinase and amylase hydrolytic enzymes were tested individually and in combinatory approaches. The optimum activity was obtained with the Cellic CTec 2 mix (Novozymes, Denmark) - which combines several enzymatic activities (exo-, endo-glucanase, and proteinase) - at an industrially relevant concentration (1 % v/v), temperature of 50.0 °C, and pH 5.0 (50.0 mm, Sodium acetate) for 72 h. Biomass-glucose conversion efficiencies reached 90–100% compared to chemical hydrolysis.

Following ultrafiltration, the hydrolysate rich in monomeric sugars and deficient in nitrogen (high C:N ratio) was used as a sole fermentation medium for cultivation of the oleaginous yeasts *C. oleaginosus*, *C. curvatus* and *R. toruloides*. Only *C. oleaginosus* was able to accumulate high amounts of intracellular

lipids, as indicated by a high-throughput Nile red analysis. In shake flasks studies, *S. obtusiusculus* hydrolysate, devoid of any expensive nutritional addition (e.g., biotin, yeast extract, pure glucose…), allowed for a lipid yield of 3.6 $g.L^{-1}$ compared to 5.1 $g.L^{-1}$ with the expensive synthetic minimal media. At industrial scale, this renewable biomass could prove a cost-effective feedstock for SCOs production.

Bioprocess and Biosystems Engineering (2020) 43:1629–1638
https://doi.org/10.1007/s00449-020-02354-0

RESEARCH PAPER

Microbial lipid production by oleaginous yeasts grown on *Scenedesmus obtusiusculus* microalgae biomass hydrolysate

Samer Younes[1] · Felix Bracharz[1] · Dania Awad[1] · Farah Qoura[1] · Norbert Mehlmer[1] · Thomas Brueck[1]

Received: 18 February 2020 / Accepted: 13 April 2020 / Published online: 28 April 2020

Abstract

Due to increasing oil prices and climate change concerns, biofuels have become increasingly important as potential alternative energy sources. However, the use of arable lands and valuable resources for the production of biofuel feedstock compromises food security and negatively affect the environment. Single cell oils (SCOs), accumulated by oleaginous yeasts, show great promise for efficient production of biofuels. However, the high production costs attributed to feedstocks or raw materials present a major limiting factor. The fermentative conversion of abundant, low-value biomass into microbial oil would alleviate this limitation. Here, we explore the feasibility of utilizing microalgae-based cell residues as feedstock for yeast oil production. We developed an efficient, single-step enzymatic hydrolysis to generate *Scenedesmus obtusiusculus* hydrolysate (SH) without thermo-chemical pretreatment. With this eco-friendly process, glucose conversion efficiencies reached 90–100%. *Cutaneotrichosporon oleaginosus*, *Cryptococcus curvatus* and *Rhodosporidium toruloides* were cultivated on SH as sole nutrients source. Only *C. oleaginosus* was able to accumulate intracellular lipids, with a 35% (g lipid/g DCW) content and a yield of 3.6 g/L. Our results demonstrate the potential valorization of algal biomass into desired end-products such as biofuels.

Samer Younes and Felix Bracharz contributed equally to the work.

✉ Thomas Brueck
brueck@tum.de

[1] Werner Siemens-Lehrstuhl für Synthetische Biotechnologie, Technische Universität München, Garching, Germany

Graphic Abstract

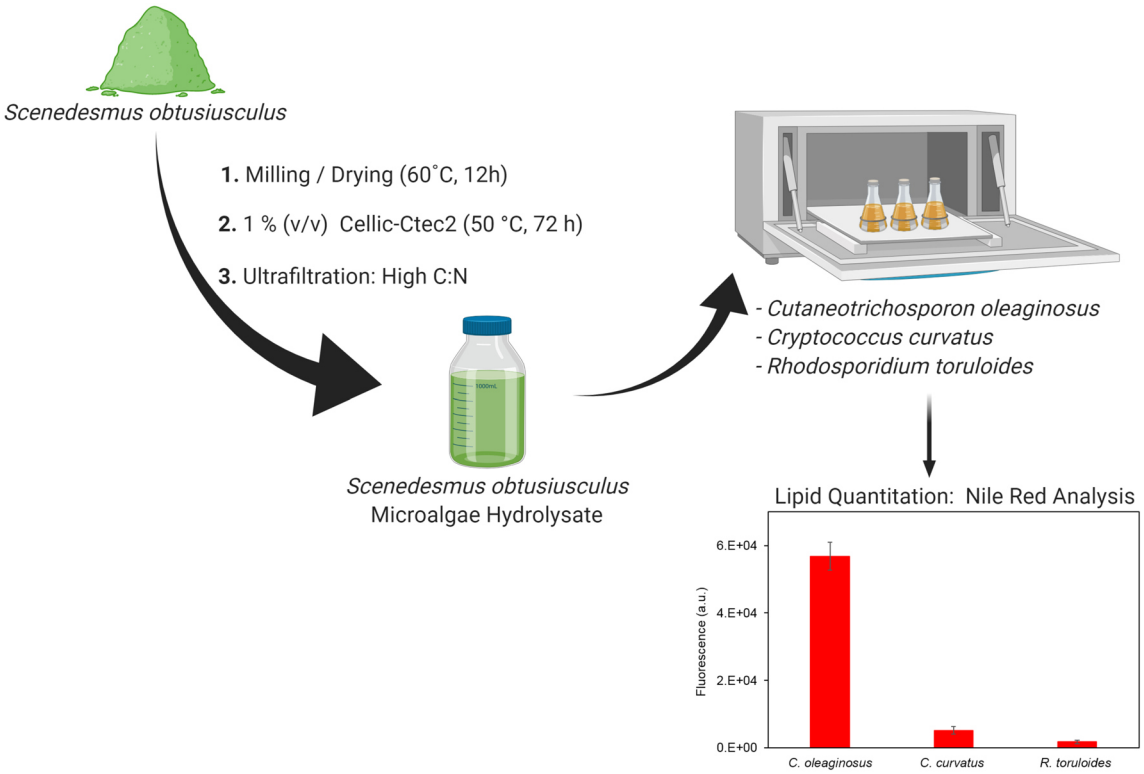

Keywords *Scenedesmus obtusiusculu* · *Cutaneotrichosporon oleaginosus* · Enzymatic hydrolysis · Microalgae biomass · Lipid production

Introduction

The ever-increasing energy demand in today's industrial world led to the widespread use of non-renewable fossil fuels such as petroleum. The transition from a society with waste generating, linear production routes to one cyclic valorization path in conjunction with renewable resource management is one of the most demanding technological goals for establishing sustainable bioeconomy [1, 2]. This scenario particularly applied renewable energy supply routes that demand a switch from finite fossilto sustainable platform solutions. Moreover, dwindling of fossil resources, escalating environmental pollution, surging CO_2 and greenhouse gas emissions, in addition to climate change have collectively driven the search for alternative energy sources [3]. Accordingly, technological innovations that enable a more sustainable lifestyle are coveted [4].

Biofuels have garnered great interest in recent years as alternatives for fossil fuel. In fact, plant-derived biofuel offers a partial solution to the ever-increasing energy demand, due to their renewability. However, this first-generation of biofuels, generated from edible crops, impacts agricultural activity and jeopardizes food security [1] To meet the current annual global-demand of biodiesel, more than double of the currently arable land would be required to grow crops that are explicitly grown for fuel production [5]. Consequently, alternative sources for biofuel production that do not affect food security are in high demand [1]. One of those alternatives is the use of oleaginous microorganisms such as algae and yeast [6].

Oleaginous microorganisms accumulate lipid at a minimum of 20% (g lipids/g dry cell weight (DCW)) [7]. However, lipid accumulation in oleaginous microorganisms, such as yeast, fungi and microalgae, is not a constitutive feature, but rather an adaptive response to particular environmental factors [8]. In environmental conditions abundant in carbon source and deficient in specific nutrients such as nitrogen, phosphorus or sulfur, oleaginous microorganisms convert excess carbon into fatty acids and incorporate them into triglycerides (TAGs) as a form of energy storage [9]. TAGs are stored in specialized organelles called lipid bodies (also known as lipid droplets) [10]. Single Cell Oils (SCOs) can be efficiently converted into biodiesel and biofuel [11, 12]. Various oleaginous yeasts have been subject to extensive

investigations such as *Yarrowia lipolytica*, *Rhodosporidium toruloids* and *Lipomyces starkeyi*, with reports of lipid accumulation in excess of 70% (g lipid/g DCW) [13, 14]. The potential biotechnological applications of these oleaginous yeasts, utilizing various carbon sources have been previously reported [9, 15, 16].

Moon et al. first isolated *Cutaneotrichosporon oleaginosus* (ATCC 20509) in 1978 from factory drain samples of the Iowa State University Dairy Farm. *C. oleaginosus* readily utilizes glucose, galactose, cellobiose, xylose, sucrose, and lactose as carbon source [1, 17–19]. Furthermore, this yeast is able to metabolize glycerol, *N*-acetylglucosamine, volatile fatty acids and ethanol and 4-hydroxymethylfurfural [20–22]. To improve the sustainability of SCOs from socio-economic aspects, *Y. lipolytica* has undergone extensive genetic engineering aimed at simultaneous sugar uptake (hexoses and pentoses) from complex and wastewater hydrolysates, which is an inherent ability in *C. oleaginosus* [8]. Depending on carbon, nitrogen sources and stress conditions (nitrogen, phosphate or sulfate limitation), cellular lipid accumulation in *C. oleaginosus* can reach up to 85% (g lipid/g DCW) [23, 24]. In addition to fast growth rate, this oleaginous yeast exhibits a fatty acid profile that mimics that of vegetable oils, specifically palm oil, with palmitic, stearic and oleic acid as dominant fatty acids [25]. McCurdy et al. reported that biodiesel B20 derived from *C. oleaginosus* TAGs meet the ASTM (D6751) certification [1, 9]. Through recycling and finding appropriate industrial sink for bio-compounds, a recent study touching on the socio-economic sustainability of *C. oleaginosus* SCOs has been recently prepared in our group [4].

Other oleaginous species that can be exploited for the biofuel sector include microalgae. In contrast to industrial crops, such as palm or canola plants, biomass generation from microalgae has high space and time yields. Globally, around 280 tons/ha of algae dry biomass and 3.9 tons/ha of forest biomass are produced every year [26]. Additionally, microalgae display high CO_2 fixation ability (513 tons of sequestered CO_2 per hectare per year). Specifically, 1.6-2 grams of CO_2 is captured for every gram of algal biomass produced, at an efficiency of 80-99% [27, 28]. While microalgae can provide renewable oils by photosynthetically converting atmospheric CO_2 to lipids, yields are conventionally lower compared to oleaginous yeast species [29–31]. In most algae oil production processes, the extracted cell residue is not contributing to the overall process economy [29, 31].

Yet recently, several value-adding outlets for this residue have been achieved, either by feeding it back into renewable production (oil, food, feed, etc.) or by recycling of resources [4, 32]. Similar waste-free biorefinery approaches have been considered in the design and optimization of biogas production processes [33]. In that respect, the residual biomass, which is rich in fermentable sugars, can be used as feedstock for oleaginous yeasts cultivation [34]. Specifically, *Scenedesmus* spp. belong to the most common freshwater green algae. *Scenedesmus obtusiusculus* A189, a newly isolated member of the *Chlorophyta* genus, is characterized by high growth rates in fresh and saline media, in addition to high inherent carbohydrate content [35]. Fermentative conversion of various biomass sources into SCOs and subsequent biofuel via oleaginous yeasts has recently received an increasing interest in the scientific and industrial community [2, 4]. Specifically, microalgae biomass does not contain recalcitrant lignin, making it suitable for eco-friendly and cost-effective hydrolysis methods [35]. To that end, efficient hydrolysis of algae biomass could provide a sustainable stream of monomeric hexose and pentose sugars for fermentative growth. However, chemical biomass hydrolysis, which is most commonly applied in industry, tarnishes the eco-friendly aspect of biofuel production [2]. Alternatively, enzymatic hydrolysis efficiently generates sugar-rich fermentation media, yet necessitates thermo-chemical pretreatment steps to break down the lignocellulosic biomass components into monomeric hexose and pentose sugars [36]. These pretreatment steps release inhibitory compounds that hinder growth of subsequent oleaginous yeast inoculum in the prospective hydrolysate. Removal of these inhibitory compounds imposes additional costs, time and effort for the production process [37].

In this study, we examine the enzymatic hydrolysis of microalgae-based cell residues and the subsequent use of its hydrolysate (SH) for the cultivation of oleaginous yeasts (*C. oleaginosus*). A single-step enzymatic hydrolysis process was devised and optimized, allowing efficient hydrolysis and saccharification of microalgae biomass, without thermo-chemical pretreatment. The resulting *S. obtusiusculus* hydrolysate (SH), barring expensive additives, was utilized as the sole fermentative media for *C. oleaginosus*, *Cryptococcus curvatus* and *Rhodosporidium toruloides*. The accumulated lipids, deposited as intracellular lipid bodies (LBs), were relatively quantified by Nile red analysis. Moreover, *C. oleaginosus* growth, dry biomass and lipid weight were evaluated.

Materials and methods

Algae strains and biomass determination

Scenedesmus obtusiusculus (A189) residues were obtained from Pharmaceutical Biology Group, Ernst Moritz Arndt University (EMAU), Griefswald, Germany. Water content was determined following the milling and drying of the algal samples at 60 °C overnight. Total carbohydrate concentration was determined by the thymol-sulfuric acid method [38]. The standard Kjeldahl procedure was utilized to determine the amount of protein in the algae biomass

[39]. Total lipids were extracted according to Folch et al., and determined gravimetrically after solvent evaporation [40]. Biomass ash content was determined by following the AOAC procedure [41]. Biological replicates ensured reproducible measurements.

Enzymatic hydrolysis and preparation of SH

Scenedesmus obtusiusculus Hydrolysate (SH) was prepared by hydrolyzing autoclaved algae biomass. Briefly, dry biomass samples weighing 50 g were transferred to 2 L glass bottles containing 1 L of 50.0 mM sodium acetate buffer, pH 5.0. Different hydrolytic enzyme mixtures were examined, including Cellic-Ctec2 (Novozymes, Denmark), Celli-Htec2 (Novozymes, Denmark), Pectinex (Novozymes, Denmark) and Fungamyl (Novozymes, Denmark). Hydrolytic Reactions were initiated by adding the enzyme solution and incubating the mixture at 50 °C for 72 h. Buffer and enzymes were sterile-filtered prior to hydrolysis. Samples were then spun down for 30 min. Cross-filtration using a 10 kDa membrane made from regenerated cellulose was completed under the following parameters: Inlet-Pressure (P1) of 2 bar, Repentant-Pressure (P2) of 0.3–0.5 bar and permeate was open to atmospheric pressure. Flow-Rates of retentate and permeate were adjusted to 2 L/min and 0.1 L/min respectively. A 0.2 µm filter capsules were installed at the outlet to sterilize the resulted hydrolysate. Biological triplicates of the SH were prepared.

Sugar analysis

Sugar composition of the hydrolysate was determined by an Agilent 1100 series HPLC with a Refractive Index (RI) detector (Shodex, RI101) and Ultraviolet Index (Sedere-France, Sedex75). Following cross-filtration, 5 µL sample was injected on an Aminex HPX-87P column (8% cross-linked resin, lead ionic, Bio-Rad) and separated at 70 °C with double-distilled water as mobile phase. Run parameters were set to a duration of 30 min, a flow rate of 0.4 mL/min and detection at 50 °C. Samples' RI signal was aligned with that of internal standard curves.

Yeast strains and culture conditions

Yeast strains *Cutaneotrichosporon oleaginosus* (ATCC 20509), *Cryptococcus curvatus* (CBS 5324) and *Rhodosporidium toruloides* (NP11) were maintained on yeast peptone dextrose (YPD) agar (20 g/L peptone, 10 g/L yeast extract, 20 g/L glucose, 20 g/L agar) at 4 °C for short-term storage. Minimal nitrogen media (MNM) (30 g/L glucose, 1.5 g/L yeast extract, 0.5 g/L NH_4Cl, 7.0 g/L KH_2PO_4, 5.0 g/L $Na_2HPO_4{\cdot}12H_2O$, 1.5 g/L $MgSO_4{\cdot}7H_2O$, 0.08 g/L $FeCl_3{\cdot}6H_2O$, 0.01 g/L $ZnSO_4{\cdot}7H_2O$, 0.1 g/L $CaCl_2{\cdot}2H_2O$, 0.1 mg/L $MnSO_4{\cdot}5H_2O$, 0.1 mg/L $CuSO_4{\cdot}5H_2O$, 0.1 mg/L $Co(NO_3)_2{\cdot}6H_2O$; pH 5.5) was adopted from Suutari et al. for induction of lipogenesis [42].

Following pre-culturing in YPD broth for 24 h, yeast cells were centrifuged, washed with PBS buffer (8 g/L NaCl, 0.2 g/L KCl, 1.44 g/L Na_2HPO_4, 0.24 g/L KH_2PO_4; pH 7.4) and inoculated in 250 mL baffled flasks, containing 50 mL of MNM, at an initial seeding OD_{600} of 0.5. Incubation lasted for 4 days in a rotary shaker at 120 rpm and 28 °C. To evaluate the capability of utilizing hydrolysates for yeast growth and lipid accumulation, the selected oleaginous strains were cultured solely on SH lacking any additives or carbon supplementation. Biological cultures of the oleaginous yeasts were carried out in triplicates.

Nile red staining

Samples were analyzed in technical triplicates using a modified protocol from Sitepu et al. [43]. Briefly, 225 µL of each yeast culture was transferred to a 96-well black microtiter plate. Serial dilutions were performed in triplicates to ensure an optical density < 1 before 50 µl DMSO was added to each well. Initial absorbance readings were taken at 600 nm and for growth monitoring and correction of fluorescence readings for growth variation. A volume of 25 µL Nile red was then added to each well (final concentration of 50 µg/mL). Fluorescence measurements (recorded before and after Nile red addition) at excitation at 530/25 nm; emission at 590/35 nm; and kinetic reading for 5 min with 30 s interval were taken. Maximal emission values were determined and fluorescence measurements were corrected for variation in cell density by dividing the fluorescence unit by background optical density OD_{600} values.

Gravimetric analysis

Technical triplicates of the total lipid content of the oleaginous yeasts were determined by a modified method by Folch et al. [40]. Briefly, 15 mL of yeast cultures were washed and homogenized using an Avestin Emulsiflex at a sample port pressure of 1200 bar and a chamber pressure of 8 bar. Lipids from the homogenate were extracted with 6 mL of Folch solution (2:1 chloroform: methanol). Lipid extraction continued overnight at room temperature and shaking speed of 120 rpm. Subsequently, 1.2 mL of 0.9% NaCl were added to aid phase separation. The lower phase was aspirated using a syringe and added to pre-weighed glass vessels. The chloroform was fully evaporated under a nitrogen stream and glass vials were weighed again. The extracted lipid samples were used to calculate lipid content as total lipid weight and as percent of dry yeast weight.

Dry biomass determination

A volume of 2 mL of each yeast culture was transferred in triplicates to pre-weighed 2 mL Eppendorf tubes. The tubes were weighed again the following centrifugation at 14,000 g for 5 min, washing and drying at 60 °C overnight. Measurements were recorded in triplicates by subtracting the weight of the sample tubes from their respective pre-weights.

Results

Algae biomass analysis

In this study, the biomass composition of *S. obtusiusculus* was determined (Table 1). This green algae displays high amounts of carbohydrates and crude proteins comprising 34% and 49% (g/g DCW) respectively. Other components encompassed water, lipids and ash measured at 3.7, 8.3 and 1.9% (g/g DCW), respectively. The acquired biomass data suggest that *S. obtusiusculus* can be quantitatively hydrolyzed by chemical and enzymatic systems to release monomeric pentose and hexose sugars, which could serve as a carbon source for microbial cultivation.

Hydrolysis of *S. obtusiusculus* dry biomass

Various commercial hydrolase enzyme mixtures were tested for their biomass liquefaction efficiencies including a cellulase mix (Cellic-Ctec2, Novozymes), a hemicellulose-mix (Cellic-Htec2, Novozymes), a pectinase mix (Pectinex, Novozymes), and an amylase mix (Fungamyl, Novozymes). Biomass to glucose conversion ratios from the various enzyme mixtures is presented in Fig. 1a. The cellulase mix (Cellic CTec 2) exhibited the best activity. Glucose monomerization reached a saturation level between 12 and 14 g/L starting from a 50 g algae biomass, which translates to a glucose yield of 0.24-0.28 g/g of DCW. Furthermore, a 1% (v/v) of cellulase mixture Cellic-Ctec2 was combined with varying concentrations of the remaining enzyme mixtures, none of which yielded a significantly better conversion ratio (Fig. 1b).

Table 1 Biochemical composition of *S. obtusiusculus*, calculated as percent of total dry weight

Biomass component	Content % % (g/g dry biomass weight)
Water	3.7
Carbohydrates	33.8
Proteins	48.7
Lipids	8.3
Pigments, secondary metabolites	3.6
Ash	1.9

Relative standard deviation for all given numbers is ≤ ± 2%

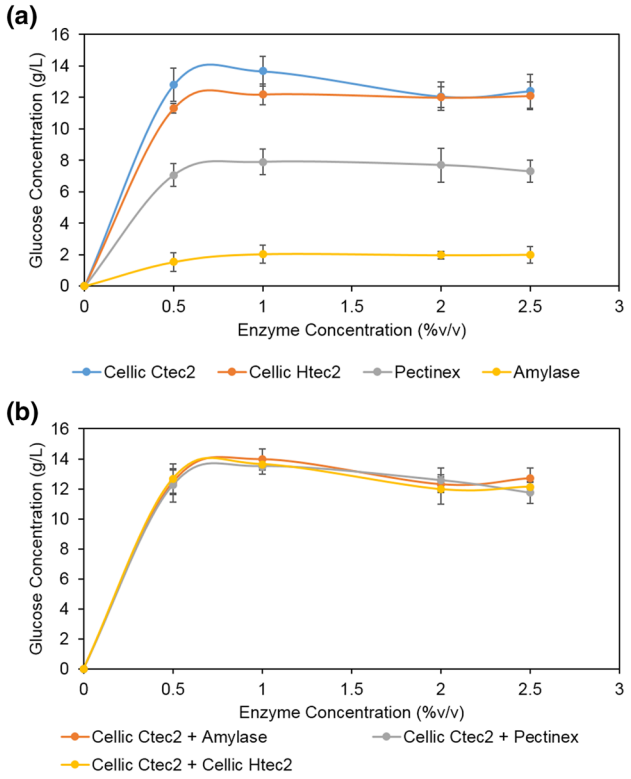

Fig. 1 Glucose concentration of SH displayed as a factor of various enzymes mixes and concentrations (**a**). Glucose concentration of SH displayed as a factor of the combination of enzyme mixtures with Cellic CTec 2 (**b**)

To assess the efficiency of glucose liberation from the algae biomass, measurements of enzymatic hydrolysis were compared with those of acidic hydrolysis. Table 2 confirms that glucose conversion efficiencies reached (90–100%), with glucose constituting up to two-thirds (g/g of DCW) of the total carbohydrate content of SH.

The combined enzymatic conversion rate of mannose and galactose, which were not distinguished by HPLC, was limited to only 20–25% (g/g DCW).

However, total sugar concentration in the hydrolysate was still relatively low (12–14 g/L glucose) given a carbohydrate content of 34% (g/g DCW). Accordingly, hydrolysis was repeated with higher amounts of biomass retaining a 1% (v/v) concentration of the cellulase mixture. As a result, glucose concentration in SH reached 48 g/L starting with a 200 g *Scenedesmus* dry biomass. This accounts fora glucose yield of 0.24 g/g of DCW, maintaining the high conversion efficiencies of (90–100%). Subsequent experiments were conducted with SH comprising this high glucose concentration (48 g/L).

Table 2 A comparison of monosaccharide content % (g/g dry biomass weight) resulting from acidic and enzymatic hydrolysis

Sugar	Acidic hydrolysis % (g/g dry biomass weight)	Enzymatic hydrolysis % (g/g dry biomass weight)	Conversion Efficiency (%)
Glucose	22	20–22	90–100
Mannose		–	–
Galactose	10	2–2.5	20–25
Rhamnose	~1	0	0
Fucose	~1	0	0
Ribose	~1	0	0

Relative standard deviation for all given numbers is ≤ ± 2%

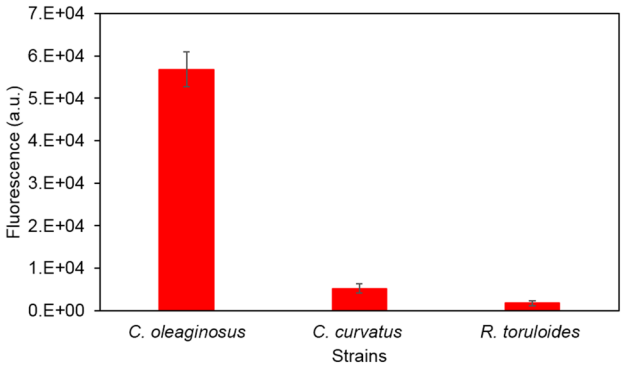

Fig. 2 Rapid estimation of lipid contents in *C. oleaginosus*, *C. curvatus* and *R. toruloides* following 4 days cultivation on SH, determined by Nile red assay

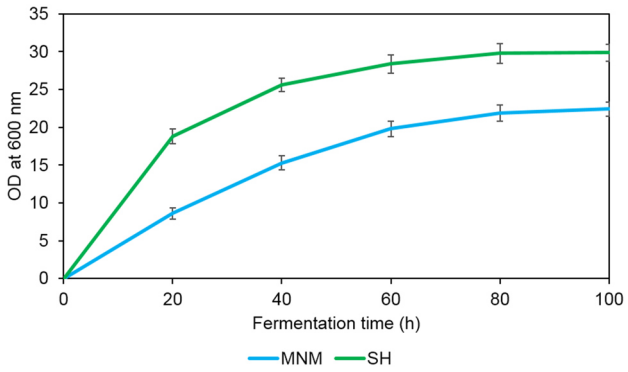

Fig. 3 *C. oleaginous* growth trend when grown on MNM and SH over 4 days in a shake flask fermentation

Yeast growth and lipid production

High throughput Nile red screening was employed to determine the lipid yield of three oleaginous yeast strains *C. oleaginosus*, *C. curvatus* and *R. toruloides*. Following a 4-day fermentative growth on SH as the sole carbon source, Nile red analysis revealed low lipid content in *C. curvatus* and *R. toruloides*. Contrarily, *C. oleaginosus* was able to accumulate a considerable amount of lipid bodies when cultivated on the same media (Fig. 2).

Thus, *C. oleaginosus* underwent subsequent experiments to determine growth rate and lipid absolute quantitation when cultivated on MNM and SH. To evaluate *C. oleaginosus* growth-rate in MNM and SH media, optical density at 600 nm was measured over 4 days (Fig. 3). SH media resulted in highest final growth for *C. oleaginosus* measured at OD_{600} of about 30, compared to OD_{600} of about 22 in MNM.

Gravimetric analysis was performed to determine total lipid content in *C. oleaginosus* following fermentation on MNM and SH in shake flasks (Fig. 4). The yeast accumulated nearly 61% and 35% (g lipid/g DCW) lipids when grown on MNM and SH, respectively. After 4 days fermentation, lipid yield in *C. oleaginosus* reached about 5.3 g/L of culture when cultivated on MNM, and 3.6 g/L of culture when cultivated on SH media.

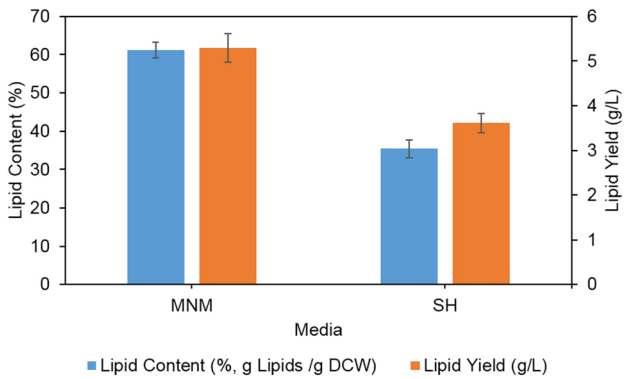

Fig. 4 Lipid content (%, g lipid/g DCW) and lipid yield (g/L) of *C. oleaginous* cultivated in MNM and SH media for 4 days in shake flask fermentation

Discussion

For years, microalgae have been exploited as a source for value-added products, with numerous commercial applications that include enhancing the nutritional value of food and animal feed, as well as being incorporated into cosmetics [44]. The significant properties of microalgae biomass as raw material for microbial cultivation include high carbohydrates contents and lack of recalcitrant lignin [45]. The use of microbes as a platform for lipid and subsequent biofuel and biodiesel production offers: (1) renewability and potential sustainability, (2) requires less labor and fewer raw materials, (3) is easier to scale up, (4) does not compete with edible-plants for land, (5) generates less waste and (6) is not affected by season or climate [46]. Recently, the valorization of seagrass and brown macroalgae biomass as feedstock for *C. oleaginosus* lipid production, in addition to the techno-economic feasibility of the bioprocesses have been conducted in our group [2, 4]. In this study, *S. obtusiusculus* biomass was chosen as feedstock for oily yeast growth, due to its high carbohydrates content 34% (g/g dry biomass weight). In comparison, *Scenedesmus obliquus*, *Chlorella vulgaris*, *Chlamydomonas rheinhardii*, and *Dunaliella salina* algae species exhibit sugar content per dry biomass weight of 10%, 12%, 17% and 32% respectively [44].

Complete chemical hydrolysis (H_2SO_4) have been regularly implemented for the production of hydrolysate from lignocellulosic biomass [47, 48]. Lately, two-stage hydrolysis processes starting with mild chemical treatment (dilute sulfuric acid) and followed by enzymatic hydrolysis have gained popularity amongst industrial applications [49]. Corn-stover biomass hydrolysis required a pretreatment of the biomass with 0.5 M NaOH at 80 °C for 75 min [50]. However, these methods often generate inhibitory substances that might hinder or completely abolish the growth of microorganisms cultivated in the resulting hydrolysates. Furfural was found to elongate the lag-phase; while benzoic acid reduced growth rate and biomass yield [51]. Thus, complex detoxification step would be necessary prior to the fermentation, ensuing additional costs and tarnishing the eco-friendly aspect of the biofuel production process [36]. Accordingly, we opted to use a single-step enzymatic approach in this study that would allow efficient hydrolysis of algae biomass without the need for any pretreatment steps. Sterilization of *S. obtusiusculus* biomass was performed in a laboratory-scale autoclave at 120 °C for 15 min to eliminate the microbial contaminants present within the microalgae residue. This not considered as a pretreatment step since hydrolysis of hemicellulose and cellulose only starts at temperatures greater than 150 °C [37]. Efficient saccharification of *S. obtusiusculus* biomass by single-step enzymatic hydrolysis using a cellulase mix was possible. In fact, the Cellic CTec 2 combines a number of different enzymatic activities (exo-, endo-glucanase activity and proteinase activity). The optimal activity was obtained at an industrially relevant concentration of 1% (v/v) at 50.0 °C and pH 5.0 in 50 mM, sodium acetate buffer for 72 h. Quantitative biomass to glucose conversion ratio remained high, even when raising substrate amounts up to 200 g/L. Beyond this point, viscosity was too high for effective hydrolysis. Notably, the diverse heteropolymeric structure of algal cell wall might account for the low conversion efficiency of mannose and galactose [52]. Commonly available enzyme mixtures including Celli-Htec2 (Novozymes), Pectinex (Novozymes) and Fungamyl (Novozymes) failed to liberate total monosaccharides from these structures.

Lipid accumulation in oleaginous yeasts is usually triggered upon excess carbon and nutrient deficiency (e.g., nitrogen phosphate or sulfur). Lipid yields and fatty acid profile vary depending on the type and concentration of the carbon and nitrogen source [1, 7, 53]. Single-step enzymatic hydrolysis generated glucose-rich hydrolysate, the preferred monomeric sugar for microbial fermentation. A 10 KDa cross-filtration was subsequently implemented, and the permeate product (SH), exhibiting now nitrogen limitation and high C/N ratio, was used as fermentation media for high lipid accumulation in yeast.

The oleaginous yeast *Cutaneotrichosporon oleaginous* is able to metabolize a broad monosaccharide spectrum including hexoses and pentoses into intracellular TAGs [23]. This yeast was also able to grow well in a model medium with a carbohydrate mixture that resembled a typical microalgae derived-hydrolysate [54]. In this work, *C. oleaginosus*, as well as *C. curvatus* and *R. toruloides* were cultivated in *S. obtusiusculus* hydrolysate. Most interestingly, in contrast to the other two oleaginous yeasts, high-throughput Nile red analysis indicated that only *C. oleaginosus* was able to accumulate significant amounts of intracellular lipids when grown in SH.

Without any nutritional addition to the hydrolysate (biotin, yeast extract, pure glucose…), SH was utilized as the sole carbon source for lipid production in *C. oleaginosus.* The assessment was conducted on the basis of lipid accumulation. The results were evaluated along with the data from cultivation in the synthetic MNM—a medium known to induce lipid biosynthesis in oleaginous yeasts [55]. *C. oleaginosus* grew faster in SH media, in comparison with MNM. The yeast yielded 61% (g lipid/g DCW) of intracellular lipid when grown on MNM, and about 35% (g lipid/g DCW) when grown on SH. Following fermentation, *C. oleaginosus* achieved total lipid yield of 3.6 g/L when cultivated on SH media. In scaled-up experiments, SH

would prove a cost-effective alternative for the relatively expensive synthetic MNM media.

To establish nutrient limitation, the microalgae hydrolysate underwent ultrafiltration thus eliminating proteins and peptides and establishing a high C/N ratio. However, other factors besides nitrogen-limitation could induce lipogenesis in *C. oleaginosus*. Effect of phosphate and sulfur limitation on lipid accumulation in oleaginous yeasts have been previously reported [56]. High C/P ratio prompted high lipid yield in *R. toruloides* even in the presence of excess nitrogen [22]. For future work, soluble phosphates could be precipitated and removed by interaction with metal ions, such as Ca^{2+}, Mg^{2+}, or Fe^{3+} [57], and the resulting hydrolysate—now exhibiting high C/N and C/P ratios—could allow for even higher for lipid accumulation by *C. oleaginosus.*

Cutaneotrichosporon oleaginosus cultivated in *S. obtusiusculus* hydrolysate achieved a high growth rate and accumulated substantial amount of intracellular lipids. Previous research showed that this yeast accumulates lipid in the form of triacylglycerides, with a fatty acid (FA) profile consisting mainly of C16 and C18 FA [58]. Palmitic acid, stearic acid and oleic acid constitute the major raw material for downstream processing and subsequent conversion into green biofuels [59]. Furthermore, chemo-catalytic conversion of lipids produced by *C. oleaginosus* into biodiesel was achieved with a 98.9% w/w recovery [9]. The physical properties of resulting B20 - comparable to Soybean B20 - meet the ASTM requirements [9]. This FA profile makes SCOs from *C. oleaginosus* a suitable alternative for plant and vegetable oils.

Conclusion

This study demonstrated that *Scenedesmus obtusiusculus* biomass could be valorized as a substrate for microbial lipid production. A single-step enzymatic hydrolysis was implemented that efficiently released monomeric sugars from the biomass without the need for any pretreatment. This approach alleviated the need for detoxification steps, reduced upstream processing costs and maintained the eco-friendly aspect of biofuel production. The oleaginous yeast *C. oleaginosus* was able to grow fast and accumulate 3.6 g/L of lipids when cultivated on the microalgae hydrolysate, and the resulting microbial oil could be converted to high-grade biodiesel. Microalgae biomass offer value-added biofuel yield potential as compared to terrestrial plantation; biomass-to-fuel conversion processes are improved by necessitating no agricultural land, alleviating direct competition with food security and requiring low water and resource demand. Furthermore, the integration of yeast and algae species in a single SCO platform towards "zero concepts" with respect to emission and excess resources has recently been reported. In one study, the oleaginous microalgae *Phaeodactylum tricornutum* was supplemented with CO_2 supplied from the oleaginous yeast *C. curvatus* in a co-fermentation approach [32]. In another study focused on the holistic valorization of unexploited marine biomass, a waste-free, microbial oil-centered cyclic bio-refinery approach integrated the production of yeast lipids and animal feed with precious metal biosorbents [4]. In that respect, the algal effluent resulting from the ultra-filtration of the algae hydrolysate should be further characterized and profiled for possible added-value in the process described in this study.

Acknowledgement Open Access funding provided by Projekt DEAL. The authors acknowledge Prof. Dr. Sabine Mundt for providing *Scenedesmus obtusiusculus* (A189) residues. TB gratefully acknowledges funding of the Werner Siemens foundation for establishing the research field of Synthetic Biotechnology at the Technical University of Munich. This work was supported by the BMBF (German Federal Ministry of Education and Research, 03SF0446A). SY, DA and NM gratefully acknowledge funding by the Bavarian State Ministry for Environmental and Consumer affairs for funding of the project Resource-efficient PHB production processes within the project consortium BayBioTech (TP7, TLK01U-69045, http://www.baybiotech.de/startseite/). The authors gratefully acknowledge HPLC sample analysis conducted by Ms. Martina Haack.

Author contributions Conceptualization of the study was conducted jointly by FB, NM, and TB. The methodological approach was designed and carried out by FB and NM. Data validation was jointly carried out by SY, DA and NM. SY and DA prepared the original draft of the manuscript. The manuscript was jointly finalized by all authors.

Data availability All datasets generated for this study are included in the manuscript.

Compliance with ethical standards

Conflict of interest statement The authors declare that the research was conducted in the absence of any commercial or financial relationships that could be construed as a potential conflict of interest.

References

1. Awad D, Bohnen F, Mehlmer N, Brueck T (2019) Multi-factorial-guided media optimization for enhanced biomass and lipid

formation by the oleaginous yeast *Cutaneotrichosporon oleaginosus*. Front Bioeng Biotechnol 7:54
2. Masri MA, Younes S, Haack M, Qoura F, Mehlmer N, Brück T (2018) A seagrass-based biorefinery for generation of single-cell oils for biofuel and oleochemical production. Energy Technol 6(6):1026–1038
3. Knothe G (2008) "Designer" biodiesel: optimizing fatty ester composition to improve fuel properties. Energy Fuels 22(2):1358–1364
4. Masri MA, Jurkowski W, Shaigani P, Haack M, Mehlmer N, Brück T (2018) A waste-free, microbial oil centered cyclic bio-refinery approach based on flexible macroalgae biomass. Appl Energy 224:1–12
5. Smith VH, Sturm BS, Billings SA (2010) The ecology of algal biodiesel production. Trends Ecol Evol 25(5):301–309
6. Kyle DJ (2010) Future development of single cell oils. Single cell oils. Elsevier, New York, pp 439–451
7. Ratledge C, Wynn JP (2002) The biochemistry and molecular biology of lipid accumulation in oleaginous microorganisms. Adv Appl Microbiol 51:1–52
8. Bracharz F, Beukhout T, Mehlmer N, Bruck T (2017) Opportunities and challenges in the development of Cutaneotrichosporon oleaginosus ATCC 20509 as a new cell factory for custom tailored microbial oils. Microb Cell Fact 16(1):178. https://doi.org/10.1186/s12934-017-0791-9
9. McCurdy AT, Higham AJ, Morgan MR, Quinn JC, Seefeldt LC (2014) Two-step process for production of biodiesel blends from oleaginous yeast and microalgae. Fuel 137:269–276
10. Coradetti ST, Pinel D, Geiselman GM, Ito M, Mondo SJ, Reilly MC, Cheng Y-F, Bauer S, Grigoriev IV, Gladden JM, Simmons BA, Brem RB, Arkin AP, Skerker JM (2018) Functional genomics of lipid metabolism in the oleaginous yeast Rhodosporidium toruloides. eLife 7:e32110. https://doi.org/10.7554/elife.32110
11. Kosa M, Ragauskas AJ (2011) Lipids from heterotrophic microbes: advances in metabolism research. Trends Biotechnol 29(2):53–61
12. Meng X, Yang J, Xu X, Zhang L, Nie Q, Xian M (2009) Biodiesel production from oleaginous microorganisms. Renew Energy 34(1):1–5
13. Rakicka M, Lazar Z, Dulermo T, Fickers P, Nicaud JM (2015) Lipid production by the oleaginous yeast Yarrowia lipolytica using industrial by-products under different culture conditions. Biotechnol Biofuels 8:104. https://doi.org/10.1186/s13068-015-0286-z
14. Azambuja SPH, Bonturi N, Miranda EA, Gombert AK (2018) Physiology and lipid accumulation capacity of different *Yarrowia lipolytica* and *Rhodosporidium toruloides* strains on glycerol. bioRxiv. https://doi.org/10.1101/278523
15. Rakicka M, Lazar Z, Dulermo T, Fickers P, Nicaud JM (2015) Lipid production by the oleaginous yeast Yarrowia lipolytica using industrial by-products under different culture conditions. Biotechnol Biofuels 8(1):104
16. Wang R, Wang J, Xu R, Fang Z, Liu A (2014) Oil production by the oleaginous yeast *Lipomyces starkeyi* using diverse carbon sources. BioResources 9(4):7027–7040
17. Moon NJ, Hammond E, Glatz BA (1978) Conversion of cheese whey and whey permeate to oil and single-cell protein1. J Dairy Sci 61(11):1537–1547
18. Evans CT, Ratledge C (1983) A comparison of the oleaginous yeast, *Candida curvata*, grown on different carbon sources in continuous and batch culture. Lipids 18(9):623–629
19. Liang Y, Jarosz K, Wardlow AT, Zhang J, Cui Y (2014) Lipid production by *Cryptococcus curvatus* on hydrolysates derived from corn fiber and sweet sorghum bagasse following dilute acid pretreatment. Appl Biochem Biotechnol 173(8):2086–2098
20. Chi Z, Ahring BK, Chen S (2012) Oleaginous yeast *Cryptococcus curvatus* for biofuel production: ammonia's effect. Biomass Bioenerg 37:114–121
21. Iassonova DR (2009) Lipid synthesis and encapsulation by *Cryptococcus curvatus*. Iowa State University, Ames
22. Wu S, Hu C, Zhao X, Zhao ZK (2010) Production of lipid from *N*-acetylglucosamine by *Cryptococcus curvatus*. Eur J Lipid Sci Technol 112(7):727–733
23. Gujjari P, Suh S-O, Coumes K, Zhou JJ (2011) Characterization of oleaginous yeasts revealed two novel species: trichosporon *Cacaoliposimilis* sp. nov. and *Trichosporon oleaginosus* sp. nov. Mycologia 103(5):1110–1118
24. Masri MA, Garbe D, Mehlmer N, Brück TB (2019) A sustainable, high-performance process for the economic production of waste-free microbial oils that can replace plant-based equivalents. Energy Environ Sci 12(9):2717–2732
25. Ageitos JM, Vallejo JA, Veiga-Crespo P, Villa TG (2011) Oily yeasts as oleaginous cell factories. Appl Microbiol Biotechnol 90(4):1219–1227
26. Bai A, Popp J, Pető K, Szőke I, Harangi-Rákos M, Gabnai Z (2017) The significance of forests and algae in CO_2 balance: a hungarian case study. Sustainability 9(5):857
27. Bhola V, Swalaha F, Ranjith Kumar R, Singh M, Bux F (2014) Overview of the potential of microalgae for CO_2 sequestration. Int J Environ Sci Technol 11(7):2103–2118. https://doi.org/10.1007/s13762-013-0487-6
28. Sayre R (2010) Microalgae: the potential for carbon capture. Bioscience 60(9):722–727. https://doi.org/10.1525/bio.2010.60.9.9
29. Koutinas AA, Chatzifragkou A, Kopsahelis N, Papanikolaou S, Kookos IK (2014) Design and techno-economic evaluation of microbial oil production as a renewable resource for biodiesel and oleochemical production. Fuel 116:566–577
30. Guo M, Cheng S, Chen G, Chen J (2019) Improvement of lipid production in oleaginous yeast *Rhodosporidium toruloides* by ultraviolet mutagenesis. Eng Life Sci 19(8):548–556
31. André A, Chatzifragkou A, Diamantopoulou P, Sarris D, Philippoussis A, Galiotou-Panayotou M, Komaitis M, Papanikolaou S (2009) Biotechnological conversions of bio-diesel-derived crude glycerol by Yarrowia lipolytica strains. Eng Life Sci 9(6):468–478
32. Dillschneider R, Schulze I, Neumann A, Posten C, Syldatk C (2014) Combination of algae and yeast fermentation for an integrated process to produce single cell oils. Appl Microbiol Biotechnol 98(18):7793–7802. https://doi.org/10.1007/s00253-014-5867-4
33. Achinas S, Achinas V, Euverink GJW (2017) A technological overview of biogas production from biowaste. Engineering 3(3):299–307. https://doi.org/10.1016/J.ENG.2017.03.002
34. Htet AN, Noguchi M, Ninomiya K, Tsuge Y, Kuroda K, Kajita S, Masai E, Katayama Y, Shikinaka K, Otsuka Y, Nakamura M, Honda R, Takahashi K (2018) Application of microalgae hydrolysate as a fermentation medium for microbial production of 2-pyrone 4,6-dicarboxylic acid. J Biosci Bioeng 125(6):717–722. https://doi.org/10.1016/j.jbiosc.2017.12.026
35. Wirth R, Lakatos G, Böjti T, Maróti G, Bagi Z, Kis M, Kovács A, Ács N, Rákhely G, Kovács KL (2015) Metagenome changes in the mesophilic biogas-producing community during fermentation of the green alga *Scenedesmus obliquus*. J Biotechnol 215:52–61
36. Huang H, Guo X, Li D, Liu M, Wu J, Ren H (2011) Identification of crucial yeast inhibitors in bio-ethanol and improvement of fermentation at high pH and high total solids. Bioresour Technol 102(16):7486–7493
37. Silveira MHL, Morais ARC, da Costa Lopes AM, Olekszyszen DN, Bogel-Łukasik R, Andreaus J, Pereira Ramos L (2015) Current pretreatment technologies for the development of cellulosic ethanol and biorefineries. Chemsuschem 8(20):3366–3390

38. Shetlar M, Masters YF (1957) Use of thymol-sulfuric acid reaction for determination of carbohydrates in biological material. Anal Chem 29(3):402–405
39. Kjeldhal J (1883) A new method for estimation of nitrogen in organic compounds. Z Anal Chem 22:366
40. Folch J, Lees M, Sloane-Stanley G (1957) A simple method for the isolation and purification of total lipids from animal tissues. J Biol Chem 226(1):497–509
41. Chemists AoOA (1990) Official methods of analysis: changes in official methods of analysis made at the annual meeting. Supplement, vol 15. Association of Official Analytical Chemists,
42. Suutari T, Priha P, Laakso S (1993) Temprature shifts in regulation of lipids accumulated by *Lippmyces starkeyi*, p. 891–894
43. Sitepu I, Ignatia L, Franz A, Wong D, Faulina S, Tsui M, Kanti A, Boundy-Mills K (2012) An improved high-throughput Nile red fluorescence assay for estimating intracellular lipids in a variety of yeast species. J Microbiol Methods 91(2):321–328
44. Spolaore P, Joannis-Cassan C, Duran E, Isambert A (2006) Commercial applications of microalgae. J Biosci Bioeng 101(2):87–96
45. Posten C (2009) Design principles of photo-bioreactors for cultivation of microalgae. Eng Life Sci 9(3):165–177
46. Li Q, Du W, Liu D (2008) Perspectives of microbial oils for biodiesel production. Appl Microbiol Biotechnol 80(5):749–756
47. Morales-delaRosa S, Campos-Martin JM, Fierro JL (2014) Optimization of the process of chemical hydrolysis of cellulose to glucose. Cellulose 21(4):2397–2407
48. Tsigie YA, Wang C-Y, Kasim NS, Diem Q-D, Huynh L-H, Ho Q-P, Truong C-T, Ju Y-H (2012) Oil production from *Yarrowia lipolytica* Po1g using rice bran hydrolysate. BioMed Research International, Lonon
49. Zhang Y, Zhang M, Reese RA, Zhang H, Xu B (2016) Real-time single molecular study of a pretreated cellulose hydrolysis mode and individual enzyme movement. Biotechnol Biofuels 9(1):85
50. Gong Z, Shen H, Yang X, Wang Q, Xie H, Zhao ZK (2014) Lipid production from corn stover by the oleaginous yeast *Cryptococcus curvatus*. Biotechnol Biofuels 7(1):158
51. Zha Y, Muilwijk B, Coulier L, Punt PJ (2012) Inhibitory compounds in lignocellulosic biomass hydrolysates during hydrolysate fermentation processes. J Bioprocess Biotechniq 2(1):112–122
52. Takeda H (1988) Classification of Chlorella strains by cell wall sugar composition. Phytochemistry 27(12):3823–3826
53. Granger LM, Perlot P, Goma G, Pareilleux A (1993) Efficiency of fatty acid synthesis by oleaginous yeasts: prediction of yield and fatty acid cell content from consumed C/N ratio by a simple method. Biotechnol Bioeng 42(10):1151–1156
54. Meo A, Priebe XL, Weuster-Botz D (2017) Lipid production with Trichosporon oleaginosus in a membrane bioreactor using microalgae hydrolysate. J Biotechnol 241:1–10
55. L-j MA, H-m WANG, Y-f WEN, H-l JIANG, D-h XUE (2008) Optimized culture medium and fermentation conditions for lipid production with filamentous fungus. J Changchun Univ Technol 4:023
56. Zhang G, French WT, Re Hernandez, Hall J, Sparks D, Holmes WE (2011) Microbial lipid production as biodiesel feedstock from *N*-acetylglucosamine by oleaginous microorganisms. J Chem Technol Biotechnol 86(5):642–650
57. Jenkins D, Ferguson JF, Menar AB (1971) Chemical processes for phosphate removal. Water Res 5(7):369–389
58. Kourist R, Bracharz F, Lorenzen J, Kracht ON, Chovatia M, Daum C, Deshpande S, Lipzen A, Nolan M, Ohm RA (2015) Genomics and transcriptomics analyses of the oil-accumulating basidiomycete yeast Trichosporon oleaginosus: insights into substrate utilization and alternative evolutionary trajectories of fungal mating systems. MBio 6(4):e00918–e01015
59. Zhao C, Brück T, Lercher JA (2013) Catalytic deoxygenation of microalgae oil to green hydrocarbons. Green Chem 15(7):1720–1739

3.3 Systems Biology Engineering of the Pantothenate Pathway to Enhance 3HB Productivity in *Escherichia coli*

Samer Younes, Dania Awad, Elias Kassab, Martina Haack, Claudia Schuler, Norbert Mehlmer & Thomas Brueck

Published in: Biotechnology and Bioprocess Engineering

Editor-in-Chief: Jong Won Yun, Sang Yup Lee

Date of Publication: 09 September 2021

DOI: 10.1007/s12257-021-0033-1

3.3.1 Author Contributions

Conceptualization of the study and design of the methodological approach was jointly designed by all authors. Planning and execution of experiments was carried out by the author of this thesis, Samer Younes. Data validation was jointly carried out by all authors. Samer Younes and Dania Awad prepared the original draft of the manuscript, which was jointly finalized and reviewed by all authors.

3.3.2 Summary III

Sustainable production of high-value chemicals via biological processes has recently received considerable attention. 3-hydroxybutyrate (3HB) is the monomeric unit of polyhydroxybutyrate (PHB), a polyester that is naturally produced by several non-conventional microorganisms such as *Halomonas boliviensisis*, *Ralstonia eutropha*, and *Bacillus megaterium* [130]. PHB, by its very nature, is a bio-derived, biocompatible, and biodegradable polymer. The monomer 3HB is an interesting molecule since it contains a chiral center and two active functional groups that can be easily modified: a hydroxyl group and a carboxyl group. This allows it to be used as precursor in the synthesis of fine chemicals, polymers, and pharmaceuticals such as antibiotics and vitamins [131].

3HB can be produced via several routes: (a) chemical synthesis, (b) chemical hydrolysis of PHB, (c) enzymatic hydrolysis of PHB (in vitro and in vivo) or (d) metabolically engineered microorganisms (e.g. *Escherichia coli*). Among these methods, recombinant production is the most coveted because it is a one-step process and bypasses the use of non-environmentally friendly organic solvents [132]. An often-employed pathway for 3HB production in recombinant E. coli consists of three-steps: (1) condensation of two acetyl-CoA molecules to acetoacetyl-CoA, (2) reduction of acetoacetyl-CoA to 3-hydroxybutyrate-CoA, and (3) hydrolysis of 3-hydroxybutyrate-CoA to 3-hydroxybutyrate by thioesterase [133]. A major drawback for microbial-derived 3HB/PHB is the high production costs compared to chemically synthesized 3HB and petroleum-derived plastics [133]. Hence, any significant improvement in space-time yields of the product is essential for industrial deployment and commercialization of this technology.

The central metabolite in the 3HB production pathway is acetyl-CoA, the derivative of coenzyme A (CoA). Enriching the intracellular pool of these cofactors could improve 3HB titers [134]. In this study, increasing CoA titers, and subsequently 3HB titers, was attempted by upregulating pantothenate kinase (PanK), the rate limiting step in CoA biosynthetic pathway [114]. To this end, 4 PanKs genes of different taxonomic origins (mammalian, fungal and bacterial) were individually expressed and evaluated in 3HB producing *E. coli* BL 21cells. The design employed a 2-plasmid system: (1) the low-copy plasmid pJBGT3RX harboring β-ketothiolase (t3), an acetoacetyl-CoA reductase (rx) and

chloramphenicol resistance genes allowed the production of 3HB; and (2) plasmid pET28a harboring kanamycin resistance gene and one of four Panks genes (*E. coli* PankI, *Aspergillus nidulans* PankII, *Mus musculus* PanK1β or *Bacillus subtilis* PankII). To the best of our knowledge, this constitutes the first report on the expression of the murine PanK1β in an *E. coli* host system. In shake flask studies, and under nitrogen limitation, strains expressing *A. nidulans* PankII and *M. musculus* PanK1β achieved the highest 3HB titers. In a 1.3L bioreactor fermentation, the strain harboring murine PanK1β resulted in 7.6 $g.L^{-1}$ compared to 5.4 $g.L^{-1}$ of 3HB in the control strain, constituting a 41 % increase.

Although structurally different from the bacterial PankI, our study showed that eukaryotic Panks can supplement the kinase activity in prokaryotes. Expressing the exogenous PanKs offer several advantages over the host's enzyme; PanKII is only inhibited by acetyl-CoA, for which the 3HB-production system would provide a constant metabolic sink [135]. Additionally, PanK1β is weakly regulated by acetyl-CoA, and its activity is stimulated by free CoA [136]. Overexpressing eukaryotic PanKs constitutes a suitable strategy for improving 3HB titers in *E. coli* and elevating the development of recombinant production platforms. Further enhancement of the titers could be achieved by integrating a one-plasmid system, adopting other nutrient-limitation (e.g. phosphate) modes, or carrying out high cell-density (2 stage) fermentations [133].

Biotechnology and Bioprocess Engineering 26: 621-629 (2021)
DOI 10.1007/s12257-021-0033-1

pISSN 1226-8372
eISSN 1976-3816

RESEARCH PAPER

Systems Biology Engineering of the Pantothenate Pathway to Enhance 3HB Productivity in *Escherichia coli*

Samer Younes, Dania Awad, Elias Kassab, Martina Haack, Claudia Schuler, Norbert Mehlmer, and Thomas Brueck

Received: 23 February 2021 / Revised: 6 June 2021 / Accepted: 7 June 2021

Abstract The monomer, 3-hydroxybutyrate (3HB), plays an interesting role as a precursor for antibiotics, vitamins, and bioplastics such as polyhydroxybutyrates (PHB). The biotechnological production of both compounds in *Escherichia coli* has seen increased interest in the last decade. The central metabolite in the 3HB production pathway is acetyl-CoA, the derivative of coenzyme A (CoA). Enriching the intracellular pool of these cofactors could improve 3HB titers. In our study, we opted to increase CoA titers by upregulating pantothenate kinase (PanK), the rate limiting step in CoA biosynthetic pathway. To this end, 4 PanKs genes of different taxonomic origins (mammalian, fungal, and bacterial) were individually expressed and evaluated in 3HB producing *E. coli* cells. In shake flask studies, strains expressing *Aspergillus nidulans* PankII and *Mus musculus* PanK1β achieved the highest 3HB titers. In a bioreactor fermentation, the strain harboring murine PanK1β resulted in 7.6 g/L compared to 5.4 g/L of 3HB in the control strain. Although structurally different from the bacterial PankI, our study showed that eukaryotic Panks can supplement the kinase activity in prokaryotes. Expressing the exogenous PanKs offer several advantages over the host's enzyme; PanKII is only inhibited by acetyl-CoA, for which the 3HB-production system would provide a constant metabolic sink. Additionally, PanK1β is weakly regulated by acetyl-CoA, and its activity is stimulated by free CoA. Overexpressing eukaryotic PanKs constitutes a suitable strategy for improving 3HB titers in *E. coli*.

Samer Younes†, Dania Awad†, Elias Kassab, Martina Haack, Claudia Schuler, Norbert Mehlmer, Thomas Brueck*
Werner Siemens-Chair of Synthetic Biotechnology, Department of Chemistry, Technical University of Munich (TUM), Garching 85748, Germany
Tel: +49-89-289-13250; Fax: +49-89-289-13255
E-mail: brueck@tum.de

†Both authors contributed equally to this work

Keywords: 3-hydroxybutyrate, pantothenate kinase, *Escherichia coli*, bioplastics, CoA, acetyl-CoA

1. Introduction

Dwindling fossil resources, escalating environmental pollution, and rapid climate change drives the search for alternatives to petroleum-based products [1,2]. Sustainable production of high-value chemicals via biological processes has recently received considerable attention [1-3]. β-hydroxybutyrate (3HB), the monomer of polyhydroxybutyrate (PHB), is a versatile chiral C4 molecule [4,5]. Both compounds are commercially valuable with applications in the chemical, plastic, food, and pharmaceutical industries [4-6]. PHB, by its very nature, is a bio-derived, biocompatible and biodegradable polymer. Possessing similar properties to various synthetic thermoplastics such as polypropylene, PHB is suitable for bioplastic production [7]. Several non-conventional microorganisms such as *Halomonas boliviensis*, *Ralstonia eutropha*, and *Bacillus megaterium* naturally produce PHB, where it serves as both a source of energy and as a carbon storage [5,8,9]. In the halophile *H. boliviensis*, three enzymes are involved in the metabolism of PHB: (1) acetoacetyl-CoA thiolase which catalyzes condensation of two acetyl-CoA molecules into acetoacetyl-CoA, (2) acetoacetyl-CoA reductase which reduces acetoacetyl-CoA to 3-hydroxybutyrate-CoA, and (3) PHB synthase which polymerizes this monomer into PHB [4]. Although *H. boliviensis* is capable of accumulating high PHB yield (80% g/g of the cell dry weight (CDW)), the fermentative growth conditions of this strain (*e.g.* high salt concentrations) can lead to corrosive damage in industrial stainless steel bioreactors [5,6]. Furthermore, the lack of genomic and transcriptomic data, and the halophile's

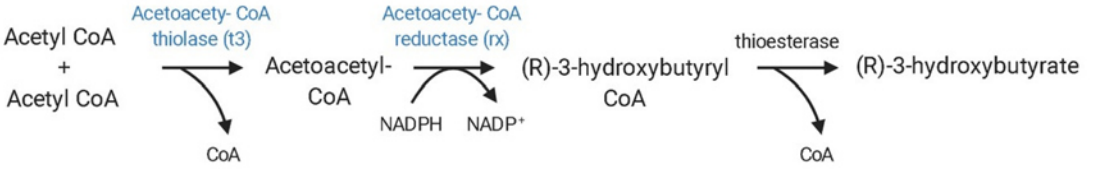

Fig. 1. Key steps of the recombinant production of 3HB in *Escherichia coli* [4].

protective mechanisms impede its genetic and metabolic manipulation [4,5]. Thus, a more suitable host for the production of PHB and its monomer (3HB) is desired.

The monomer 3HB serves as an intermediate in the synthesis of bioplastics, antibiotics, vitamins, and aromatic derivatives [3,6]. 3HB and its lactone derivative 3-hydroxybutyrolactone (3HBL) have been identified as high value-added chemicals from biomass in a report by the U.S. Department of Energy [10]. 3HB can be produced via several routes: (a) chemical synthesis, (b) chemical hydrolysis of PHB, (c) enzymatic hydrolysis of PHB (*in vitro* and *in vivo*) or (d) metabolically engineered microorganisms (*e.g. Escherichia coli*) [4,11-13]. Recombinant production of 3HB is mostly coveted since it is environmentally friendly, sustainable and yields enantiomerically pure product [3-5,8, 13]. 3HB has been successfully produced in *E. coli* via the heterologous expression of thiolase (t3) and reductase (rx) from *H. boliviensis*, save for the polymerization step (PHB synthase) (Fig. 1). Hydrolysis of 3-hydroxybutyryl-CoA to 3-hydroxybutyrate is achieved by native *E. coli* thioesterases [3-6,11,13]. Coupled with media and strain optimization, genetic manipulation of various precursors and pathways, in addition to scale up fermentation, recombinant production of 3HB in *E. coli* achieved titers between 4 and 16 g/L [3-6,11]. A major drawback for microbial-derived 3HB/PHB is the high production costs compared to chemically synthesized 3HB and petroleum-derived plastics. Hence, any significant improvement in space-time yields of the product is essential for industrial deployment and commercialization of this technology.

The central metabolite in the recombinant production of 3HB is acetyl-CoA [4,5]. Coenzyme A (CoA) and its thioester derivative acetyl-CoA are essential intermediates (cofactors) in numerous biosynthetic pathways and a wide variety of biochemical reactions, including the oxidation of fatty acids, carbohydrates, pyruvate, lactate, ketone bodies, and amino acids [14-17]. Although this molecule is a major precursor for various pathways, the heterologous expression of t3 and rx promote the flux of acetyl-CoA into 3HB biosynthesis [4,5]. In order to maximize 3HB yields, various studies opted for increasing the intracellular pool sizes of several cofactors such as NADH, NADPH, and ATP within microbial cells. Yet, no reports on the concurrent enhancement of intracellular CoA /acetyl-CoA pools with 3HB production are available [6,14].

The universal CoA biosynthetic pathway consists of five enzymatic steps (Fig. 2) [18]. Pantothenate kinase (PanK) catalyzes the first and rate-limiting step, where pantothenate (vitamin B5) is phosphorylated to 4'-phosphopantothenate [15-17,19]. Three distinct types of PanK have been characterized in various organisms. Encoded by the coaA gene, type I (PanK-I) is found exclusively in prokaryotes such as *E. coli* and *Staphylococcus aureus*. Eukaryotes, including yeast, fungi, plants, and mammals carry the second type (PanK-II). Mammalian cells express several isoforms of the second type, including Pank1α, present predominately in heart and skeletal muscles, and PanK1β

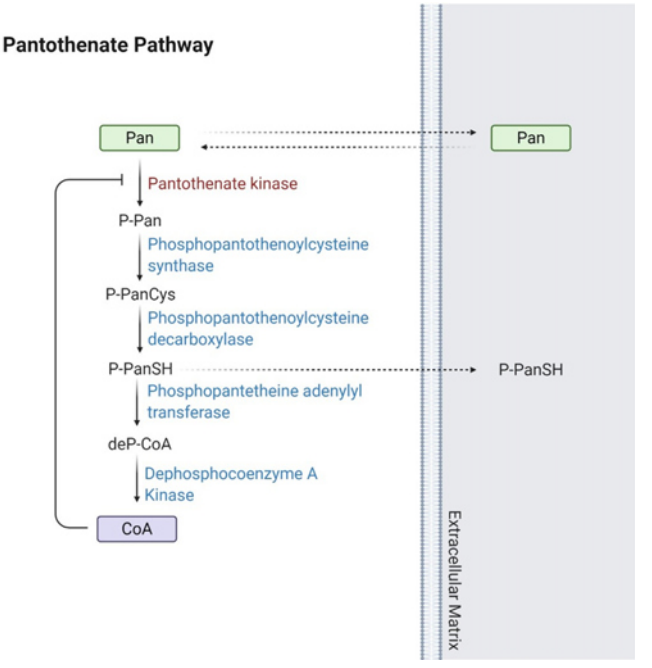

Fig. 2. The universal biosynthetic pathway of CoA. Vitamin B5 or Pantothenate (Pan) is first phosphorylated to 4'-phosphopantothenate (P-Pan) by pantothenate kinase. In prokaryotes, this enzyme is highly regulated by CoA. P-Pan is then condensed with cysteine into 4'-phosphopantothenoylcysteine (P-PanCys) and decarboxylated to form 4'-phosphopantetheine (P-PanSH). These two reactions are catalyzed by different domains of a bifunctional enzyme in prokaryotes, and by two distinct proteins in eukaryotes. P-PanSH is subsequently converted to dephospho-CoA (deP-CoA) which is ultimately phosphorylated to form CoA. These two reactions are catalyzed by two distinct enzymes in prokaryotes and plants but fused in a bifunctional enzyme in mammals [15,18].

detected primarily in the liver and kidneys, in addition to PanK2, PanK3, and PanK4 [19-22]. Although PanK type I and II do not possess high sequence similarity, they share common regulatory mechanisms based on feedback inhibition by CoA and/or acetyl-CoA [16,19]. Recently, a third type (PanK-III), encoded by CoaX, was identified in several pathogenic bacteria, including *Helicobacter pylori*, *Pseudomonas aeruginosa*, *Bordetella pertussis*, and *Mycobacterium tuberculosis* [23,24]. Moreover, some bacteria such as *Bacillus subtilis* have genes that code for both PanK-I and PanK-III. In contrast to the first two types, PanK-III exhibits distinct biochemical properties, including resistance to feedback inhibition by CoA and its thioesters [21,24-26]. Various studies attempted to relieve this feedback mechanism by co-overexpressing distinct PanK enzymes in recombinant host cells. The differential modulation of the various types (I, II, and III) resulted in specific increases (between 2-30 fold) of CoA/acetyl-CoA intracellular pools [14,16,19].

The aim of this work is to improve the production titers of 3HB in recombinant *E. coli* BL21, by increasing pools of its precursors: CoA and acetyl-CoA. Plasmid harboring the key enzymes t3 and rx was first introduced into the cells to allow for the production of 3HB. *E. coli* PankI, *Aspergillus nidulans* PankII, *Mus musculus* PanK1β (PANK II family), and *B. subtilis* PankIII were individually overexpressed in the production strain. Growth and 3HB titers were then assessed in shake flask experiments. Subsequently, the best 3HB producer strain was cultivated in a bioreactor with glucose (40 g/L) as the sole carbon source.

2. Materials and Methods

2.1. Strains and plasmids

E. coli strains and their corresponding plasmids utilized in this study are listed in Table 1. Cells were stored in glycerol stocks at -80°C and plasmids were stored at -20°C. The *E. coli* strain DH5α was used for all cloning and amplification procedures. *E. coli* BL21 (DE3) strain was used for expression and 3HB production.

For 3HB production, the low-copy plasmid pJBGT3RX harboring β-ketothiolase (t3), an acetoacetyl-CoA reductase (rx) and chloramphenicol resistance genes was transformed into *E. coli* BL21 cells. This plasmid was gratefully provided by Prof. Gen Larsson from KTH Royal Institute of Technology in Sweden. The 3HB producing strain is henceforth termed HB-1.

To increase the CoA/acetyl-CoA intracellular pool, plasmid pET28a (Novagen/Merk Millipore) was utilized to express the different pantothenate kinases in the production strain. This plasmid expresses kanamycin resistance gene. DNA sequences of *A. nidulans* PanKII (GenBank: AAD09811.1), *M. musculus* panK1β (GenBank: NP_076281.1) and *B. subtilis* panKIII (GenBank: WP_024713081.1) were obtained from NCBI database (https://www.ncbi.nlm.nih.gov). The mature sequences were codon optimized for expression in *E. coli* and chemically synthesized by Eurofins Scientific (https://eurofinsgenomics.eu/). All three panK genes, in addition to *E. coli* panKI, were amplified by PCR with complementary sites to the NcoI and HindIII restriction sites, which were later used to be cloned into an empty pET28a. The cloned genes were confirmed by sequencing (Eurofins Scientific). All primers were synthesized by Eurofins Scientific. Strain HB-2 harbors pJBGT3RX and empty pET28a plasmids. In addition to t3 and rx, strains HB-3 to HB-6 express *E. coli* panKI, *A. nidulans* panKII, *M. musculus* panK1β, and *B. subtilis* panKIII, respectively.

Bacterial strains were maintained on Luria-Bertani (LB) agar with the appropriate antibiotics (Kanamycin 50 μg/mL and/or Chloramphenicol 34 μg/mL), at 4°C for short-term storage. For preculture preparation, a single colony of *E. coli* (HB1 to HB-6) was inoculated in a 125 mL Erlenmeyer flask holding 50 mL LB liquid medium for 24 h at 37°C and 170 rpm in a rotary incubator. Cultures were then centrifuged and washed with PBS buffer prior to inoculation.

2.2. Cultivation in shake flasks

Pre-cultures of *E. coli* strains HB1 to HB-6 were used to inoculated sterile baffled 500 mL shake flasks holding 50 mL Minimal M9 media, with starting OD_{600} of 0.05. The

Table 1. Strains and plasmids

Strains	Description	References
E. coli BL21 (DE3)	Expression host, F- ompT gal dcm hsdSB (rB- mB-) λ(DE3)	NEB
E. coli HB-1	*E. coli* BL21 (DE3)- pJBGT3RX	This study
E. coli HB-2	*E. coli* BL21 (DE3)- pJBGT3RX- pet28	This study
E. coli HB-3	*E. coli* BL21 (DE3)- pJBGT3RX- pETpanKI	This study
E. coli HB-4	*E. coli* BL21 (DE3)- pJBGT3RX- pETpanKII	This study
E. coli HB-5	*E. coli* BL21 (DE3)- pJBGT3RX- pETpanK1β	This study
E. coli HB-6	*E. coli* BL21 (DE3)- pJBGT3RX- pETpanKIII	This study

cultivation media consists of 1 g/L NH_4Cl, 0.5 g/L NaCl, 3 g/L KH_2PO_4, 6 g/L Na_2HPO_4, 0.493 g/L $MgSO_4 \cdot 7H_2O$, 0.011 g/L $CaCl_2$, 0.42 g/L $FeCl_3$- $6 \cdot H_2O$ and supplemented with 0.4% glucose (pH of 6.9). The media was additionally supplemented with the appropriate antibiotics (chloramphenicol, kanamycin). Pantothenate (pantothenic acid), the substrate for the pantothenate kinase enzymatic step, was added to an initial concentration of 5 mM. 3HB production was induced by the addition of 150 μM isopropyl-β-D-1-thiogalactopyranoside (IPTG) at an optical density OD_{600} of 0.6. Cultivation was carried out at 37°C and 170 rpm. Samples were collected 24 h after induction with IPTG, to measure 3HB titers.

2.3. Fermentation

Fed-batch cultivation of *E. coli* HB-5 was performed in a DASGIP® 1.3 L parallel reactor system (Eppendorf AG) with a working volume of 1 L of a modified M9 media consisting of 8 g/L NH_4Cl, 13.3 g/L KH_2PO_4, 1.24 g/L $MgSO_4 \cdot 7H_2O$, 0.42 g/L $FeCl_3 \cdot 6H_2O$, supplemented with 40 g/L glucose. Pantothenate was added to the culture medium to an initial concentration of 5 mM. Cultivation media was additionally supplemented with the appropriate antibiotics. The feed solution consisted of 500 g/L glucose, 20 g/L $MgSO_4 \cdot 7H2O$, 2 mg/L thiamine-HCl, 16 mL 100 × trace elements solution (5 g/L EDTA; 0.83 g/L $FeCl_3 \cdot 6H_2O$; 84 mg/L $ZnCl_2$, 13 mg/L $CuCl_2$-$\cdot 2H_2O$, 10 mg/L $CoCl_2 \cdot 2H_2O$, 10 mg/L H_3BO_3, and 1.6 mg/L $MnCl_2 \cdot 4H_2O$) and (pH=7.00). Samples were taken at different time points to determine the OD_{600}. Fermenters were inoculated with an overnight pre-culture with a starting OD_{600} of 0.1. The cultivation temperature was kept constant at 37°C. Initial stirring velocity and airflow was set to 200 rpm and to 0.2 volumes of air per volume of medium per min (vvm), respectively. Dissolved oxygen was maintained at 30% by successive increases of the stirrer velocity, the oxygen concentration, and eventually the airflow. A pH value of 7.00 was controlled by the addition of 6 M aqueous NaOH. A pH value shift above 7.05 initiated a feed shot of 40 mL. Another 7 g/L of NH_4Cl was added during fermentation to allow high cell density. Once cells reached the stationary phase of growth, 3HB production was induced with 150 μM IPTG. Samples were collected at different intervals to measure 3HB titers.

2.4. Growth and 3HB analysis

To monitor cell growth, OD_{600} was measured at regular intervals for all cultivations. Samples were withdrawn and diluted to an estimated OD_{600} of 0.1-0.4 and measurements were recorded using a spectrophotometer GENESYS™ 10S UV/VIS spectrophotometer (Thermo Fisher Scientific, Germany) was utilized and 1 mL cuvettes.

To quantify 3HB concentration in *E. coli* strains HB1-HB6 for shake flask experiments and fed-batch fermentation, 5 mL of samples were withdrawn on regular intervals and centrifuged at 2,000 g for 5 min. The supernatant was then filtered (VWR collection, 0.45 μm) and 3HB content was determined using Megazyme D-3-Hydroxybutyric Acid Assay Kit Cat No. K-HDBA (Megazyme, Germany). All analysis were performed in triplicates and a student t-test was performed.

2.5. Protein extraction and visualization

To extract the soluble protein fraction from HB-2 (control) and HB-5, the cells from a volume of 50 mL culture were pelleted and washed. The cells were then lysed using a French Press (Avestin, Canada) in Extraction buffer (25 mM Tris, 5 mM EDTA, 5 mM beta-mercaptoethanol, 1 mM PMSF, pH 8,0). Following high-speed centrifugation (12,000 rpm at 4°C) for 10 min, the supernatant, corresponding to the soluble protein fraction, was resolved on a 12% one-dimensional SDS polyacrylamide gel electrophoresis. PageRuler™ Unstained Protein Ladder (Thermo Fisher Scientific) was used to estimate protein band size. Proteins were visualized following Coomassie Brilliant Blue staining.

2.6. In-gel tryptic digestion

Following SDS-PAGE, protein bands in the region between 40 and 50 kDa were excised. In-gel tryptic digestion followed according to a modified protocol Shevchenko *et al.* and Granvogl *et al*. [27,28]. Briefly, the excised gel bands were shredded into small pieces (< 1 mm^3) and washed with acetonitrile until the Coomassie Brilliant Blue stain was washed out. Then, the gel pieces were dried at room temperature under vacuum for 15 min. using a SpeedVac (GeneVac, UK). Samples were reduced (10 mM DTT, 50 mM ammonium bicarbonate) at 56°C for 30 min., washed with acetonitrile, and alkylated (55 mM iodoacetamide, 50 mM ammonium bicarbonate) at room temperature for 20 min. The gel pieces were then washed with acetonitrile again and dried under vacuum for 15 min. Tryptic digestion was carried out overnight at 37°C and 300 rpm using Trypsin Gold (Promega, USA), according to the manufacturers' specifications (1:20 trypsin: protein). Peptides were extracted from the gel pieces by a series of incubation steps (15 min each) using 50 mM ammonium bicarbonate, acetonitrile, and 5% formic acid solution respectively. Collected solutions were dried under vacuum, dissolved in 1% formic acid, filtered through a 13.3 kDa spin-filter.

2.7. LC-MS/MS

Peptide analysis and protein identification was performed using a Tims-TOF Pro mass spectrometer (TIMS) connected

to a NanoEltute LC System (Bruker Daltonik GmbH, Germany), equipped with an Aurora column (250 × 0.075 mm, 1.6 μm, IonOptics, Australia). The mobile phase consisted of a 0.1% (v/v) water-formic acid mixture (A) and a 0.1% (v/v) acetonitrile-formic acid mixture (B), added as a binary gradient and running at a flow rate of 0.4 μL/min. The gradient started at 2% (v/v) B and was increased to 17% (v/v) B after 18 min. After 9 min, another gradient step was started at 25% (v/v) B and increased to 37% (v/v) B after 3 min. After 35 min, buffer B was increased to 95% (v/v). The oven temperature during the measurement was set to 50°C.

The Tims-TOF Pro mass spectrometer (TIMS) was used in PASEF Mode with the following settings: mass range 100-1,700 m/z, ion mobility ramp 0.6-1.6 $V \cdot s/cm^2$, 10 MS/MS Scans per ion mobility ramp (total cycle time 1.16 s), charge range 0-5, active exclusion for 0.4 min, a target intensity of 20000 and an intensity threshold of 1000. Collision energy was ramped stepwise, appropriate to the ion mobility ramp, from 20 to 59 eV. The ESI source parameters were 1600 V for the capillary voltage, 3 L/min N2 as dry gas, and dry gas temperature of 180°C. The measurements were performed in a positive mode. Mass calibration was performed with sodium formiate cluster and the TIMS was calibrated using Hexais (2,2-difluoroethoxy) phosphazene, Hexakis (2,2,3,3-tetrafluoropropoxy) phospazene and the Chip cube high mass reference (m/z 622, 922, and 1222) [29,30].

2.8. Bioinformatics

Peptide sequencing and subsequent protein identification were performed using PEAKS software, version 10.6 (Bioinformatics Solutions Inc., Canada) software [31-33]. Monoisotopic mass was searched with parent and fragment mass error tolerance of 25 ppm and 0.05 Da, respectively. Up to 2 missed cleavages were tolerated for trypsin with cysteine residues (57.02 Da) and methionine residues (15.99 Da) as constant and variable modifications, respectively. Peptide sequences were searched against a uniprot database that comprised *E. coli* proteins and also included *M. musculus* panK1β protein sequence (www.uniprot.com). False discovery rate (FDR) was set to 1% and protein identification was based on significant peptides with a minimum of 1 unique peptide.

3. Results and Discussion

This study provides the first evidence on recombinant expression of panK1β in *E. coli* and its metabolic effects on engineered 3HB production. To that end, soluble proteins of BL21 expressing empty pET28a vector (control) and of BL21 expressing pETpanK1β were first resolved on SDS-PAGE (Fig. S1) in order to clean up the bands to allow a more efficient downstream in-gel digestion and mass spectrometry based protein identification. As expected for the crude, soluble *E. coli* protein extract, the protein bands were not well resolved, with several endogenous *E. coli* proteins in the region of interest (between 40 kDa and 50 kDa) that would overlay the target panK1β protein band. Therefore, we opted for identifying the target protein by excising the bands between 40 and 50 kDa from both sample and control *E. coli* extracts and subjecting them to mass spectrometry based protein identification. In that repertoire, one cut in particularly in the region of 41,642 Da emerged in the pETpanK1β sample and was not detected in the control (Table S1). It showed 20 unique peptides that were unambiguously assigned to *M. musculus* panK1β with a 34% coverage. It is noteworthy, that the endogenous *E. coli* pantothenate kinase shares no significant similarities with panK1β (BLAST®), an expected outcome given that these particular enzymes are of two distinct types (PanKI and PanKII) [15,16]. To the best of our knowledge, this constitutes the first report on the expression of the murine PanK1β in an *E. coli* host system.

3.1. PanKs shake flasks

Production of 3HB was previously achieved in recombinant *E. coli* AF1000 strains with the heterologous expression of acetoacetyl-CoA thiolase (t3) and acetoacetyl-CoA reductase (rx) genes from *H. boliviensis* [4,5] . In our study, the low-copy plasmid pJBGT3RX, harboring t3 and rx genes, was transformed into *E. coli* BL21 (DE3) cells. 3HB production was validated in shake flask experiments, by cultivating the control strain HB-1 on nitrogen-limited media with glucose as sole carbon source.

To investigate the influence of pantothenate kinase on 3HB titers, BL21 (DE3) harboring pETpanKI, pETpanKII, pETpanKIII, or pETpanK1β, in addition to the production plasmid pJBGT3RX, were evaluated in shake-flask cultures. Notably, all 3 PanK proteins share the same function and hence are assigned an identical EC number (2.7.1.33). An excess of pantothenate (5 mM) was added to culture media in order to saturate the enzymatic activity of the overexpressed PanKs. Previous studies showed that high concentrations of pantothenate in the medium does not affect the growth of recombinant cells [14]. HB-2 strain harboring an empty pet28a plasmid (pJBGT3RX-pET) was also tested under the same conditions. 3HB titers and OD_{600} of the various strains are presented in Table 2. The control strain HB-1 produced 0.11 g/L of 3HB, while HB-5 expressing PanK1β yielded the highest titers of 0.15 g/L. This corresponds to a 36% increase compared to the control strain. Previous results indicate that an increase in

Table 2. Optical density and 3HB titers (g/L) of *Escherichia coli* strains (HB1-6) cultivated in shake flasks with glucose as the sole carbon source

Escherichia coli strain	Final OD_{600}	3HB Titers (g/L)
HB-1	3.6 ± 0.1	0.11 ± 0.00
HB-2	3.3 ± 0.0	0.09 ± 0.01
HB-3	3.4 ± 0.1	0.11 ± 0.01
HB-4	3.5 ± 0.1	0.13 ± 0.00
HB-5	3.5 ± 0.0	0.15 ± 0.01
HB-6	3.4 ± 0.1	0.10 ± 0.01

intracellular acetyl-CoA level with pantothenate kinase overexpression does not translate to an observable change in the growth rate of *E. coli* [14]. Our results confirm these findings.

CoA and acetyl-CoA are essential cofactors and key regulators in numerous metabolic pathways. Across species, phosphorylation of pantothenate by PanK is the rate-limiting step in the CoA biosynthesis pathway [14,15]. Several studies attempted to increase CoA/acetyl-CoA pools by overexpressing various forms of PanK [14,16,19,34]. Notably, acetyl-CoA occupied more than 70% of the total CoA group whether the pantothenate kinases were overexpressed or not, indicating the feasibility of increasing CoA availability to improve acetyl-CoA-derived biochemical processes [35]. In our study, 3HB-producing strains reflect cytosolic CoA/acetyl-CoA levels as acetyl-CoA is the precursor of 3-hydroxybutyrate.

E. coli PanKI is potently inhibited by CoA and to a lesser extent by acetyl-CoA [15,36]. The latter is an end-product of glucose metabolism. The decreased sensitivity of PanKI to acetyl-CoA allows this pool to grow and accommodate the metabolic needs of the cell, particularly when cultivated on glucose-rich medium [15,22,23]. In a previous study, overexpression of PanKI in *E. coli* lead to a 10-fold increase in CoA levels and a 5-fold increase in acetyl-CoA levels during fermentation in rich media. However, the same strain achieved only a 2.5-fold increase in intracellular CoA levels with no detectable change in acetyl-CoA levels when cultivated on M9 media [14]. Previous studies reported increased metabolic flux towards 3HB was promoted by nutrient (*e.g.* nitrogen) limitation [3-6,11]. In our study, the lack of increase in 3HB levels observed in the PanKI overexpression strain (HB-3) - compared to HB-1 - could be attributed to the constraint for cultivation on minimal media.

In contrast to PanKI, acetyl-CoA selectively and potently inhibits eukaryotic PanKII, whereas free (unesterified) CoA has little or no effect [19,22]. This differential regulation by CoA/acetyl-CoA may be related to the differences in subcellular compartmentalization and metabolism among species. In prokaryotes, the cytosol harbors the various enzymes, substrates, products, and regulators. In eukaryotes, CoA and its derivates are mostly concentrated in the mitochondria and peroxisomes, while PanKII is a cytosolic enzyme [19,20,22]. The rationale behind overexpressing PanKII in recombinant *E. coli* lies in that 3HB-production system would provide a metabolic sink for the accumulated acetyl-CoA, constantly alleviating the feedback inhibition. This was demonstrated in this study with *E. coli* HB-4 expressing *A. nidulens* PanKII, which achieved higher 3HB titers compared to *E. coli* HB-1 and HB-3 strains. Interestingly, strains overexpressing *M. musculus* PanK1β (HB-5) yielded the highest 3HB titers, with a 15% increase compared to HB-4 expressing its fungal variant. Across eukaryotic species, from fungi to humans, panthonate kinase type II and its isoforms share primary sequence similarities, similar cytoplasmic localization and strong feedback inhibition by acetyl-CoA [16, 19, 20, 22]. PanK1β in particular exhibits distinctive biochemical properties, as it is weakly regulated by acetyl-CoA [16, 19, 20]. *In vitro* studies have showed that 10-fold concentration of acetyl-CoA was needed to attain IC_{50} for PanK1β compared to other eukaryotic isoforms [16]. *In vivo* (liver and kidney) overexpression of this enzyme lead to a 33-fold increase in intracellular CoA levels. Synergistic *in vivo* and *in vitro* data generated demonstrated that PanK1β overexpression influenced both the uptake and metabolism of pantothenate [19]. Most interestingly, the activity of PanK1β is stimulated by free CoA, a unique feature of this particular enzyme [16, 19, 20]. Both PanK1 isoforms (PanK1α and PanK1β) possess a common catalytic domain. However, PanK1α has a 184 amino acid regulatory module attached to the amino-terminus of the catalytic core (compared to just 10-amino acid terminus in PanK1β), which imparts more stringent feedback regulation [19, 20]. PanKII from *A. nidulans* exhibited significant similarity to both PanK1 isoforms in the catalytic core region. The fungal enzyme also possesses a long N-terminus domain and its biochemical properties were found to be intermediate between PanK1α and PanK1β [19,20,22]. The unique properties of isoform PanK1β allowed recombinant *E. coli* to achieve high 3HB titers in our study.

Pantothenate kinase type III, identified in a number of bacteria, differs from the first two types in that it is refractory to feedback inhibition by CoA and acetyl-CoA. *In vitro* studies showed that the ability of PankIII to phosphorylate pantothenate was completely unaffected by high concentrations of the aforementioned cofactors [21,24,26,37]. Surprisingly, in our study, the strain expressing PanKIII (HB-6) was not the best 3HB producer, with titers similar to that expressing *E. coli* PanKI, itself highly

regulated by CoA. Gene disruption studies in bacteria possessing both types showed that the contribution of PanKI to the formation of the intracellular CoA pool is larger than that of PanKIII. These experiments also showed that PanKI is an essential gene while PanKIII is not [23-25]. It might also be possible that PanKIII requires an environment for optimal activity that is not present in heterologous host systems.

3.2. Bioreactor: PanK1β

Shake-flasks experiments clearly indicated, that over-expression of *M. musculus* PanK1β in *E. coli* production strain lead to a significant increase in 3HB titers. To validate the performance of this enhanced strain under controlled conditions, fed-batch fermentations were performed in a 1.3 L parallel stirred tank bioreactor. Strain HB-5 overexpressing PanK1β and the control strain HB-1, were cultivated in fed-batch mode with excess glucose and nitrogen-limited media. Both strains exhibited the same final OD_{600} of about 27. With the HB-5 strain, the maximal 3HB concentration (7.6 g/L) was achieved at a fermentation time point of 24 h. This 3HB yield represents a 41% increase compared to the control production strain (5.4 g/L) (Fig. 3 and 4). Previously published work on 3HB production by recombinant *E. coli* reported titers between 4 and 16 g/L [3-6,11,13,38].

The low initial 3HB titers of the HB-5 (3.5 g/L) compared to HB-1 (5.0 g/L) strain at 6 h fermentation time could be attributed to several factors, including increased metabolic burden due to utilization of a 2 plasmids system. Another plausible explanation is the initial high level of CoA expected in HB-5 (due to PanK1β overexpression). Free CoA competitively inhibits acetoacetyl-CoA thiolase (t3), which catalyzes the first step in 3HB production [39]. During exponential growth, high levels of CoA would hinder the activity of this enzyme; however, upon nitrogen depletion CoA level drop, relieving the inhibition. A previous study reported similar observation, where acetoacetyl-CoA thiolase was almost completely inhibited by CoA during growth phase, and regained 75% of its maximum activity during PHB accumulation [40].

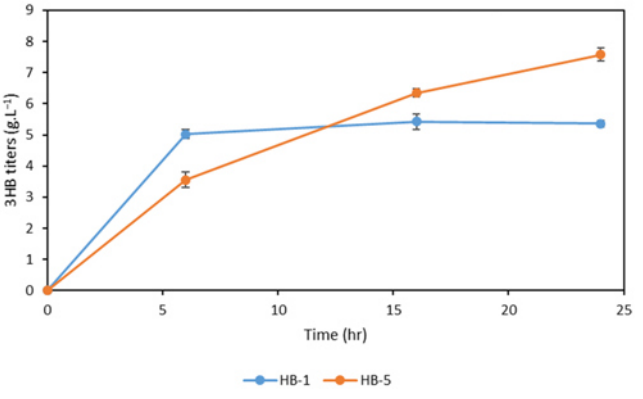

Fig. 3. Production of 3HB in HB-1 (blue) and HB-5 (orange) during fed-batch cultivation with glucose as the sole carbon source ($p < 0.5$).

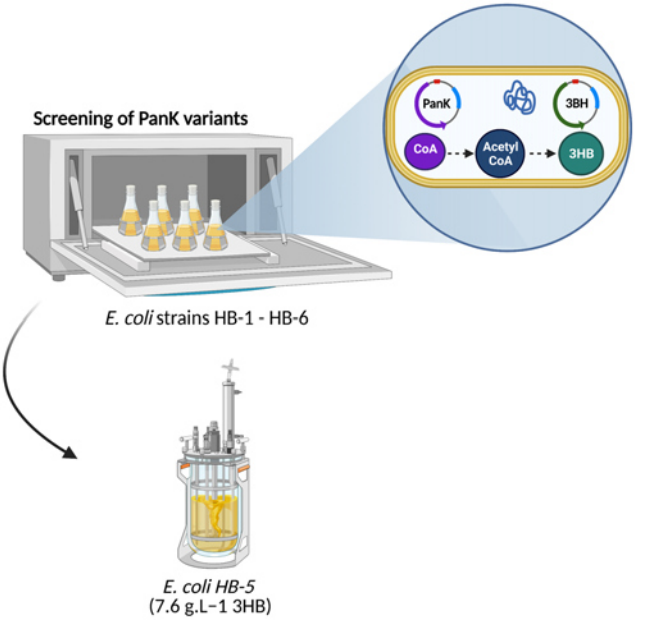

Fig. 4. Schematic illustration of the PanK evaluation and upscaling experiments in this study.

4. Conclusion

To the best of our knowledge, this is the first study that systematically evaluates pantothenate kinase overexpression in recombinant *E. coli* with a focus on 3HB yield optimization. Overexpressing mammalian resulted in a 41% increase in 3HB titers. Future work could elucidate the detailed metabolomics- and transcriptomic networks of *E. coli* based, recombinant 3HB production systems in conjunction with the stoichiometry governing panthonate and acetyl coA. This comprehensive study would enable identification of further metabolic bottlenecks, which can be addressed by genomic approaches towards an optimized 3HB production system. In that context, further enhancement of the titers could be achieved by integrating a one-plasmid system, adopting other nutrient-limitation (*e.g.* phosphate) modes [5], or carrying out high cell-density (2 stage) fermentations [6,11]. Combinatory approaches could also be employed, where a metabolic "push and pull" strategy would drive the carbon flux more stringently towards 3HB production. In combination with increased CoA/acetyl-CoA pools, improving the supply of other cofactors (*e.g.*

NADPH) (push) [6], overexpressing endogenous thioesterases (pull) [3], and blocking competing pathways could help improve the overall 3HB titers further.

Funding

This work was supported by the Bavarian State Ministry for Environmental and Consumer affairs for funding of the project Resource-efficient PHB production processes within the project consortium BayBioTech (TP7, TLK01U-69045, http://www.baybiotech.de/startseite/).

Availability of Data and Material

All datasets generated for this study are included in the manuscript.

Authors' Contributions

Conceptualization of the study was conducted jointly by SY, NM, and TB. The methodological approach was designed and carried out by SY, DA, EK and NM. Data validation was jointly carried out by SY, NM. SY and DA prepared the original draft of the manuscript. The manuscript was jointly finalized by all authors.

Acknowledgements

TB gratefully acknowledges funding of the Werner Siemens foundation for establishing the research field of Synthetic Biotechnology at the Technical University of Munich. SY, DA and NM gratefully acknowledge funding of the Bavarian State Ministry for Environmental and Consumer affairs. The authors gratefully acknowledge Prof. Gen Larsson from KTH Royal Institute of Technology in Sweden for providing the 3HB production plasmid.

Conflicts of Interest

The authors declare that the research was conducted in the absence of any commercial or financial relationships.

Informed Consent

Neither ethical approval nor informed consent was required for this study.

Electronic Supplementary Material (ESM)

The online version of this article (doi: 10.1007/s12257-021-0033-1) contains supplementary material, which is available to authorized users.

References

1. Awad, D., F. Bohnen, N. Mehlmer, and T. Brueck (2019) Multi-factorial-guided media optimization for enhanced biomass and lipid formation by the oleaginous yeast *Cutaneotrichosporon oleaginosus*. *Front. Bioeng. Biotechnol*. 7: 54.
2. Younes, S., F. Bracharz, D. Awad, F. Qoura, N. Mehlmer, and T. Brueck (2020) Microbial lipid production by oleaginous yeasts grown on *Scenedesmus obtusiusculus* microalgae biomass hydrolysate. *Bioprocess Biosyst. Eng*. 43: 1629-1638.
3. Guevara-Martinez, M., M. Perez-Zabaleta, M. Gustavsson, J. Quillaguaman, G. Larsson, and A. J. A. van Maris (2019) The role of the acyl-CoA thioesterase "YciA" in the production of (R)-3-hydroxybutyrate by recombinant *Escherichia coli*. *Appl. Microbiol. Biotechnol*. 103: 3693-3704.
4. Jarmander, J., J. Belotserkovsky, G. Sjoberg, M. Guevara-Martinez, M. Perez-Zabaleta, J. Quillaguaman, and G. Larsson (2015) Cultivation strategies for production of (*R*)-3-hydroxybutyric acid from simultaneous consumption of glucose, xylose and arabinose by *Escherichia coli*. *Microb. Cell Fact*. 14: 51.
5. Guevara-Martinez, M., K. Sjoberg Gallno, G. Sjoberg, J. Jarmander, M. Perez-Zabaleta, J. Quillaguaman, and G. Larsson (2015) Regulating the production of (R)-3-hydroxybutyrate in *Escherichia coli* by N or P limitation. *Front. Microbiol*. 6: 844.
6. Perez-Zabaleta, M., G. Sjoberg, M. Guevara-Martinez, J. Jarmander, M. Gustavsson, J. Quillaguaman, and G. Larsson (2016) Increasing the production of (*R*)-3-hydroxybutyrate in recombinant *Escherichia coli* by improved cofactor supply. *Microb. Cell Fact*. 15: 91.
7. Wei, Y. H., W. C. Chen, H. S. Wu, and O. M. Janarthanan (2011) Biodegradable and biocompatible biomaterial, polyhydroxybutyrate, produced by an indigenous *Vibrio* sp. BM-1 isolated from marine environment. *Mar. Drugs*. 9: 615-624.
8. Lee, S. Y., Y. Lee, and F. Wang (1999) Chiral compounds from bacterial polyesters: sugars to plastics to fine chemicals. *Biotechnol. Bioeng*. 65: 363-368.
9. Quillaguaman, J., R. Hatti-Kaul, B. Mattiasson, M. T. Alvarez, and O. Delgado (2004) *Halomonas boliviensis* sp. nov., an alkalitolerant, moderate halophile isolated from soil around a Bolivian hypersaline lake. *Int. J. Syst. Evol. Microbiol*. 54: 721-725.
10. Werpy, T. and G. Petersen (2004) Top value added chemicals from biomass: volume I--results of screening for potential candidates from sugars and synthesis gas. National Renewable Energy Lab., Golden, CO, USA.
11. Perez-Zabaleta, M., M. Guevara-Martinez, M. Gustavsson, J. Quillaguaman, G. Larsson, and A. J. A. van Maris (2019) Comparison of engineered *Escherichia coli* AF1000 and BL21 strains for (R)-3-hydroxybutyrate production in fed-batch cultivation. *Appl. Microbiol. Biotechnol*. 103: 5627-5639.
12. de Roo, G., M. B. Kellerhals, Q. Ren, B. Witholt, and B. Kessler (2002) Production of chiral R-3-hydroxyalkanoic acids and R-3-hydroxyalkanoic acid methylesters via hydrolytic degradation of polyhydroxyalkanoate synthesized by pseudomonads. *Biotechnol. Bioeng*. 77: 717-722.
13. Liu, Q., S. P. Ouyang, A. Chung, Q. Wu, and G. Q. Chen (2007)

Microbial production of R-3-hydroxybutyric acid by recombinant *E. coli* harboring genes of phbA, phbB, and tesB. *Appl. Microbiol. Biotechnol*. 76: 811-818.
14. Vadali, R. V., G. N. Bennett, and K. Y. San (2004) Cofactor engineering of intracellular CoA/acetyl-CoA and its effect on metabolic flux redistribution in *Escherichia coli*. *Metab. Eng*. 6: 133-139.
15. Rock, C. O., H. W. Park, and S. Jackowski (2003) Role of feedback regulation of pantothenate kinase (CoaA) in control of coenzyme A levels in *Escherichia coli*. *J. Bacteriol*. 185: 3410-3415.
16. Zhang, Y. M., C. O. Rock, and S. Jackowski (2005) Feedback regulation of murine pantothenate kinase 3 by coenzyme A and coenzyme A thioesters. *J. Biol. Chem*. 280: 32594-32601.
17. Yun, M., C. G. Park, J. Y. Kim, C. O. Rock, S. Jackowski, and H. W. Park (2000) Structural basis for the feedback regulation of *Escherichia coli* pantothenate kinase by coenzyme A. *J. Biol. Chem*. 275: 28093-28099.
18. Leonardi, R., Y. M. Zhang, C. O. Rock, and S. Jackowski (2005) Coenzyme A: back in action. *Prog. Lipid. Res*. 44: 125-153.
19. Rock, C. O., R. B. Calder, M. A. Karim, and S. Jackowski (2000) Pantothenate kinase regulation of the intracellular concentration of coenzyme A. *J. Biol. Chem*. 275: 1377-1383.
20. Rock, C. O., M. A. Karim, Y. M. Zhang, and S. Jackowski (2002) The murine pantothenate kinase (Pank1) gene encodes two differentially regulated pantothenate kinase isozymes. *Gene*. 291: 35-43.
21. Yang, K., Y. Eyobo, L. A. Brand, D. Martynowski, D. Tomchick, E. Strauss, and H. Zhang (2006) Crystal structure of a type III pantothenate kinase: insight into the mechanism of an essential coenzyme A biosynthetic enzyme universally distributed in bacteria. *J. Bacteriol*. 188: 5532-5540.
22. Calder, R. B., R. S. Williams, G. Ramaswamy, C. O. Rock, E. Campbell, S. E. Unkles, J. R. Kinghorn, and S. Jackowski (1999) Cloning and characterization of a eukaryotic pantothenate kinase gene (panK) from *Aspergillus nidulans*. *J. Biol. Chem*. 274: 2014-2020.
23. Ogata, Y., H. Katoh, M. Asayama, and S. Chohnan (2014) Role of prokaryotic type I and III pantothenate kinases in the coenzyme A biosynthetic pathway of *Bacillus subtilis*. *Can. J. Microbiol*. 60: 297-305.
24. Brand, L. A. and E. Strauss (2005) Characterization of a new pantothenate kinase isoform from *Helicobacter pylori*. *J. Biol. Chem*. 280: 20185-20188.
25. Awasthy, D., A. Ambady, J. Bhat, G. Sheikh, S. Ravishankar, V. Subbulakshmi, K. Mukherjee, V. Sambandamurthy, and U. Sharma (2010) Essentiality and functional analysis of type I and type III pantothenate kinases of *Mycobacterium tuberculosis*. *Microbiology (Reading)*. 156: 2691-2701.
26. Nicely, N. I., D. Parsonage, C. Paige, G. L. Newton, R. C. Fahey, R. Leonardi, S. Jackowski, T. C. Mallett, and A. Claiborne (2007) Structure of the type III pantothenate kinase from *Bacillus anthracis* at 2.0 Å resolution: implications for coenzyme A-dependent redox biology. *Biochemistry*. 46: 3234-3245.
27. Strand, D. D. and D. M. Kramer (2014) Control of non-photochemical exciton quenching by the proton circuit of photosynthesis. pp. 387-408. In: B. Demmig-Adams, G. Garab, W. W. Adams III, and Govindjee (eds.). *Non-Photochemical Quenching and Energy Dissipation in Plants, Algae and Cyanobacteria*. Springer Netherlands, Dordrecht, Netherlands.
28. Granvogl, B., P. Gruber, and L. A. Eichacker (2007) Standardisation of rapid in-gel digestion by mass spectrometry. *Proteomics*. 7: 642-654.
29. Sandow, J. J., G. Infusini, L. F. Dagley, R. Larsen, and A. I. Webb (2019) Simplified high-throughput methods for deep proteome analysis on the timsTOF Pro. *BioRxiv*. 657908.
30. Meier, F., A. D. Brunner, S. Koch, H. Koch, M. Lubeck, M. Krause, N. Goedecke, J. Decker, T. Kosinski, M. A. Park, N. Bache, O. Hoerning, J. Cox, O. Räther, and M. Mann (2018) Online parallel accumulation-serial fragmentation (PASEF) with a novel trapped ion mobility mass spectrometer. *Mol. Cell. Proteomics*. 17: 2534-2545.
31. Tran, N. H., M. Z. Rahman, L. He, L. Xin, B. Shan, and M. Li (2016) Complete *de novo* assembly of monoclonal antibody sequences. *Sci. Rep*. 6: 31730.
32. Tran, N. H., X. Zhang, L. Xin, B. Shan, and M. Li (2017) *De novo* peptide sequencing by deep learning. *Proc. Natl. Acad. Sci. USA*. 114: 8247-8252.
33. Tran, N. H., R. Qiao, L. Xin, X. Chen, C. Liu, X. Zhang, B. Shan, A. Ghodsi, and M. Li (2019) Deep learning enables *de novo* peptide sequencing from data-independent-acquisition mass spectrometry. *Nat. Methods*. 16: 63-66.
34. Liu, W., B. Zhang, and R. Jiang (2017) Improving acetyl-CoA biosynthesis in *Saccharomyces cerevisiae* via the overexpression of pantothenate kinase and PDH bypass. *Biotechnol. Biofuels*. 10: 41.
35. Ku, J. T., A. Y. Chen, and E. I. Lan (2020) Metabolic engineering design strategies for increasing acetyl-CoA flux. *Metabolites*. 10: 166.
36. Song, W. J. and S. Jackowski (1994) Kinetics and regulation of pantothenate kinase from *Escherichia coli*. *J. Biol. Chem*. 269: 27051-27058.
37. Paige, C., S. D. Reid, P. C. Hanna, and A. Claiborne (2008) The type III pantothenate kinase encoded by coaX is essential for growth of *Bacillus anthracis*. *J. Bacteriol*. 190: 6271-6275.
38. Gao, H. J., Q. Wu, and G. Q. Chen (2002) Enhanced production of D-(-)-3-hydroxybutyric acid by recombinant *Escherichia coli*. *FEMS Microbiol. Lett*. 213: 59-65.
39. Suzuki, F., W. L. Zahler, and D. W. Emerich (1987) Acetoacetyl-CoA thiolase of *Bradyrhizobium japonicum* bacteroids: purification and properties. *Arch. Biochem. Biophys*. 254: 272-281.
40. Mothes, G., I. S. Rivera, and W. Babel (1996) Competition between β-ketothiolase and citrate synthase during poly(β-hydroxybutyrate) synthesis in *Methylobacterium rhodesianum*. *Arch. Microbiol*. 166: 405-410.

4. Discussion and Outlook Chapter 1

4.1 Eukaryotic Platforms Development

Currently, various technical and environmental challenges hinder viable economic applications of SCOs at industrial scale. Costly feedstock or raw material, complex and toxic carbon-source procurement methods, in addition to low lipid yields constitute major limiting factors [7,56] For the successful implementation of SCOs in industry, these factors must be tackled.

This work primarily addresses the main technical and environmental constraints pertaining to SCOs production from oleaginous yeasts. Eukaryotic platform development was pursued with respect to:

- → **Section 4.2: Sustainable feedstock acquirement, which involves the characterization of promising marine biomass**
- → **Section 4.3: Development of an efficient, eco-friendly and cost-effective biomass hydrolysis method**
- → **Section 4.4: Marine Biomass hydrolysate as feedstock for the assessment and validation of promising yeast platforms**

4.2 Sustainable feedstock

Various studies investigated the use of renewable feedstock including glycerol, molasses and lignocellulosic biomass as carbon sources for lipid accumulation in oleaginous yeasts [137,138]. In our work, we opted for marine biomass, specifically seagrass and microalgae, to circumvent the use of fresh water and arable lands, and any associated environmental and sustainability concerns (e.g., deforestation, food security). This section pertains to the biomass analysis of marine biomass under study.

4.2.1 Seagrass Biomass

In this work, we examined the value-added use of aged seagrass waste as a readily available, low-cost, raw feedstock for production of microbial lipids in oleaginous yeasts. To the best of our knowledge, utilization of beach-cast seagrass biomass as feedstock for single-cell oils (SCOs) production has not been previously considered. To that end, seven seagrass samples from six different seagrass eco-regions were collected, and a phylogenetic classification of each sample was constructed using 18s rRNA sequencing. The samples were identified as *Zostera marina*, *Zostera noltii*, *Syringodium filiforme*, *Posidonia australis*, *Posidonia oceanica*, and *Thalassia testudinum*.

Comprehensive biomass analysis was performed on the various seagrass samples. In contrast to terrestrial biomass (e.g., wheat straw), the absence of lignin from this marine biomass meant that physicochemical pre-treatment can be avoided, contributing to a better energy and ecosystem impact

in a life cycle analysis. Most importantly, all samples displayed a high carbohydrate content of 73–81 % $g.g^{-1}$ DCW. Glucose was found to be the dominant monomeric carbohydrate, mainly originating from cellulosic leaf fibers [139]. Given that, glucose is the preferred carbon source for a diverse array of pro- and eukaryotic microorganisms, our data supports seagrass biomass as a potentially suitable feedstock for SCO platforms.

Notably, ash constituted 12–13 % $g.g^{-1}$ DCW. Minerals contained in the ash are vital for yeast fermentation as some trace elements play an essential role in lipid production [140]. In iron deficient environments, reduced α-linolenic acid content in yeast has been linked to a decrease in the activity of desaturases, as its activity depends on the presence of iron [141]. The main inorganic elements constituting the ash structure are Ca^{2+} and Mg^{2+}, followed by smaller amounts of Al and S. The concentrations of these elements vary extensively between the seagrass species; this is mainly due to the availability of nutrients in the original marine ecosystem. Interestingly, phosphate was completely absent from *P. oceanica*. The high Ca^{2+} and Mg^{2+} content could be responsible for the precipitation of phosphate compounds. This technique is commonly applied on yeast culture media to deplete phosphates for the induction of lipid accumulation [142]. Thus, this strain can play an integral role for the development of SCO platforms, whereby lipogenesis is also triggered by phosphate limitation [143,144].

High density and low moisture content in biomass material are associated with reduced transport and operation costs. To that end, dewatering of marine biomass (e.g., macro and microalgae) is of particular interest for sustainable biofuel and oleochemical applications. Wet biomass is subject to rapid deterioration in quality, heavy to transport, bulky to store and the energy extraction from such feedstocks is costly [145,146]. Biomass analysis of the collected aged seagrass samples showed low water content (8-10 % $g.g^{-1}$ DCW). Furthermore, structural analysis, in particular that of *P. oceanica*, revealed a dense (non-hollow) structure, with fiber bundles interspersed within the leaf matrix. Seagrass biomass, specifically of *P. oceanica*, exhibiting high density and minimal water content, is an advantageous raw material for cost-effective industrial applications.

The presented results of biomass analysis can guide culture media preparation with respect to applied nutrient limitations, including organic (i.e., C: N and C: P) and mineral (Fe^{3+}, Ca^{2+} and Mg^{2+}) components and ratios. The characterization of *P. oceanica* biomass, one of the most promising seagrasses under study, is detailed in **Table 3**.

Table 3. Detailed characterization of *P. oceanica* biomass.

Origin	Location	Mediterranean Sea (Malta2)
	GPS coordinates	35°49'15.4"N 14°33'32.1"E
	Identification via	ITS1 and 18S rRNA sequencing
	Structure	fiber bundles interspersed within the leaf matrix
Biochemical composition (%, $g.g^{-1}$ DCW)	Lipids	2.3 ± 0.41
	Proteins	05.1 ± 0.06
	Sugars	80.8 ± 0.57
	Ash	11.8 ± 0.68
	Phosphate	n.d.
Carbohydrate composition (%, $g.g^{-1}$ DCW)	glucose	55.99 ± 0.17
	galacturonic acid	6.61 ± 0.10
	xylose, mannose, fructose	3.67 ± 0.09
	rhamnose	7.17 ± 0.12
	fucose	1.23 ± 0.02
Mineral composition (%, $g.g^{-1}$ DCW)	O	69.3
	Mg	12.7
	Al	1
	S	2.6
	Ca	14.1
	Sr	0.3
Fatty acid content (%, $g.g^{-1}$ DCW)	C16:0	0.471 ± 0.308
	C18:0	0.152 ± 0.125
	C18:1 (Ω9)	0.206 ± 0.196
	C24:0	0.435 ± 0.606
	other	0.794 ± 0.022

4.2.2 Microalgae biomass

Scenedesmus spp. are of high interest as they constitute the most common freshwater green algae. In this work, we explored the feasibility of utilizing microalgae-based cell residues of this species as feedstock for yeast oil production. Specifically, *Scenedesmus obtusiusculus* was the focus point of this work, since previous research in our group found that this microalgae strain allowed for high lipid accumulation.

The significant properties of microalgae biomass as raw material for microbial cultivation lies in its high carbohydrates contents and lack of recalcitrant lignin [107]. *Scenedesmus spp.* has been previously exploited for bioethanol fermentation in yeasts, following acid hydrolysis. In this study, the biochemical composition of *S. obtusiusculus* (A189) revealed high carbohydrate content (34%, $g.g^{-1}$

DCW) [147]. In comparison, *Scenedesmus obliquus*, *Chlorella vulgaris* and *Chlamydomonas rheinhardii* microalgae species exhibited carbohydrate content of 10%, 12%, 17% $g.g^{-1}$ DCW, respectively [148,149].

The biochemical composition of *S. obtusiusculus* (A189) biomass can be found in **Table 4**. The presented results validate *S. obtusiusculus* as a carbon rich source. Subsequently we employed this biomass as feedstock for oleaginous yeast fermentation, following proper hydrolysis technique to release monomeric pentose and hexose sugars.

Table 4. Biochemical composition of *S. obtusiusculus* biomass.

Origin	Culture collection of WSSB	Pharmaceutical Biology Group of the Ernst-Moritz-Arndt University in Greifswald
Biochemical composition* (%, g.g-1 DCW)	Lipids	8.3
	Proteins	49
	Sugars	34
	Ash	1.9
	water	3.7
	Pigments/secondary metabolites	3.6

*Relative standard deviation for all given numbers is ≤ ± 2%.

4.3 Development of hydrolysis method

Following the comprehensive characterization of the various marine biomass, we developed an "eco-friendly hydrolyzation process". The single-step "green" enzymatic hydrolysis process resulted in the efficient release of monomeric sugars contained in seagrasses and microalgae biomass without the need for energy- and cost-intensive thermochemical pre-treatments. The proposed hydrolysis method also circumvents the need for costly and complex subsequent detoxification steps. Sterilization of the various marine biomass was performed in a laboratory-scale autoclave at 120 °C for 15 min. This step is crucial to eliminate microbial contaminants that may be present in the marine biomass. Sterilization also aids the disintegration of the cell wall, facilitating proximity contact with the hydrolytic enzymes [150]. As saccharification of hemicellulose and cellulose is initiated at temperatures above 150 °C, sterilization is not considered a pre-treatment step [151].

Various commercial hydrolase mixtures were chosen for their biomass liquefaction efficiencies including a cellulase mix (Cellic-Ctec2, Novozymes), a hemicellulose-mix (Cellic-Htec2, Novozymes), a pectinase mix (Pectinex, Novozymes), an amylase mix (Fungamyl, Novozymes), and a β-glucosidase (Novozymes 188). These enzymes were previously utilized as stand-alone or in mixtures for the hydrolysis of various lignocellulosic biomass, including sugarcane bagasse, sorghum bagasse, wheat straw, bamboo chips and corn stover. However, in all these reports, the enzymatic saccharification

step always necessitated a pretreatment method [152-154]. Our study constitutes the first report on a single-step enzymatic hydrolysis of marine biomass.

We also employed a stand-alone and a combinatory approach in the optimization of these enzyme systems. For all biomass residues, the total concentration of both standalone or mixtures of enzyme systems was kept at an industrially and economically relevant 1% (v/v). Finally, to achieve nitrogen-limitation (key for induction of lipogenesis in oleaginous yeasts), 10 kDa cross-filtration was performed for the various hydrolysates [81].

4.3.1 Seagrass biomass hydrolysis

For sea grass biomass, the highest biomass-to-glucose conversion efficiency was achieved by combining Cellic-Ctec2 and Cellic HTec at a ratio of 1:4, respectively. The optimal concentration of this mixture (1 %; w/w) allowed 0.38 $g.g^{-1}$ of glucose to be released from the seagrass biomass. Method optimization led to a further enhanced glucose recovery of 0.47 $g.g^{-1}$ DCW, with the addition of 0.3% β-glucosidase. The combinatory effect of cellulase, hemicellulase and glucosidase enzymes led to a biomass-glucose conversion efficiency of about 82% ($g.g^{-1}$). The experimental set up of the hydrolytic treatment is summarized in **Table 5**. Applying one or more of these commercial enzyme systems, other studies reported conversion efficiencies ranging from 28% - 85% ($g.g^{-1}$). However, as previously stated, a pre-treatment step remained crucial.

Table 5. The parameters of the optimal hydrolysis method developed in this work for sea grass biomass.

Sterilization method	Autoclave (120˚C, 15 min)
Enzymes	Cellic CTec 2, Cellic Htec and β-glucosidase
Enzyme system	1:4 (C: H; w/w) and 0.3% β-glucosidase
Temperature (˚C)	50
pH	5
Buffer	Sodium acetate, 50 mM
Incubation period (h)	72
Nitrogen Depletion	10 kDa filtration

The developed one-step “green” hydrolytic treatment was applied to the seven seagrass samples under study. *Z. noltii* and *P. oceanica* hydrolysates comprised the highest glucose content with 32 $g.L^{-1}$ and 28.5 $g.L^{-1}$, respectively. Calculating nitrogen content via the Kjeldahl method, and factoring in glucose content as main carbon source, *T. testudinum* and *P. oceanica* hydrolysates displayed the highest C: N ratios with 48 and 52, respectively. As high C: N are advantageous for downstream applications, i.e. lipid accumulation induction in nitrogen minimal conditions, *P. oceanica* was selected

as a feedstock for subsequent yeast fermentation at bioreactor scale (1L) (**Section 4.4.1: Fermentation on seagrass hydrolysate**) [87,155]. The composition of *P. oceanica* hydrolysate is detailed in **Table 6**.

Table 6. Characterization of *P. oceanica* hydrolysate.

Sugar composition ($g.L^{-1}$)	Glucose	28.50 ± 0.59
	Galacturonic acid	0.630 ± 0.02
	Xyl, Man, Gal, Fruc	5.530 ± 0.26
	Arabinose	0.150 ± 0.01
	Fucose	0.200 ± 0.01
Kjeldahl Data	Protein content (%, $g.g^{-1}$ DCW)	0.36
	Nitrogen content (%, $g.g^{-1}$ DCW)	0.06
	Nitrogen concentration ($g.L^{-1}$)	0.55
Ratio	C: N	52

4.3.2 Microalgae hydrolysate

For the microalgae, *S. obtusiusculus,* the highest biomass-to-glucose conversion efficiency was achieved by the cellulase mix Cellic-Ctec2 at 1% (w/w). Although a combinatory approach was applied, standalone Cellic-Ctec2 retained the highest conversion activity. The experimental set up of the hydrolytic treatment is summarized in **Table 7.** With this enzymatic hydrolysis the glucose-conversion efficiency reached of 90–100% ($g.g^{-1}$). This work resulted in one of the highest reported conversion efficiencies, when compared to published reports on hydrolytic treatment (comprising a pre-treatment step) of macro- and microalgae biomass [109,156-159]. At a biomass-glucose recovery of 0.24 $g.g^{-1}$ DCW, 48 $g.L^{-1}$ of glucose were obtained from 200 g of *S. obtusiusculus* dry biomass. Accordingly, *S. obtusiusculus* hydrolysate was implemented as a feedstock for yeast fermentation.

Table 7. The parameters of the optimal hydrolysis method developed in this work for *S. obtusiusculus* biomass.

Sterilization method	Autoclave (120˚C, 15 min)
Enzymes	Cellic CTec 2
Enzyme system	1%
Temperature (˚C)	50
pH	5
Buffer	Sodium acetate, 50 mM
Incubation period (h)	72
Nitrogen Depletion	10 kDa filtration

4.4 Marine Biomass hydrolysate as feedstock for oleaginous yeasts

The potential use of marine biomass hydrolysates as sole carbon source, specifically *P. oceanica* and *S. obtusiusculus,* for lipid production in oleaginous yeast was evaluated in this section. This study was conducted without any expensive nutritional additives (e.g., yeast extract, biotin, glucose). The fermentative growth and lipid accumulation of the yeasts on the hydrolysates was compared to that of the well-established minimal nitrogen media (MNM). This medium is known to induce lipogenesis in oleaginous yeast as it contains high glucose and low nitrogen content, with a high C: N of 150. Consequently, this media has been utilized for technical-scale fermentation (15 L fermenter) and SCOs production from yeasts [160].

4.4.1 Fermentation on seagrass hydrolysate

In shake flasks studies (300 mL), *Cutaneotrichosporon oleaginosus* was grown on the 7 seagrass strains under study. The yeast recorded the highest growth rate on *P. oceanica* hydrolysate, reaching an OD_{600} of 45 following 5 days of fermentation, compared to an OD_{600} of 23 on MNM. Despite the lower C: N of *P. oceanica* hydrolysate, compared to MNM (150), *C. oleaginosus* also displayed higher lipid titers (6.8 $g.L^{-1}$), when grown on this hydrolysate (5.1 $g.L^{-1}$ lipids on MNM). Other factors, besides nitrogen-limitation, may be driving the fast growth and high lipid accumulation in the yeast cultivated on the seagrass hydrolysate. In that respect, phosphate limitation may contribute to lipid induction in this process. The effect of phosphate limitation on lipogenesis in yeast strains has been previously determined [161]. High carbon: phosphorus (C: P) ratio allowed for lipid accumulation in *Rhodosporidium toruloides*, which was maintained even in the presence of excess nitrogen [162]. As mentioned in **section 4.2.1: Seagrass Biomass**, phosphate was completely absent *P. oceanica* biomass. The enhanced performance of *C. oleaginosus* grown on the hydrolysate could be explained by the high C: P and relatively high C: N of *P. oceanica* biomass. Ideally, this hydrolysate could be exhibiting an optimal or golden C: N: P ratio, whereby allowing simultaneous high cell density and high lipid yield.

To validate the potential of this favorable feedstock, fed-batch fermentations were performed in a 1 L scale. Utilizing *P. oceanica* hydrolysate as the sole carbon-source in the base and the feed media, *C. oleaginosus* accumulated 24.5 $g.L^{-1}$ lipids, following 96h of fermentation. Seagrass biomass - to - microbial lipid conversion coefficient reached 208.4 $mg.g^{-1}$. In another study, microalgae hydrolysate of *Scenedesmus spp.* origin was supplemented with pure glucose as feedstock for *C. oleaginosus* fermentation to achieve a conversion coefficient of 120 $mg.g^{-1}$ [163].

A techno-economic analysis was performed for the fermentation process described in **Table 8**. Accordingly, the cost of microbial oil obtained from seagrass hydrolysate is estimated at 6.2 $€.kg^{-1}$. Although this value exceeds the production cost of vegetable oils (0.95 – 1.8 $€.kg^{-1}$), the environmental

and agricultural security concerns associated with these plantation crops outweighs their economic benefit [164]. Converting half the globally available seagrass via microbial fermentation into biodiesel is comparable to the entire B100 production of USA in 2015 (4.8 billion liters), 53 % of which is generated from edible crops [165]. Implementing seagrass biomass as feedstock in microbial lipid production platforms, as described in this work, can boost global B100 production by 26%. This carbon rich biomass thus represents a sustainable route for biodiesel production, reducing the need for fresh water and arable land in industrial applications.

Table 8. The parameter of *P. oceanica* hydrolysate-based fermentation at bioreactor scale (1L) and the fermentative potential of *C. oleaginosus*.

Parameters	Strain	*C. oleaginosus*
	Fermentation mode	fed-batch
	Volume (L)	1
	Fermentation time (h)	96
	Base media	*P. oceanica* hydrolysate
	Feed media	10x concentrated *P. oceanica* hydrolysate
Fermentative potential	Biomass ($g.L^{-1}$) at 72 h	42
	Lipid content (%, $g.g^{-1}$ DCW)	54.4
	Total lipid concentration ($g.L^{-1}$)	24.5
	Lipid productivity ($g.L^{-1}.h^{-1}$)	0.35
	Lipid coefficient ($mg.g^{-1}$)	208.4
	Fatty acid content (%, $g.g^{-1}$ DCW)	C16:0 (34.7) C18:0 (6.2) C18:1 (51.2) other (7.9)

4.4.2 Fermentation on microalgae hydrolysate

Three industrially relevant oleaginous yeast strains, *C. oleaginosus*, *C. curvatus* and *R. toruloides* were cultivated on *S. obtusiusculus* hydrolysate as the sole carbon source in shake flasks experiments (50 mL) for 4 days. *C. oleaginosus* recorded the highest growth rate on *S. obtusiusculus* hydrolysate, reaching an OD_{600} of 30 following 4 days of fermentation, compared to an OD_{600} of 22 on MNM. In comparison, *C. curvatus* and *R. toruloides* exhibited deterred growth. This phenomenon could be explained by the high tolerance of *C. oleaginosus,* compared to these strains, to inhibitory compounds including phenolic acids and bacteriostatic agents. These compounds are usually found in fresh microalgae samples, and could still be present, albeit at low concentration, in *S. obtusiusculus* hydrolysate [166,167]. *C. oleaginosus* also displayed higher lipid titers than the other 2 strains, as indicated by Nile red analysis, a relative quantitation method for rapid estimation of lipid titers in MTP scale.

Based on these results, we underscore the compatibility of *S. obtusiusculus* hydrolysate as feedstock for *C. oleaginosus* production platforms.

Compared to MNM (5.3 $g.L^{-1}$), fermentation of *C. oleaginosus* on *S. obtusiusculus* hydrolysate resulted in the accumulation of 3.6 $g.L^{-1}$ lipids. Although the yeast displayed 36% higher biomass accumulation on *S. obtusiusculus* hydrolysate, intracellular lipid accumulation was higher on MNM (61% $g.g^{-1}$) than the hydrolysate (35% $g.g^{-1}$), thus resulting in higher total productivity on MNM. Compared to our experimental setup (50 mL shake flask), oleaginous yeasts cultivated in a 2 L fermenter of macroalgae hydrolysate achieved similar lipid content of 37% ($g.g^{-1}$) [168]. Improved lipid yields could be obtained at scaled-up experiments, where *S. obtusiusculus* hydrolysate would prove a cost-effective alternative for the expensive synthetic MNM media components.

4.5 Outlook

The development of biorefinery industry of SCOs requires inexpensive sugar streams for downstream biological fermentation [169]. In order to improve the economics of these platforms, several aspects of the process require further development.

Commercially available enzyme systems remain pricey, which add to the overall costs of the upstream process. Enzymatic preparation from various microorganisms, namely fungi (e.g. *Trichoderma spp.*), could offer a cost-effective alternative to their commercial counterpart [170]. This field is particularly active in the bio-detergent sector [171]. Cost reductions in bioprocessing could also be achieved via modified microorganisms capable of producing both: the hydrolase and lipids [172]. In this context, co-culturing of a hydrolytic enzyme-producing strain with a high lipid producing strain is another alternative approach [173].

More work should be conducted towards constructing phylogenetic relatedness of global seagrass populations, as it is predicted that 91 % of the entire seagrass diversity remains unknown [174]. In that respect, newly identified species could hold more potential (advantageous traits) for SCOs processes. Furthermore, the fermentative potential of prominent oleaginous yeasts (e.g*., Y. lipolytica*, *L. starkeyi* and *R. toruloides*) should be also evaluated to assess their compatibility with the seagrass hydrolysate. Despite its many industrial advantages (high density and low moisture content), the use of seagrass as feedstock for SCO production still suffers from logistic drawbacks. Collection and transportation of beach-cast residues from around the globe contribute largely to the cost of the overall process. We thus suggest a decentralized model for processing of biofuels, where small hydrolysis/fermentation units could be established at seagrass collection sites, near remote beaches and coastal areas.

With respect to *S. obtusiusculus* biomass, a more detailed biomass analysis is necessary to better elucidate the composition of the resulting hydrolysate, and accurately determine C: N and C: P. As stated previously (**section 4.2.1: Seagrass Biomass**), soluble phosphates could be precipitated and quenched by various metal ions, such as Ca^{2+}, Mg^{2+}, or Fe^{3+}, resulting in a hydrolysate with both nitrogen and phosphate limitations [161]. Upscaling the bioprocess to a bioreactor fermenter, in addition to conducting techno-economic studies, would validate the use of microalgae hydrolysate for industrial applications. Finally, a waste-free, cyclic and "zero concept" biorefinery process could be implemented by integrating yeast and algae species in a single SCO platform. This could be achieved in a co-culture or via consecutive fermentation processes, where CO_2 is photosynthetically converted to lipids in the algae, the residue of which is then fed to the yeast for more lipid generation [128]. Visual illustration of such a process is presented in **Fig. 4.**

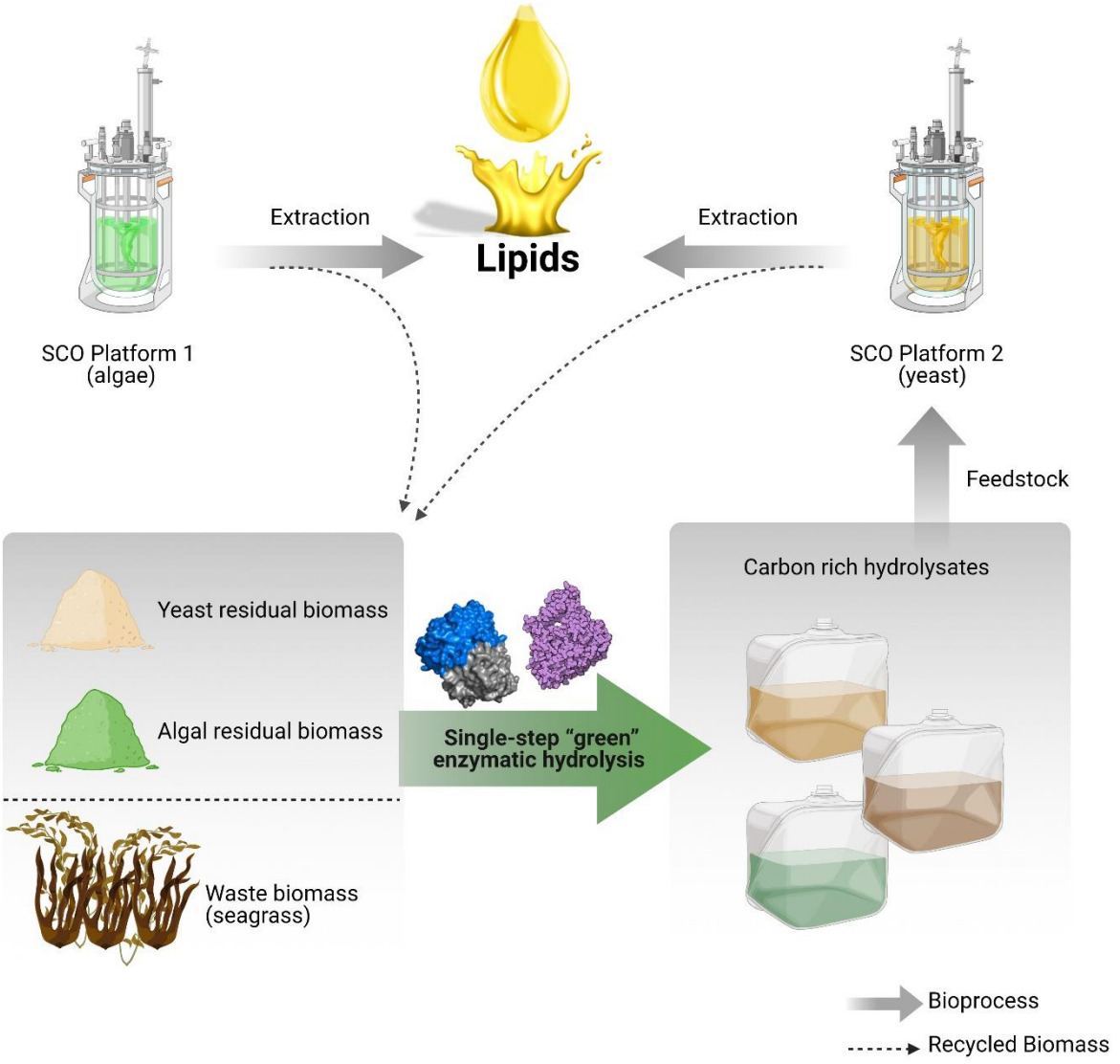

Fig. 4 Illustration of waste-free, cyclic "zero concept" biorefinery process

Further characterization of *C. oleaginosus* with respect to nutrient requirements, including essential vitamins and minerals is requisite to the development of this SCO production platform. Additionally, strain development can be performed by accelerated adaptation to a desired nutrient environment. This can be achieved by repeatedly subjecting the yeast to a mutagenic agent (e.g., UV and fast neutron radiation) during cultivation on the desired hydrolysate [58]. Screening for enhanced mutant strains displaying improved characteristics (enhanced biomass and lipid yields) typically follows. Finally, to evaluate the fermentative potentials of various yeasts cultivated in proposed hydrolysates, a fast lipid qualification methodology is needed. To that end, we have recently developed a high-throughput miniaturized Nile red method, that efficiently, rapidly and reliably allows for the absolute lipid quantitation $g.L^{-1}$ (compared to the widely used but limited relative lipid quantitation % $g.g^{-1}$ technique) of intracellular lipids for large samples pool [58]. Briefly, the approach implements oleic acid (C18:1) as a standard the determination of lipid titers at a 96-wells microtiter plates (MTP)-scale. Compared to commercially available standards (e.g., triolein), oleic acid is inexpensive, easy to handle and does not require a toxic organic solvent carrier. This high-throughput and miniaturized technique enables greater depth of strain characterization and can be applied for the screening of various oleaginous microorganisms such as *Y. lipolytica*, *L. starkeyi* and *R. toruloides* [58].

5. Discussion and Outlook Chapter 2

5.1 Prokaryotic platform development

As for their eukaryotic counterparts, industrial applications of bacterial-derived valuable products, including bioplastics and biopolymers (e.g. PHB, PHA), still suffer from various technical and environmental challenges [133]. These include costly feedstock, underdeveloped host systems, low product yields and inconsistent fermentation processes, in addition to physical (thermoplastic properties) limitations of the end-products [92,132].

This work primarily addresses several of the aforementioned technical constraints pertaining to bacterial bioplastic production. Prokaryotic platform development was pursued with respect to:

- → **Section 5.2: Selection of proper host system for subsequent production of 3HB**
- → **Section 5.3: Improving 3HB yield by engineering cofactor supply**

5.2 Selection of proper host system

As stated previously, utilizing native PHB producers (mainly halophiles) as production platforms suffers from various drawbacks, including extreme fermentation conditions and inaccessibility to genomic modulation [92,131]. Nevertheless, these bacteria are an attractive source of enzymes for the production of 3HB and PHB. To overcome the challenges posed by halophilic microorganisms, we opted for recombinant expression of enzymes from the PHB metabolic pathway in the model host, *E. coli*. In this work, we transformed the 3HB production platform (gratefully provided by Prof. Gen Larsson from KTH Royal Institute of Technology in Sweden), which includes the recombinant genes t3 and rx, into *E. Coli* BL21 strains [133]. This 3HB production platform would be easily amenable to any subsequent genetic and metabolic manipulation. Furthermore, amongst the various *E. coli* strains, BL-21 in particular is a low acetate-forming host, the main competing pathway for 3HB [132].

5.3 Improving 3HB yield by engineering cofactor supply

Despite the increase in 3HB titers by using nutrient-limited cultivation processes, a ceiling is reached when relying on bioprocess design strategies alone [92,131]. Strain development via genetic engineering can bypass these limitations. As stated previously (**section 3.3.2: Summary III.**), 3HB production involves three catalytic steps, starting from the central metabolite acetyl-CoA [133]. In this study, we pursued the enhancement of 3HB titers by enriching the intracellular CoA/acetyl-CoA pools. This strategy targets alleviating the bottleneck in the universal CoA biosynthesis system by modulating pantothenate kinase (PanK) gene. Four PanKs genes of distinct taxonomic origins (mammalian, fungal and bacterial) were codon-optimized and individually cloned in pet28a plasmid, and subsequently expressed in 3HB producing *E. coli* BL-21 cells. The rationale behind overexpressing eukaryotic PanKs

(PanKII family) in a prokaryotic system (PanKI family) lies in the differential regulation by CoA/acetyl-CoA. In contrast to PanKI enzyme, PanKII is selectively and potently inhibited by acetyl-CoA rather than free CoA [136]. In our designed strains, the recombinant 3HB-production system would direct the metabolic flux from acetyl-CoA to 3HB, constantly alleviating the feedback inhibition on PanKII. This rationale was validated in shake flask studies**,** where 3HB titers reflect cytosolic CoA/acetyl-CoA levels. Strains overexpressing *Aspergillus nidulans* PankII and *Mus musculus* PanK1β (PanKII family) produced 0.13 and 0.15 $g.L^{-1}$ of 3HB respectively, compared to only 0.11 $g.L^{-1}$ of 3HB produced by both the control strain (pJBGT3RX alone) and strain overexpressing prokaryotic PanKI. The significant increase in 3HB titers (36 %) in PanK1β strain compared to the control strain can be attributed to the unique characteristics of this particular enzyme. In contrast to its eukaryotic family members (PankII), PanK1β is only weakly regulated by acetyl-CoA, and, interestingly, its activity is stimulated by free CoA [175].

To evaluate the potential of this enhanced strain at industrial scale, fed-batch fermentations were performed in a 1.3 L parallel bioreactor. Following 24 h of fermentation, *E. coli* PanK1β strain produced 7.6 $g.L^{-1}$ of 3HB, compared to 5.4 $g.L^{-1}$ in the control strain. Previous work on recombinant 3HB production in *E. coli* reported titers ranging between 4 to 16 $g.L^{-1}$ [92,130,133,132]. As CoA and acetyl-CoA are essential intermediates (co-factors) in numerous biosynthetic pathways and a wide variety of biochemical reactions, overexpressing pantothenate kinase, in particular PanK1β, constitutes a suitable strategy for prokaryotic platform development.

5.4 Outlook

The strategies for the development of 3HB microbial platform investigated in this study, resulted in improved overall titers. Whether this production system is viable for industrial applications could be determined by a detailed techno-economic analysis in a subsequent step. For the successful industrial implementation of this technology, further process optimization may include:

- Utilizing lignocellulosic biomass hydrolysate (e.g., wheat, straw, or marine biomass) as a cheap, sustainable alternative to expensive carbon-sources (e.g., glucose), and subsequent implementation of cyclic biorefinery concept. However, given that hydrolysates containing pentoses and hexoses represent a difficult fermentation media for *E. coli*, we are actively developing a ptsG knockout strain that enables simultaneous utilization of these lignocellulosic-based monosaccharides [176]. Deletion of the glucose-specific permease of the phosphotransferase system (ptsG), relieves the carbon catabolite repression (ccr) that controls the order in which different carbon sources are metabolized (initiated by glucose) [176]. Additionally, we designed and incorporated an artificial Dahms metabolic pathway in the

recombinant strain in order to drive the flux of pentoses to key intermediates of 3HB, thus improving its titers. Bacteria such as *E. coli* metabolizes xylose via the pentose phosphate pathway (PPP) generating pyruvate, and eventually feeding into the acetyl-CoA pool. In *Pseudomonas,* xylose metabolism occurs through the distinct Dahms pathway, which converts xylose into glycoaldehyde and pyruvate via 3 enzymatic steps, representing a metabolic shortcut or sink for xylose [177,178]. Heterologous expression of enzymes from the Dahms pathway in *E. coli* led to the production of numerous high-value chemicals from xylose, including xylonic acid, ethylene glycol, and biopolymers [179-181].

- Integrating a one-plasmid system, adopting other nutrient-limitation (e.g., phosphate) modes, and carrying out high cell-density fermentations (uncoupling growth and product formation), are of high-importance and should be investigated [133].
- Modulating the thermodynamic "push and pull" for 3HB biosynthesis would drive the carbon flux more stringently towards 3HB production, and away from unfavorable pathways (e.g., acetate). Accordingly, combining the strategy set in this work with increasing other co-factors pools (e.g., NADPH), engineering a thioesterase with increased substrate specificity for 3HB-CoA, and knocking down competing pathways, could greatly improve 3HB titers [130,132,133].

The findings of this work are not only relevant for 3HB monomer production but also contribute to the general knowledge and the industrial application of various 3HB-derived products, mainly the biopolymer PHB. Even with improved titers and economics, recombinantly produced PHB and PHA, as in the case of its natural counterpart, still suffers from poor physio-chemical properties (high crystallinity, brittleness, stiffness, high melting point) [182].

- Utilizing the robust *Pseudomonas sp.* as host for PHA/PHB biosynthesis could help tackle these issues. This natural PHA producer has high tolerance to solvents and oxidative stress conditions, and is capable to breakdown various recalcitrant compounds [183]. Recently, due to its metabolic versatility and the advancement in synthetic biology, *Pseudomonas sp.* have been utilized as platform for tailor-made biopolymers. Incorporation of functional chemical groups and monomers (e.g., methyl, phenyl, phenoxy groups, halogenated monomers) helped improve the physiochemical proprieties of the biopolymer [184]. Challenges still hinder the efficient biopolymer production in *Pseudomonas sp.* Enriching the intracellular pool of cofactors (e.g., CoA, acetyl-CoA) could improve the monomers and PHA titers in this bacterium.
- And stated previously, the biopolymers are almost entirely in R- configuration due to the substrate and stereo-specificity of enzymes involved in their biosynthesis. Enzyme

engineering could help improve their proprieties, and meet the required demands in terms of activity, selectivity and stability [185]. Random and directed evolution can be applied to modulate target enzymes *in vivo* or *in vitro*, via metabolic engineering (where an external carbon source such as glucose is used) and enzymatic cascades approaches (where a defined precursor molecule is added) [185]. Enzyme Enantioselectivity have been the focus of various studies [186,187].

- In order to modulate the tacticity of the final polymer product, we propose a 2-step enzymatic strategy: (1) in-vivo lactonization of 3HB into 3-hydroxyburyrolactone (3HBL), followed by (2) an in-vitro ring-opening polymerization. The rational is that the 2nd step would randomly open and polymerize the lactones, generating a polymer with mixture of R and S entities (**Fig. 5**)

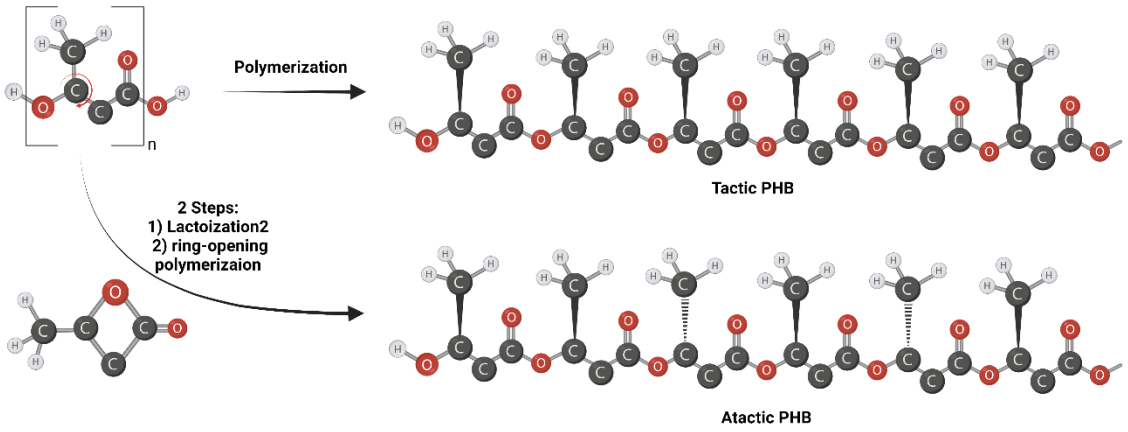

Fig. 5 Schematic for a 2-step enzymatic strategy to generate atactic PHB.

6. Final Outlook

The ultimate goal for microbial-based processes is sustainable and profitable production of biofuels, bioenergy, oleochemicals and high-value compounds. Early research has improved our understanding of the fermentation process and biochemical events that lead to SCOs accumulation. That said, these substantial advancements have failed to lead to wide-spread industrial implementation of microbial-based biorefineries. The major barriers remain the total cost of the bioprocess and the overall yield of the desired product. Valorization of low-value biomass in cyclic "Zero concept" biorefinery approach is crucial for the commercial viability of the bioprocesses. Ongoing development of synthetic biology tools (genetic engineering), analytical methods (selection methods), systems biology models (predictive tools), and protein design/evolution methods are also central to circumvent these barriers [188-190]. Finally, state-of-the-art robotics, artificial neural networks (ANNs) as well as Big Data analysis might hold the key for universal implementation SCO-based biorefineries [191-193].

7. List of Publications

7.1 A Seagrass-Based Biorefinery for Generation of Single-Cell Oils for Biofuel and Oleochemical Production

Mahmoud A. Masri, Samer Younes, Martina Haack, Farah Qoura, Norbert Mehlmer, and Thomas Brück

Energy Technology, 2017 September 27

DOI: 10.1002/ente.201700604

Page 29, Section 3: Overview of Included Publications

7.2 Microbial lipid production by oleaginous yeasts grown on *Scenedesmus obtusiusculus* microalgae biomass hydrolysate

Samer Younes, Felix Bracharz, Dania Awad, Farah Qoura, Norbert Mehlmer & Thomas Brueck

Bioprocess and Biosystems Engineering, 2020 April 28

DOI: 10.1007/s00449-020-02354-0

Page 47, Section 3: Overview of Included Publications

7.3 Systems Biology Engineering of the Pantothenate Pathway to Enhance 3HB Productivity in Escherichia coli

Samer Younes, Dania Awad, Elias Kassab, Martina Haack, Claudia Schuler, Norbert Mehlmer & Thomas Brueck

Biotechnology and Bioprocess Engineering, 2021, September 09

DOI: 10.1007/s12257-021-0033-1

Page 61, Section 3: Overview of Included Publications

7.4 Towards High-Throughput Optimization of Microbial Lipid Production: From Strain Development to Process Monitoring

Dania Awad, Samer Younes, Matthias Glemser, Franz Wagner, Gerhard Schenk, Norbert Mehlmer and Thomas Brueck

Sustainable Energy and Fuels, 2020 June 17

DOI: 10.139/D0SE00540A

Page 123, Section 12: Additional Full Length Publication

8. References

1 Fernando, S., Adhikari, S., Chandrapal, C. & Murali, N. Biorefineries: current status, challenges, and future direction. *Energy & Fuels* **20**, 1727-1737 (2006).

2 Cheah, W. Y. *et al.* Pretreatment methods for lignocellulosic biofuels production: current advances, challenges and future prospects. *Biofuel Research Journal* **7**, 1115 (2020).

3 Ainsworth, E., Lemonnier, P. & Wedow, J. The influence of rising tropospheric carbon dioxide and ozone on plant productivity. *Plant Biology* **22**, 5-11 (2020).

4 *Commodity Markets Review*, <https://ycharts.com/indicators/europe_natural_gas_price> (2021).

5 Bhatt, S. M. & Bal, J. S. in *Sustainable Approaches for Biofuels Production Technologies* 1-23 (Springer, 2019).

6 Nations, U. *The 17 Goals*, <https://sdgs.un.org/goals> (

7 Awad, D., Bohnen, F., Mehlmer, N. & Brueck, T. Multi-factorial-guided media optimization for enhanced biomass and lipid formation by the oleaginous yeast Cutaneotrichosporon oleaginosus. *Frontiers in bioengineering and biotechnology* **7**, 54 (2019).

8 Masri, M. A. *et al.* A Seagrass-Based Biorefinery for Generation of Single-Cell Oils for Biofuel and Oleochemical Production. *Energy Technology* **6**, 1026-1038 (2018).

9 Den, W., Sharma, V. K., Lee, M., Nadadur, G. & Varma, R. S. Lignocellulosic biomass transformations via greener oxidative pretreatment processes: access to energy and value-added chemicals. *Frontiers in chemistry* **6**, 141 (2018).

10 de Jong, E., Higson, A., Walsh, P. & Wellisch, M. Bio-based chemicals value added products from biorefineries. *IEA Bioenergy, Task42 Biorefinery* **34** (2012).

11 Piemonte, V. Wood residues as raw material for biorefinery systems: LCA case study on bioethanol and electricity production. *Journal of Polymers and the Environment* **20**, 299-304 (2012).

12 Nguyen, T. K. https://www. sciencedirect. com/science/article/abs/pii/S1755458621000293? via% 3Dihub#! (2021).

13 Luo, L., van der Voet, E. & Huppes, G. Biorefining of lignocellulosic feedstock–Technical, economic and environmental considerations. *Bioresource technology* **101**, 5023-5032 (2010).

14 Moncada, J., Cardona, C. A. & Rincón, L. E. Design and analysis of a second and third generation biorefinery: The case of castorbean and microalgae. *Bioresource Technology* **198**, 836-843 (2015).

15 Maity, S. K. Opportunities, recent trends and challenges of integrated biorefinery: Part I. *Renewable and Sustainable Energy Reviews* **43**, 1427-1445 (2015).

16 Cherubini, F. *et al.* Toward a common classification approach for biorefinery systems. *Biofuels, Bioproducts and Biorefining* **3**, 534-546 (2009).

17 Gunstone, F. D. & Hamilton, R. J. *Oleochemical manufacture and applications*. Vol. 4 (CRC Press, 2001).

18 Pfleger, B. F., Gossing, M. & Nielsen, J. Metabolic engineering strategies for microbial synthesis of oleochemicals. *Metabolic engineering* **29**, 1-11 (2015).

19 Yan, Q. & Pfleger, B. F. Revisiting metabolic engineering strategies for microbial synthesis of oleochemicals. *Metabolic engineering* **58**, 35-46 (2020).

20 Zhou, Y. J. *et al.* Production of fatty acid-derived oleochemicals and biofuels by synthetic yeast cell factories. *Nature communications* **7**, 1-9 (2016).

21 Biermann, U., Bornscheuer, U., Meier, M. A., Metzger, J. O. & Schäfer, H. J. Oils and fats as renewable raw materials in chemistry. *Angewandte Chemie International Edition* **50**, 3854-3871 (2011).

22 Vaughn, S. F. & Holser, R. A. Evaluation of biodiesels from several oilseed sources as environmental friendly contact herbicides. *Industrial Crops and Products* **26**, 63-68 (2007).

23 Yu, A.-Q., Pratomo Juwono, N. K., Leong, S. S. J. & Chang, M. W. Production of fatty acid-derived valuable chemicals in synthetic microbes. *Frontiers in bioengineering and biotechnology* **2**, 78 (2014).
24 Lu, X. A perspective: photosynthetic production of fatty acid-based biofuels in genetically engineered cyanobacteria. *Biotechnology advances* **28**, 742-746 (2010).
25 Lee, I., Johnson, L. A. & Hammond, E. G. Use of branched-chain esters to reduce the crystallization temperature of biodiesel. *Journal of the American Oil Chemists' Society* **72**, 1155-1160 (1995).
26 Tao, H., Guo, D., Zhang, Y., Deng, Z. & Liu, T. Metabolic engineering of microbes for branched-chain biodiesel production with low-temperature property. *Biotechnology for biofuels* **8**, 1-11 (2015).
27 Guo, D., Zhu, J., Deng, Z. & Liu, T. Metabolic engineering of Escherichia coli for production of fatty acid short-chain esters through combination of the fatty acid and 2-keto acid pathways. *Metabolic engineering* **22**, 69-75 (2014).
28 Longo, M. A. & Sanromán, M. A. Production of food aroma compounds: microbial and enzymatic methodologies. *Food Technology and Biotechnology* **44**, 335-353 (2006).
29 Bruder, S., Moldenhauer, E. J., Lemke, R. D., Ledesma-Amaro, R. & Kabisch, J. Drop-in biofuel production using fatty acid photodecarboxylase from Chlorella variabilis in the oleaginous yeast Yarrowia lipolytica. *Biotechnology for biofuels* **12**, 1-13 (2019).
30 Kargbo, H., Harris, J. S. & Phan, A. N. "Drop-in" fuel production from biomass: Critical review on techno-economic feasibility and sustainability. *Renewable and Sustainable Energy Reviews* **135**, 110168 (2021).
31 Buijs, N. A., Zhou, Y. J., Siewers, V. & Nielsen, J. Long-chain alkane production by the yeast Saccharomyces cerevisiae. *Biotechnology and bioengineering* **112**, 1275-1279 (2015).
32 Jannin, V. & Cuppok, Y. Hot-melt coating with lipid excipients. *International journal of pharmaceutics* **457**, 480-487 (2013).
33 Kassab, E., Fuchs, M., Haack, M., Mehlmer, N. & Brueck, T. B. Engineering Escherichia coli FAB system using synthetic plant genes for the production of long chain fatty acids. *Microbial cell factories* **18**, 1-10 (2019).
34 Kassab, E., Mehlmer, N. & Brueck, T. GFP Scaffold-Based Engineering for the Production of Unbranched Very Long Chain Fatty Acids in Escherichia coli With Oleic Acid and Cerulenin Supplementation. *Frontiers in bioengineering and biotechnology* **7**, 408 (2019).
35 Lu, C., Napier, J. A., Clemente, T. E. & Cahoon, E. B. New frontiers in oilseed biotechnology: meeting the global demand for vegetable oils for food, feed, biofuel, and industrial applications. *Current opinion in biotechnology* **22**, 252-259 (2011).
36 Miwa, T. K. Structural determination and uses of jojoba oil. *Journal of the American Oil Chemists' Society* **61**, 407-410 (1984).
37 Taylor, D. C. *et al.* Brassica carinata–a new molecular farming platform for delivering bio-industrial oil feedstocks: case studies of genetic modifications to improve very long-chain fatty acid and oil content in seeds. *Biofuels, Bioproducts and Biorefining* **4**, 538-561 (2010).
38 Wisniak, J. Potential uses of jojoba oil and meal—a review. *Industrial Crops and products* **3**, 43-68 (1994).
39 Rupilius, W. & Ahmad, S. The changing world of oleochemicals. *Palm Oil Dev* **44**, 21-28 (2006).
40 Smith, V. H., Sturm, B. S., Denoyelles, F. J. & Billings, S. A. The ecology of algal biodiesel production. *Trends in ecology & evolution* **25**, 301-309 (2010).
41 Danielsen, F. *et al.* Biofuel plantations on forested lands: double jeopardy for biodiversity and climate. *Conservation Biology* **23**, 348-358 (2009).
42 Koizumi, T. Biofuels and food security. *Renewable and Sustainable Energy Reviews* **52**, 829-841 (2015).
43 Li, Q., Du, W. & Liu, D. Perspectives of microbial oils for biodiesel production. *Applied microbiology and biotechnology* **80**, 749-756 (2008).

44 Ochsenreither, K., Glück, C., Stressler, T., Fischer, L. & Syldatk, C. Production strategies and applications of microbial single cell oils. *Frontiers in microbiology* **7**, 1539 (2016).

45 Cohen, Z. & Ratledge, C. *Single cell oils: microbial and algal oils*. (AOCS Publishing, 2005).

46 Ratledge, C. Fatty acid biosynthesis in microorganisms being used for single cell oil production. *Biochimie* **86**, 807-815 (2004).

47 Koch, B., Schmidt, C. & Daum, G. Storage lipids of yeasts: a survey of nonpolar lipid metabolism in Saccharomyces cerevisiae, Pichia pastoris, and Yarrowia lipolytica. *FEMS microbiology reviews* **38**, 892-915 (2014).

48 Alvarez, H. M. Triacylglycerol and wax ester-accumulating machinery in prokaryotes. *Biochimie* **120**, 28-39 (2016).

49 Escapa, I. F., García, J. L., Bühler, B., Blank, L. M. & Prieto, M. A. The polyhydroxyalkanoate metabolism controls carbon and energy spillage in Pseudomonas putida. *Environmental Microbiology* **14**, 1049-1063 (2012).

50 Bracharz, F., Beukhout, T., Mehlmer, N. & Brück, T. Opportunities and challenges in the development of Cutaneotrichosporon oleaginosus ATCC 20509 as a new cell factory for custom tailored microbial oils. *Microbial cell factories* **16**, 1-15 (2017).

51 Ratledge, C. & Cohen, Z. Microbial and algal oils: do they have a future for biodiesel or as commodity oils? *Lipid Technology* **20**, 155-160 (2008).

52 Papanikolaou, S. & Aggelis, G. Lipids of oleaginous yeasts. Part I: Biochemistry of single cell oil production. *European Journal of Lipid Science and Technology* **113**, 1031-1051 (2011).

53 Tchakouteu, S. S. *et al.* Oleaginous yeast Cryptococcus curvatus exhibits interplay between biosynthesis of intracellular sugars and lipids. *European Journal of Lipid Science and Technology* **117**, 657-672 (2015).

54 Ageitos, J. M., Vallejo, J. A., Veiga-Crespo, P. & Villa, T. G. Oily yeasts as oleaginous cell factories. *Applied microbiology and biotechnology* **90**, 1219-1227 (2011).

55 Huang, C., Chen, X.-f., Xiong, L., Ma, L.-l. & Chen, Y. Single cell oil production from low-cost substrates: the possibility and potential of its industrialization. *Biotechnology advances* **31**, 129-139 (2013).

56 Kyle, D. J. in *Single Cell Oils* 439-451 (Elsevier, 2010).

57 Younes, S. *et al.* Microbial lipid production by oleaginous yeasts grown on Scenedesmus obtusiusculus microalgae biomass hydrolysate. *Bioprocess and biosystems engineering* **43**, 1629-1638 (2020).

58 Awad, D. *et al.* Towards high-throughput optimization of microbial lipid production: from strain development to process monitoring. *Sustainable Energy & Fuels* **4**, 5958-5969 (2020).

59 Probst, K. V., Schulte, L. R., Durrett, T. P., Rezac, M. E. & Vadlani, P. V. Oleaginous yeast: a value-added platform for renewable oils. *Critical reviews in biotechnology* **36**, 942-955 (2016).

60 Sergeeva, Y. E. *et al.* Calculation of biodiesel fuel characteristics based on the fatty acid composition of the lipids of some biotechnologically important microorganisms. *Applied biochemistry and microbiology* **53**, 807-813 (2017).

61 Meesters, P., Huijberts, G. & Eggink, G. High-cell-density cultivation of the lipid accumulating yeast Cryptococcus curvatus using glycerol as a carbon source. *Applied microbiology and biotechnology* **45**, 575-579 (1996).

62 Ratledge, C. & Wynn, J. P. The biochemistry and molecular biology of lipid accumulation in oleaginous microorganisms. *Advances in applied microbiology* **51**, 1-52 (2002).

63 Papanikolaou, S. *et al.* Importance of the methyl-citrate cycle on glycerol metabolism in the yeast Yarrowia lipolytica. *Journal of biotechnology* **168**, 303-314 (2013).

64 Jacob, Z. Yeast lipid biotechnology. *Advances in applied microbiology* **39**, 185-212 (1993).

65 Volkman, J., Jeffrey, S., Nichols, P., Rogers, G. & Garland, C. Fatty acid and lipid composition of 10 species of microalgae used in mariculture. *Journal of experimental marine biology and ecology* **128**, 219-240 (1989).

66 Pinzi, S., Mata-Granados, J., Lopez-Gimenez, F., de Castro, M. L. & Dorado, M. Influence of vegetable oils fatty-acid composition on biodiesel optimization. *Bioresource technology* **102**, 1059-1065 (2011).
67 Patel, A. *et al.* An overview of potential oleaginous microorganisms and their role in biodiesel and omega-3 fatty acid-based industries. *Microorganisms* **8**, 434 (2020).
68 Thevenieau, F. & Nicaud, J.-M. Microorganisms as sources of oils. *Ocl* **20**, D603 (2013).
69 Tibocha-Bonilla, J. D., Zuñiga, C., Godoy-Silva, R. D. & Zengler, K. Advances in metabolic modeling of oleaginous microalgae. *Biotechnology for biofuels* **11**, 1-15 (2018).
70 Elrayies, G. M. Microalgae: prospects for greener future buildings. *Renewable and Sustainable Energy Reviews* **81**, 1175-1191 (2018).
71 Sing, S. F., Isdepsky, A., Borowitzka, M. A. & Moheimani, N. R. Production of biofuels from microalgae. *Mitigation and Adaptation Strategies for Global Change* **18**, 47-72 (2013).
72 Ratledge, C. Microbial oils: an introductory overview of current status and future prospects. *Ocl* **20**, D602 (2013).
73 Eroshin, V., Satroutdinov, A., Dedyukhina, E. & Chistyakova, T. Arachidonic acid production by Mortierella alpina with growth-coupled lipid synthesis. *Process Biochemistry* **35**, 1171-1175 (2000).
74 Patel, A., Arora, N., Sartaj, K., Pruthi, V. & Pruthi, P. A. Sustainable biodiesel production from oleaginous yeasts utilizing hydrolysates of various non-edible lignocellulosic biomasses. *Renewable and sustainable energy reviews* **62**, 836-855 (2016).
75 Meng, X. *et al.* Biodiesel production from oleaginous microorganisms. *Renewable energy* **34**, 1-5 (2009).
76 Maina, S. *et al.* Microbial oil production from various carbon sources by newly isolated oleaginous yeasts. *Engineering in Life Sciences* **17**, 333-344 (2017).
77 Lamers, D. *et al.* Selection of oleaginous yeasts for fatty acid production. *BMC biotechnology* **16**, 1-10 (2016).
78 Moon, N. J., Hammond, E. & Glatz, B. A. Conversion of cheese whey and whey permeate to oil and single-cell protein. *Journal of Dairy Science* **61**, 1537-1547 (1978).
79 Evans, C. T. & Ratledge, C. A comparison of the oleaginous yeast, Candida curvata, grown on different carbon sources in continuous and batch culture. *Lipids* **18**, 623-629 (1983).
80 Wu, S., Hu, C., Zhao, X. & Zhao, Z. K. Production of lipid from N-acetylglucosamine by Cryptococcus curvatus. *European journal of lipid science and technology* **112**, 727-733 (2010).
81 Masri, M. A. *et al.* A waste-free, microbial oil centered cyclic bio-refinery approach based on flexible macroalgae biomass. *Applied Energy* **224**, 1-12 (2018).
82 Masri, M. A., Garbe, D., Mehlmer, N. & Brück, T. B. A sustainable, high-performance process for the economic production of waste-free microbial oils that can replace plant-based equivalents. *Energy & Environmental Science* **12**, 2717-2732 (2019).
83 Awad, D. & Brueck, T. Optimization of protein isolation by proteomic qualification from Cutaneotrichosporon oleaginosus. *Analytical and bioanalytical chemistry* **412**, 449-462 (2020).
84 Fabiszewska, A., Misiukiewicz-Stępień, P., Paplińska-Goryca, M., Zieniuk, B. & Białecka-Florjańczyk, E. An insight into storage lipid synthesis by Yarrowia lipolytica yeast relating to lipid and sugar substrates metabolism. *Biomolecules* **9**, 685 (2019).
85 Beopoulos, A. *et al.* Yarrowia lipolytica as a model for bio-oil production. *Progress in lipid research* **48**, 375-387 (2009).
86 Garay, L. A., Boundy-Mills, K. L. & German, J. B. Accumulation of high-value lipids in single-cell microorganisms: a mechanistic approach and future perspectives. *Journal of agricultural and food chemistry* **62**, 2709-2727 (2014).
87 Sitepu, I. R. *et al.* Oleaginous yeasts for biodiesel: current and future trends in biology and production. *Biotechnology advances* **32**, 1336-1360 (2014).

88 Anjum, M. N. *et al.* Polyhydroxyalkanoates-based bionanocomposites. *Bionanocomposites*, 321-333 (2020).

89 Riaz, S., Rhee, K. Y. & Park, S. J. Polyhydroxyalkanoates (PHAs): biopolymers for biofuel and biorefineries. *Polymers* **13**, 253 (2021).

90 Amstutz, V., Hanik, N., Pott, J., Utsunomia, C. & Zinn, M. Tailored biosynthesis of polyhydroxyalkanoates in chemostat cultures. *Methods in enzymology* **627**, 99-123 (2019).

91 Ye, J. *et al.* Engineering of Halomonas bluephagenesis for low cost production of poly (3-hydroxybutyrate-co-4-hydroxybutyrate) from glucose. *Metabolic engineering* **47**, 143-152 (2018).

92 Jarmander, J. *et al.* Cultivation strategies for production of (R)-3-hydroxybutyric acid from simultaneous consumption of glucose, xylose and arabinose by Escherichia coli. *Microbial cell factories* **14**, 1-12 (2015).

93 Doi, Y. in *Macromolecular Symposia.* 585-599 (Wiley Online Library).

94 Yu, J. in *Bioprocessing for value-added products from renewable resources* 585-610 (Elsevier, 2007).

95 Anderson, A. J. & Dawes, E. A. Occurrence, metabolism, metabolic role, and industrial uses of bacterial polyhydroxyalkanoates. *Microbiological reviews* **54**, 450-472 (1990).

96 Wang, L., Chen, L., Yang, S. & Tan, X. Photosynthetic conversion of carbon dioxide to oleochemicals by cyanobacteria: Recent advances and future perspectives. *Frontiers in microbiology* **11**, 634 (2020).

97 Ji, X.-J., Ren, L.-J., Nie, Z.-K., Huang, H. & Ouyang, P.-K. Fungal arachidonic acid-rich oil: research, development and industrialization. *Critical reviews in biotechnology* **34**, 197-214 (2014).

98 Qin, L., Liu, L., Zeng, A.-P. & Wei, D. From low-cost substrates to single cell oils synthesized by oleaginous yeasts. *Bioresource technology* **245**, 1507-1519 (2017).

99 Mallick, N., Bagchi, S. K., Koley, S. & Singh, A. K. Progress and challenges in microalgal biodiesel production. *Frontiers in microbiology* **7**, 1019 (2016).

100 Webb, C., Koutinas, A. & Wang, R. Developing a sustainable bioprocessing strategy based on a generic feedstock. *Biomanufacturing*, 195-268 (2004).

101 Jin, M. *et al.* Microbial lipid-based lignocellulosic biorefinery: feasibility and challenges. *Trends in biotechnology* **33**, 43-54 (2015).

102 Valdés, G., Mendonça, R. T. & Aggelis, G. Lignocellulosic biomass as a substrate for oleaginous microorganisms: a review. *Applied Sciences* **10**, 7698 (2020).

103 Østby, H., Hansen, L. D., Horn, S. J., Eijsink, V. G. & Várnai, A. Enzymatic processing of lignocellulosic biomass: principles, recent advances and perspectives. *Journal of Industrial Microbiology & Biotechnology: Official Journal of the Society for Industrial Microbiology and Biotechnology* **47**, 623-657 (2020).

104 Zha, Y. *et al.* Identifying inhibitory compounds in lignocellulosic biomass hydrolysates using an exometabolomics approach. *BMC biotechnology* **14**, 1-16 (2014).

105 Huang, H. *et al.* Identification of crucial yeast inhibitors in bio-ethanol and improvement of fermentation at high pH and high total solids. *Bioresource technology* **102**, 7486-7493 (2011).

106 Chung, I. K., Beardall, J., Mehta, S., Sahoo, D. & Stojkovic, S. Using marine macroalgae for carbon sequestration: a critical appraisal. *Journal of applied phycology* **23**, 877-886 (2011).

107 Wirth, R. *et al.* Metagenome changes in the mesophilic biogas-producing community during fermentation of the green alga Scenedesmus obliquus. *Journal of Biotechnology* **215**, 52-61 (2015).

108 Subhadra, B. & Edwards, M. An integrated renewable energy park approach for algal biofuel production in United States. *Energy Policy* **38**, 4897-4902 (2010).

109 Htet, A. N. *et al.* Application of microalgae hydrolysate as a fermentation medium for microbial production of 2-pyrone 4, 6-dicarboxylic acid. *Journal of bioscience and bioengineering* **125**, 717-722 (2018).

110 Mahajan, D., Sengupta, S. & Sen, S. Strategies to improve microbial lipid production: Optimization techniques. *Biocatalysis and Agricultural Biotechnology* **22**, 101321 (2019).
111 Purnick, P. E. & Weiss, R. The second wave of synthetic biology: from modules to systems. *Nature reviews Molecular cell biology* **10**, 410-422 (2009).
112 Liang, M.-H. & Jiang, J.-G. Advancing oleaginous microorganisms to produce lipid via metabolic engineering technology. *Progress in lipid research* **52**, 395-408 (2013).
113 Krivoruchko, A., Zhang, Y., Siewers, V., Chen, Y. & Nielsen, J. Microbial acetyl-CoA metabolism and metabolic engineering. *Metabolic engineering* **28**, 28-42 (2015).
114 Rock, C. O., Park, H.-W. & Jackowski, S. Role of feedback regulation of pantothenate kinase (CoaA) in control of coenzyme A levels in Escherichia coli. *Journal of bacteriology* **185**, 3410-3415 (2003).
115 Yun, M. *et al.* Structural basis for the feedback regulation of Escherichia coli pantothenate kinase by coenzyme A. *Journal of Biological Chemistry* **275**, 28093-28099 (2000).
116 Suutari, M. & Laakso, S. Effect of growth temperature on the fatty acid composition of Mycobacterium phlei. *Archives of microbiology* **159**, 119-123 (1993).
117 Kjeldahl, C. A new method for the determination of nitrogen in organic matter. *Z Anal Chem* **22**, 366 (1883).
118 TSCHESCHE, H., GREENE, L. & TRUSCHEIT, E. agrammatic aid. The last section provides some 60 examples of every possible type of cosmetic emulsion with its specific formula and procedure for manufacture. This listing should prove particu-larly useful for academicians involved in teaching courses in cos-metic formulation.
119 Shetlar, M. & Masters, Y. F. Use of thymol-sulfuric acid reaction for determination of carbohydrates in biological material. *Analytical Chemistry* **29**, 402-405 (1957).
120 Díez, B., Pedrós-Alió, C. & Massana, R. Study of genetic diversity of eukaryotic picoplankton in different oceanic regions by small-subunit rRNA gene cloning and sequencing. *Applied and environmental microbiology* **67**, 2932-2941 (2001).
121 Kurtzman, C. & Robnett, C. Identification of clinically important ascomycetous yeasts based on nucleotide divergence in the 5'end of the large-subunit (26S) ribosomal DNA gene. *Journal of clinical microbiology* **35**, 1216-1223 (1997).
122 Bligh, E. G. & Dyer, W. J. A rapid method of total lipid extraction and purification. *Canadian journal of biochemistry and physiology* **37**, 911-917 (1959).
123 Folch, J., Lees, M. & Stanley, G. S. A simple method for the isolation and purification of total lipides from animal tissues. *Journal of biological chemistry* **226**, 497-509 (1957).
124 Sitepu, I. *et al.* An improved high-throughput Nile red fluorescence assay for estimating intracellular lipids in a variety of yeast species. *Journal of microbiological methods* **91**, 321-328 (2012).
125 McCurdy, A. T., Higham, A. J., Morgan, M. R., Quinn, J. C. & Seefeldt, L. C. Two-step process for production of biodiesel blends from oleaginous yeast and microalgae. *Fuel* **137**, 269-276 (2014).
126 Enríquez, S., Duarte, C. M. & Sand-Jensen, K. Patterns in decomposition rates among photosynthetic organisms: the importance of detritus C: N: P content. *Oecologia* **94**, 457-471 (1993).
127 Bai, A. *et al.* The significance of forests and algae in CO2 balance: A Hungarian case study. *Sustainability* **9**, 857 (2017).
128 Dillschneider, R., Schulze, I., Neumann, A., Posten, C. & Syldatk, C. Combination of algae and yeast fermentation for an integrated process to produce single cell oils. *Applied microbiology and biotechnology* **98**, 7793-7802 (2014).
129 Yen, H.-W. *et al.* Microalgae-based biorefinery–from biofuels to natural products. *Bioresource technology* **135**, 166-174 (2013).

130 Guevara-Martínez, M. *et al.* The role of the acyl-CoA thioesterase "YciA" in the production of (R)-3-hydroxybutyrate by recombinant Escherichia coli. *Applied microbiology and biotechnology* **103**, 3693-3704 (2019).

131 Guevara-Martínez, M. *et al.* Regulating the production of (R)-3-hydroxybutyrate in Escherichia coli by N or P limitation. *Frontiers in microbiology* **6**, 844 (2015).

132 Perez-Zabaleta, M. *et al.* Comparison of engineered Escherichia coli AF1000 and BL21 strains for (R)-3-hydroxybutyrate production in fed-batch cultivation. *Applied microbiology and biotechnology* **103**, 5627-5639 (2019).

133 Perez-Zabaleta, M. *et al.* Increasing the production of (R)-3-hydroxybutyrate in recombinant Escherichia coli by improved cofactor supply. *Microbial cell factories* **15**, 1-10 (2016).

134 Vadali, R. V., Bennett, G. N. & San, K.-Y. Cofactor engineering of intracellular CoA/acetyl-CoA and its effect on metabolic flux redistribution in Escherichia coli. *Metabolic engineering* **6**, 133-139 (2004).

135 Calder, R. B. *et al.* Cloning and characterization of a eukaryotic pantothenate kinase gene (panK) from Aspergillus nidulans. *Journal of Biological Chemistry* **274**, 2014-2020 (1999).

136 Rock, C. O., Karim, M. A., Zhang, Y.-M. & Jackowski, S. The murine pantothenate kinase (Pank1) gene encodes two differentially regulated pantothenate kinase isozymes. *Gene* **291**, 35-43 (2002).

137 Rakicka, M., Lazar, Z., Dulermo, T., Fickers, P. & Nicaud, J. M. Lipid production by the oleaginous yeast Yarrowia lipolytica using industrial by-products under different culture conditions. *Biotechnology for biofuels* **8**, 1-10 (2015).

138 Wang, R., Wang, J., Xu, R., Fang, Z. & Liu, A. Oil production by the oleaginous yeast Lipomyces starkeyi using diverse carbon sources. *BioResources* **9**, 7027-7040 (2014).

139 Torbatinejad, N. M., Annison, G., Rutherfurd-Markwick, K. & Sabine, J. R. Structural constituents of the seagrass Posidonia australis. *Journal of agricultural and food chemistry* **55**, 4021-4026 (2007).

140 Granger, L.-M., Perlot, P., Goma, G. & Pareilleux, A. Effect of various nutrient limitations on fatty acid production by Rhodotorula glutinis. *Applied Microbiology and Biotechnology* **38**, 784-789 (1993).

141 Shanklin, J. & Cahoon, E. B. Desaturation and related modifications of fatty acids. *Annual review of plant biology* **49**, 611-641 (1998).

142 Jenkins, D., Ferguson, J. F. & Menar, A. B. Chemical processes for phosphate removal. *Water research* **5**, 369-389 (1971).

143 Wang, Y. *et al.* Systems analysis of phosphate-limitation-induced lipid accumulation by the oleaginous yeast Rhodosporidium toruloides. *Biotechnology for biofuels* **11**, 1-15 (2018).

144 Huang, X. *et al.* Enhancement of lipid accumulation by oleaginous yeast through phosphorus limitation under high content of ammonia. *Bioresource technology* **262**, 9-14 (2018).

145 Gallagher, J. A., Turner, L. B., Adams, J. M., Dyer, P. W. & Theodorou, M. K. Dewatering treatments to increase dry matter content of the brown seaweed, kelp (Laminaria digitata ((Hudson) JV Lamouroux)). *Bioresource technology* **224**, 662-669 (2017).

146 Milledge, J. J., Smith, B., Dyer, P. W. & Harvey, P. Macroalgae-derived biofuel: a review of methods of energy extraction from seaweed biomass. *Energies* **7**, 7194-7222 (2014).

147 Miranda, J., Passarinho, P. C. & Gouveia, L. Bioethanol production from Scenedesmus obliquus sugars: the influence of photobioreactors and culture conditions on biomass production. *Applied microbiology and biotechnology* **96**, 555-564 (2012).

148 Spolaore, P., Joannis-Cassan, C., Duran, E. & Isambert, A. Commercial applications of microalgae. *Journal of bioscience and bioengineering* **101**, 87-96 (2006).

149 Richmond, A. *Handbook of microalgal culture: biotechnology and applied phycology*. (John Wiley & Sons, 2008).

150 Rodrigues, E. L. *et al.* Enzymatically and/or thermally treated Macroalgae biomass as feedstock for fermentative H2 production. *Matéria (Rio de Janeiro)* **24** (2019).

151 Silveira, M. H. L. *et al.* Current pretreatment technologies for the development of cellulosic ethanol and biorefineries. *ChemSusChem* **8**, 3366-3390 (2015).
152 Baral, P., Jain, L., Kurmi, A. K., Kumar, V. & Agrawal, D. Augmented hydrolysis of acid pretreated sugarcane bagasse by PEG 6000 addition: a case study of Cellic CTec2 with recycling and reuse. *Bioprocess and biosystems engineering* **43**, 473-482 (2020).
153 Sun, F. F. *et al.* Accessory enzymes influence cellulase hydrolysis of the model substrate and the realistic lignocellulosic biomass. *Enzyme and microbial technology* **79**, 42-48 (2015).
154 Ramos, L. P. *et al.* Enzymatic hydrolysis of steam-exploded sugarcane bagasse using high total solids and low enzyme loadings. *Bioresource technology* **175**, 195-202 (2015).
155 Lopes, H. J. S., Bonturi, N., Kerkhoven, E. J., Miranda, E. A. & Lahtvee, P.-J. C/N ratio and carbon source-dependent lipid production profiling in Rhodotorula toruloides. *Applied microbiology and biotechnology* **104**, 2639-2649 (2020).
156 Yanagisawa, M., Nakamura, K., Ariga, O. & Nakasaki, K. Production of high concentrations of bioethanol from seaweeds that contain easily hydrolyzable polysaccharides. *Process Biochemistry* **46**, 2111-2116 (2011).
157 Shokrkar, H., Ebrahimi, S. & Zamani, M. Bioethanol production from acidic and enzymatic hydrolysates of mixed microalgae culture. *Fuel* **200**, 380-386 (2017).
158 Kim, N.-J., Li, H., Jung, K., Chang, H. N. & Lee, P. C. Ethanol production from marine algal hydrolysates using Escherichia coli KO11. *Bioresource technology* **102**, 7466-7469 (2011).
159 Seon, G. *et al.* Effect of post-treatment process of microalgal hydrolysate on bioethanol production. *Scientific reports* **10**, 1-12 (2020).
160 Li, Y., Zhao, Z. K. & Bai, F. High-density cultivation of oleaginous yeast Rhodosporidium toruloides Y4 in fed-batch culture. *Enzyme and microbial technology* **41**, 312-317 (2007).
161 Zhang, G. *et al.* Microbial lipid production as biodiesel feedstock from N-acetylglucosamine by oleaginous microorganisms. *Journal of Chemical Technology & Biotechnology* **86**, 642-650 (2011).
162 Wu, S., Hu, C., Jin, G., Zhao, X. & Zhao, Z. K. Phosphate-limitation mediated lipid production by Rhodosporidium toruloides. *Bioresource technology* **101**, 6124-6129 (2010).
163 Meo, A., Priebe, X. L. & Weuster-Botz, D. Lipid production with Trichosporon oleaginosus in a membrane bioreactor using microalgae hydrolysate. *Journal of biotechnology* **241**, 1-10 (2017).
164 Koutinas, A. A., Chatzifragkou, A., Kopsahelis, N., Papanikolaou, S. & Kookos, I. K. Design and techno-economic evaluation of microbial oil production as a renewable resource for biodiesel and oleochemical production. *Fuel* **116**, 566-577 (2014).
165 Conti, J. *et al.* International energy outlook 2016 with projections to 2040. (USDOE Energy Information Administration (EIA), Washington, DC (United States …, 2016).
166 Pradhan, J., Das, S. & Das, B. K. Antibacterial activity of freshwater microalgae: A review. *African Journal of Pharmacy and Pharmacology* **8**, 809-818 (2014).
167 Braidy, N. *et al.* Neuroprotective effects of rosmarinic acid on ciguatoxin in primary human neurons. *Neurotoxicity research* **25**, 226-234 (2014).
168 Abeln, F. *et al.* Lipid production through the single-step microwave hydrolysis of macroalgae using the oleaginous yeast Metschnikowia pulcherrima. *Algal research* **38**, 101411 (2019).
169 Ragauskas, A. J. *et al.* The path forward for biofuels and biomaterials. *science* **311**, 484-489 (2006).
170 Kancelista, A., Chmielewska, J., Korzeniowski, P. & Łaba, W. Bioconversion of Sweet Sorghum Residues by Trichoderma citrinoviride C1 Enzymes Cocktail for Effective Bioethanol Production. *Catalysts* **10**, 1292 (2020).
171 Ahmed, I., Zia, M. A. & Iqbal, H. M. Detergent-compatible purified endoglucanase from the agro-industrial residue by Trichoderma harzianum under solid state fermentation. *BioResources* **11**, 6393-6406 (2016).

172 Zhang, Y.-H. P. & Lynd, L. R. Cellulose utilization by Clostridium thermocellum: bioenergetics and hydrolysis product assimilation. *Proceedings of the National Academy of Sciences* **102**, 7321-7325 (2005).

173 Schlembach, I. *et al.* Consolidated bioprocessing of cellulose to itaconic acid by a co-culture of Trichoderma reesei and Ustilago maydis. *Biotechnology for biofuels* **13**, 1-18 (2020).

174 Trivedi, S., Ansari, A. A., Ghosh, S. K. & Rehman, H. in *Aqaba International Conference on Marine and Coastal Environment, Status and Challenges in Arab World. Aqaba, Jordan.* (Springer).

175 Zhang, M., Mileykovskaya, E. & Dowhan, W. Cardiolipin is essential for organization of complexes III and IV into a supercomplex in intact yeast mitochondria. *Journal of Biological Chemistry* **280**, 29403-29408 (2005).

176 Jarmander, J., Hallström, B. M. & Larsson, G. Simultaneous uptake of lignocellulose-based monosaccharides by Escherichia coli. *Biotechnology and bioengineering* **111**, 1108-1115 (2014).

177 Liu, H., Valdehuesa, K. N. G., Nisola, G. M., Ramos, K. R. M. & Chung, W.-J. High yield production of D-xylonic acid from D-xylose using engineered Escherichia coli. *Bioresource technology* **115**, 244-248 (2012).

178 Stephens, C. *et al.* Genetic analysis of a novel pathway for D-xylose metabolism in Caulobacter crescentus. *Journal of bacteriology* **189**, 2181-2185 (2007).

179 Bator, I., Wittgens, A., Rosenau, F., Tiso, T. & Blank, L. M. Comparison of three xylose pathways in Pseudomonas putida KT2440 for the synthesis of valuable products. *Frontiers in bioengineering and biotechnology* **7**, 480 (2020).

180 Liu, H. *et al.* Biosynthesis of ethylene glycol in Escherichia coli. *Applied microbiology and biotechnology* **97**, 3409-3417 (2013).

181 Choi, S. Y. *et al.* Engineering the xylose-catabolizing Dahms pathway for production of poly (d-lactate-co-glycolate) and poly (d-lactate-co-glycolate-co-d-2-hydroxybutyrate) in Escherichia coli. *Microbial biotechnology* **10**, 1353-1364 (2017).

182 Madison, L. L. & Huisman, G. W. Metabolic engineering of poly (3-hydroxyalkanoates): from DNA to plastic. *Microbiology and molecular biology reviews* **63**, 21-53 (1999).

183 Nikel, P. I. & de Lorenzo, V. Pseudomonas putida as a functional chassis for industrial biocatalysis: from native biochemistry to trans-metabolism. *Metabolic engineering* **50**, 142-155 (2018).

184 Mezzina, M. P., Manoli, M. T., Prieto, M. A. & Nikel, P. I. Engineering native and synthetic pathways in Pseudomonas putida for the production of tailored polyhydroxyalkanoates. *Biotechnology Journal* **16**, 2000165 (2021).

185 Otte, K. B. & Hauer, B. Enzyme engineering in the context of novel pathways and products. *Current Opinion in Biotechnology* **35**, 16-22 (2015).

186 Song, J. W. *et al.* Multistep enzymatic synthesis of long-chain α, ω-dicarboxylic and ω-hydroxycarboxylic acids from renewable fatty acids and plant oils. *Angewandte Chemie International Edition* **52**, 2534-2537 (2013).

187 Sattler, J. H. *et al.* Introducing an in situ capping strategy in systems biocatalysis to access 6-aminohexanoic acid. *Angewandte Chemie* **126**, 14377-14381 (2014).

188 Lee, J.-E., Vadlani, P. V. & Faubion, J. Corn bran bioprocessing: Development of an integrated process for microbial lipids production. *Bioresource technology* **243**, 196-203 (2017).

189 Pham, N. *et al.* Genome-scale metabolic modeling underscores the potential of Cutaneotrichosporon oleaginosus ATCC 20509 as a cell factory for biofuel production. *Biotechnology for Biofuels* **14**, 1-17 (2021).

190 Park, J. H., Lee, S. Y., Kim, T. Y. & Kim, H. U. Application of systems biology for bioprocess development. *Trends in biotechnology* **26**, 404-412 (2008).

191 Sewsynker-Sukai, Y., Faloye, F. & Kana, E. B. G. Artificial neural networks: an efficient tool for modelling and optimization of biofuel production (a mini review). *Biotechnology & Biotechnological Equipment* **31**, 221-235 (2017).
192 Daniels, C., Rodriguez, J., Lim, E. & Wenger, M. An integrated robotic system for high-throughput process development of cell and virus culture conditions: Application to biosafety level 2 live virus vaccines. Report No. 1618-0240, (Wiley Online Library, 2016).
193 Janzen, N. H. *et al.* Implementation of a fully automated microbial cultivation platform for strain and process screening. *Biotechnology journal* **14**, 1800625 (2019).

9. List of Abbreviations

3HA	3-hydroxyalkanoates
3HB	3-hydroxybutyrate
3HBL	3-hydroxyburyrolactone
Acetyl-CoA	Acetyl-coenzyme A
ACL	ATP citrate lyase
AMP	Adenosine monophosphate
AMPD	Adenosine monophosphate deaminase
ANN	Artificial neural networks
ARA	arachidonic acid
C	Carbon
Ccr	Carbon catabolite repression
C:N	Carbo to nitrogen ratio
CN	Cetane number
CO_2	Carbon dioxide
CoA	coenzyme A
CRISPR	Clustered regularly interspaced short palindromic repeats
DCW	Dry cell weight
DHA	docosahexaenoic acid
EPA	eicosapentaenoic acid
FA	Fatty acids
FABCEs	Fatty acid branched-chain esters
FAEs	Fatty acids esters
FAEEs	Fatty acid ethyl-esters
FAMEs	Fatty acid methyl esters
FAOH	Fatty acids alcohols
FAS	Fatty acid synthase
FFAs	Free fatty acids
GHGs	Greenhouse gases
GLA	gamma-linolenic acid
HHV	Higher Heating Value
IEA	International Energy Agency
IMP	Inosine monophosphate
IPTG	Isopropyl β-d-1-thiogalactopyranoside

IV	Iodine Value
KV	Kinematic Viscosity
MMT	Million metric tons
MNM	Minimal-nitrogen media
MTP	Microtiter plate
N	Nitrogen
NADPH	Nicotinamide adenine dinucleotide phosphate
NH3	Ammonia
P	Phosphate
PanK	Pantothenate kinase
PHA	Polyhydroxyalkanoates
PHB	Polyhydroxybutyrates
PPP	Pentose phosphate pathway
ptsG	Glucose-specific permease of the phosphotransferase system
SCOs	Single cell oils
SDGs	Sustainable Development Goals
TAGs	Triacylglycerides
UN	United Nations
YPD	Yeast Peptone Dextrose

10. List of Figures and Tables

11. Preprint Permissions

Microbial lipid production by oleaginous yeasts grown on Scenedesmus obtusiusculus microalgae biomass hydrolysate
Author: Samer Younes et al
Publication: Bioprocess and Biosystems Engineering
Publisher: Springer Nature
Date: Apr 28, 2020
Copyright © 2020, Springer Nature

Rights and permissions

Systems Biology Engineering of the Pantothenate Pathway to Enhance 3HB Productivity in Escherichia coli
Author: Samer Younes et al
Publication:
Biotechnology and Bioprocess Engineering
Publisher:
Springer Nature
Date:
Sep 9, 2021

A Seagrass-Based Biorefinery for Generation of Single-Cell Oils for Biofuel and Oleochemical Production

Author: Masri et al

Publication: Energy Technology

Publisher: Wiley-VCH Verlag GmbH & Co. KGaA.

Date: 27 September 2017

12. Additional Full Length Publication

12.1 Towards High-Throughput Optimization of Microbial Lipid Production: From Strain Development to Process Monitoring

Dania Awad, Samer Younes, Matthias Glemser, Franz M. Wagner, Gerhard Schenk, Norbert Mehlmer and Thomas Brueck

Featured on the Front cover of *Sustainable Energy & Fuels*: Issue 12 (December 2020)

Published in *Sustainable Energy and Fuels*

Date of Publication: 17 June 2020

DOI: 10.1039/D0SE00540A

Volume 4
Number 12
December 2020
Pages 5871–6332

Sustainable Energy & Fuels

Interdisciplinary research for the development of sustainable energy technologies

rsc.li/sustainable-energy

ISSN 2398-4902

ROYAL SOCIETY OF CHEMISTRY

PAPER

Thomas Brueck *et al.*

Towards high-throughput optimization of microbial lipid production: from strain development to process monitoring

Sustainable Energy & Fuels

ROYAL SOCIETY OF CHEMISTRY

PAPER

View Article Online
View Journal | View Issue

Cite this: *Sustainable Energy Fuels*, 2020, **4**, 5958

Towards high-throughput optimization of microbial lipid production: from strain development to process monitoring†

Dania Awad, ‡[a] Samer Younes,‡[a] Matthias Glemser,[a] Franz M. Wagner,[b] Gerhard Schenk, [cd] Norbert Mehlmer [a] and Thomas Brueck *[a]

Received 4th April 2020
Accepted 12th June 2020

DOI: 10.1039/d0se00540a

rsc.li/sustainable-energy

Digitalization drives accelerated process optimization by comprehensive automation. In the advanced biofuels sector this demands automatable high-throughput processes for production strain development and downstream process performance monitoring. In that context, the unit operations of oleaginous yeast-based biodiesel production are amenable to high-throughput process development. *Cutaneotrichosporon oleaginosus* is a leading production strain for high-energy biofuel options, that is capable of utilizing a broad range of substrates as carbon sources, thereby generating in excess of 60% (w/w) lipids under nutrient limiting conditions. For the first time, we report on the use of fast neutron (FN) irradiation for the rapid, high-throughput genetic enhancement of an oleaginous yeast in conjunction with high-throughput selection of enhanced lipid producing *C. oleaginosus* mutants by cultivation in the presence of the fatty acid biosynthesis inhibitor cerulenin. Performance monitoring of improved mutants was accomplished by development of a high-throughput lipid qualification methodology based on a miniaturized, low cost Nile red based spectrofluorimetric assay. From the FN mutant library, this high-throughput strain development approach allowed identification of a *C. oleaginosus* variant (FN M2) displaying a 21.67% (w/v) and 22.58% (w/v) increase in biomass formation and total lipid yield compared to wild-type strain, respectively. Mutant triglyceride characterization revealed a higher content of saturated fatty acids, which is favorable with respect to biofuels production standards, determined here for the first time. This study is an initial step towards an automatable, high-throughput yeast oil optimization process that facilitates accelerated industrial deployment.

1. Introduction

Climate change and resulting environmental concerns drive the development of sustainable bioenergy and oleochemical solutions.[1–3] However, plant-derived biofuels and chemical entities only offer a partial solution as oil crops compete with agricultural crops over arable land, nutrients and water resources, ultimately affecting food prices.[1,3,4] Oleaginous microorganisms (OM), such as yeast, filamentous fungi and algae species can accumulate high amounts of intracellular lipids, which are commonly in excess of 20% (g g^{-1} of dry cell weight (DCW)).[1,2,5] Recently, utilization of single cell oils (SCOs) as a platform for biodiesel production has received considerable attention, since OM (a) do not require arable land, (b) can utilize waste material as feedstocks, (c) have short production-cycles and (d) are not affected by seasons or climate. Thereby, OM do not jeopardize food security, all the while providing triglyceride-based lipid products at a constant yield and quality independent of climate and land use change effectors.[1–3,6] The use of lipids, derived from OM and particularly oleaginous yeasts (OYs), for biofuel and bioenergy production has been reported previously.[7] However, a summary of Key Performance Indicators (KPIs) for yeast-derived fuel products has not yet been documented.

In the context of yeast-based biofuel generation, *Rhodosporidium toruloides*, *Lipomyces starkeyi*, *Cutaneotrichosporon oleaginosus*, *Yarrowia lipolytica*, *Debaryomyces hansenii* and *Rhodotorula glutinis* are amongst the most promising yeast species for industrial applications of SCOs. Several studies reported lipid accumulation of 40–70% (g g^{-1} of DCW) in these wild-type strains when cultivated under nitrogen-limiting conditions with excess carbon (glucose).[1,2,5,8,9] *C. oleaginosus*, in particular, displays industrially favorable characteristics, such as the ability to accumulate more than 60% lipids (g g^{-1} of

[a]*Werner Siemens-Chair of Synthetic Biotechnology, Department of Chemistry, Technical University of Munich (TUM), Garching, Germany. E-mail: brueck@tum.de*
[b]*Forschungs-Neutronenquelle Heinz Maier-Leibnitz II (FRM II), Technische Universität München, Garching, Germany*
[c]*School of Chemistry and Molecular Biosciences, The University of Queensland, St. Lucia, QLD 4072, Australia*
[d]*Sustainable Minerals Institute, The University of Queensland, St. Lucia, QLD 4072, Australia*

† Electronic supplementary information (ESI) available. See DOI: 10.1039/d0se00540a

‡ Both authors contributed equally to the work.

DCW), a high flexibility in carbon source utilization and a fatty acid composition similar to that of plant oils, specifically palm oil.[1,4,10–14] This yeast has been the focus of several strain development studies ranging from model-based (surface response methodology) culture media optimization, tailored fatty acid profile, development of sustainable and high performance waste-free biorefinery platforms, in addition to techno-economic studies.[1,10,13,15,16] However, yeast-derived lipids have not yet been commercialized due to technical (*e.g.* low space-time yields) and economic (*i.e.* cost of oil extraction) barriers. Moreover, high production costs, which mainly include expensive fermentation substrates (carbon sources) and complex lipid extraction protocols (cell rupture, oil extraction and purification), have prevented market entry of this technology.[3,6,17] To that end, rapid identification and optimization of OY production strains in synergy with appropriate cultivation and oil extraction conditions are required to develop a commercially viable process. Accordingly, any significant improvement in space-time yields of yeast lipids is central to the accelerated industrial deployment for this promising high-energy biofuel technology.[1,3,18]

In that context, digitalization accelerates and drives industrial process design, optimization and deployment through comprehensive automation. With respect to advanced bioprocesses, such as yeast-based biofuel production, this does not only demand specialized sensor and software development, but is also highly dependent on the availability of automatable, high-throughput processes, particularly in initial process development stages involving production strain generation, selection and performance monitoring. While this has been in part achieved for biogas and bioethanol processes, equivalent solutions are lacking for high-energy content biofuels processes.[19–22] To that end, the generation of microbial lipids for biodiesel production using yeast-based production platforms, such as *C. oleaginosus*, are amenable to implementation of high-throughput optimization of individual unit operations. Therefore, development of high-throughput methodologies for genetic production strain enhancement, rapid selection of process-relevant variants and downstream product-oriented performance monitoring are essential for automated oleaginous yeast biofuel process optimization scenarios.

With respect to rapid production strain enhancement, current methods of metabolic engineering encompass various targeted and random mutagenesis techniques.[23,24] Targeted mutagenesis, or directed evolution, *via* genetic engineering is conventionally a key technology in developing optimized strains with improved and tailored lipid production characteristics.[25] Although genomic and transcriptomic data of *C. oleaginosus* are available, this and other *de novo* OYs display protective mechanisms preventing rapid and precise genome manipulation (*via* mechanisms of homologous recombination/knockout). These organisms appear to be refractory to most targeted genetic engineering approaches, as observed by several studies performed in our group and others (*e.g.* CRISPR).[2,10,26–28] Specifically, the GC-rich genome (65%) of these organisms entails a strong bias in the codon usage, thus hindering the direct transfer of established site-directed genetic protocols from model yeasts like *Saccharomyces cerevisiae* to *C. oleaginosus* and other OYs.[10,26] However, random genetic manipulation of several OYs has been successful *via Agrobacterium tumefaciens*-mediated gene transfer (AGMT), but this method results in multiple, non-targeted insertions, is laborious and cannot be transferred into high-throughput automated formats.[2,10,26] Furthermore, with AGMT and other targeted mutagenesis techniques arises the need for selective agents (*e.g.* antibiotics) that incur additional costs and efforts, especially at industrial levels, in addition to legislative requirements involved in Genetically Modified Organism (GMO) control and containment.[29]

In contrast, strain development can also be carried out by random mutagenesis, also termed accelerated evolution. This method is (a) subject to no GMO controls, (b) requires minimal technical manipulation, (c) does not necessitate the integration of antibiotic resistance genes, (d) requires little knowledge of the genetic/biochemical mechanisms involved in the synthesis of desired products, and, most importantly, (e) can be transferred to automatable, high-throughput formats.[29–31] Generally, microbial strain improvement has previously been achieved *via* physical mutagens, such as UV light and ionizing radiation (IR, including γ-rays, α-rays, X-rays and neutron radiation), in addition to chemical mutagenic agents, such as ethyl methane sulfonate (EMS) and nitrosomethyl guanidine (NTG).[2,5,25,30,32] Chemically-induced mutations are genetically less stable and have a tendency to revert back to the wild-type form.[32,33] Similarly, UV-induced DNA damage (photo-lesions) is commonly repaired through photo-reactivation. Even in the absence of this process, photo-lesions can still be removed – albeit less efficiently – by DNA repair mechanisms.[34,35] The most commonly used IR are γ-rays, which have been implemented in the mutagenesis of diverse organisms (*e.g.* bacteria, yeasts, plants). The type of DNA damage caused by IR correlates with the relative biological effectiveness (RBE) of the specific radiation, which is a function of its linear energy transfer (LET). In that respect, fast neutron (FN) radiation shows greater LET (many folds higher) than those of low-LET radiation, such as γ- and X-rays. Amongst the various types of damage induced by mutagens the most biologically relevant are DNA double strand breaks (DSBs).[33,36] FN irradiation has been reported to cause a higher number of non-repairable DNA damage concurrent with highly delayed DNA repair mechanisms.[33,37] Thus, it is a more effective inducer of inherently stable DSBs, base substitutions or deletions/insertions compared to other mutagenic techniques (physical or chemical).[33,38,39] FN mutagenesis has been successfully and extensively employed for crop improvement in many plant species including soybean, rice, peanuts, tomato and peas.[33,40–42] However, FN irradiation is a less explored approach in the mutagenesis of yeast species, with the sole report of utilizing this specific IR in irradiating the non-oleaginous model yeast *S. cerevisiae* dating back to 1986.[43]

The main challenge associated with FN irradiation and any other random mutagenesis technique lies in the large numbers of generated mutant libraries. Thus, an efficient selection method commonly succeeds random mutagenic techniques.[5,18] With respect to OYs, selection methods should allow for the

isolation of mutants exhibiting enhanced lipid yields and enhanced biomass formation.[2,5,32] Interestingly, cerulenin, which was originally isolated from the fungus *Cephalosporium caerulens*, is a potent fatty acid synthase (FAS) inhibitor. Cerulenin results in the reduction of colony growth on culture plates.[44] This antifungal has become the standard for improved screening of OYs for lipid yield. The rational of this strategy resides in the fact that mutants displaying normal growth, in the presence of cerulenin, possess mutagenesis-induced metabolic alterations (*e.g.* enhanced FAS activity). By overcoming the inhibition, these mutants are good candidates for improved growth or lipid production.[2,5,25] When generating random mutagenesis libraries, a subsequent selective cultivation in the presence of cerulenin provides a targeted, fast, visible and labor-saving selection method for improved mutant strains. Improvements in lipid production following this combinatorial approach have been previously reported for *R. glutinis*, *R. toruloides*, *L. starkeyi* and *Y. lipolytica* but not *C. oleaginosus*.[5,18,25,45]

Generation and selection of mutant libraries still incur further qualification and characterization of fermentative growth potential. Conventional methods for the determination of OY lipid titers typically require cell disruption, solvent lipid extraction and weighing (gravimetric analysis), or derivatization of extracted fatty acids into fatty acid methyl esters (FAMES) followed by gas chromatography. These techniques are very tedious and time-consuming, especially when handling significant amounts of biological samples, such as mutant libraries.[2,5,18,46] In context of strain development for industrial commercialization of SCOs, process monitoring, which employs state-of-the-art analytical tools characterized by high-throughput and miniaturized scale, enables greater depth of strain characterization.[47] Recent advancements in efficient and fast quantification of lipids from OM have made use of several high-throughput colorimetric and spectrofluorimetric methods such as Nile red, Sudan black B and sulfo-phospho-vanillin. With the advantage of easy handling of small biological samples, these fast lipid quantitation methods can be paired with other cell component quantitation (*e.g.* protein, DNA) using the same sample for multi-analytical measurements. Specifically, Nile red analysis has been well optimized and validated. Lipid quantification *via* this assay strongly correlates with the gravimetric lipid content (%, g g^{-1} of DCW).[48–50] However, absolute quantification of lipid yields (g L^{-1}) *via* the Nile red method has been hindered by the high variability of the fluorescence measurements.[51,52] Glycerol triolein (TO) is a symmetrical triglyceride harboring one glycerol and three oleic acid (OA) units, which represent the most prominent fatty acid produced in *C. oleaginosus*. TO has previously been adopted as a standard for Nile red quantitation of lipids from OY.[53] However, the use of this standard for absolute quantitation comes with its own drawbacks. TO is expensive, difficult to handle, only linear in a narrow concentration range (2–100 μg mL^{-1}), and might result in over- or underestimation of the actual neutral lipid content in the cells.[3,54,55]

For the first time, this study employed random mutagenesis by FN irradiation for the rapid, high-throughput genetic enhancement of an OY. Following mutagenesis of *C. oleaginosus* ATCC 20509, potentially improved mutants displaying uninhibited growth on cerulenin-containing medium were rapidly selected for further qualification of their fermentative potential. Accordingly, evaluation of mutants displaying enhanced biomass and lipid formation entailed the development of a miniaturized, quantitative high-throughput assay (lipid yield, lipid content and maximal lipid productivity) based on Nile Red fluorospectrometry. This lipid detection methodology was based on a purified microbial lipid standard extracted from *C. oleaginosus*, which was further correlated with the previously reported model triglyceride, TO. Additionally, the potential of OA as a low-cost and easy-to-handle alternative standard was evaluated. Moreover, analysis of lipid profiles and biofuel KPIs of wild-type *C. oleaginosus* as well as improved mutant strains were conducted. This study provides initial processes for the development of a technology platform for automated high-throughput yeast lipid process optimization, that fosters accelerated industrial deployment of advanced high-energy biofuels, such as yeast-based biodiesel and sustainable aviation fuels. Our *C. oleaginosus* centered model study presents initial high-throughput solutions for essential unit operations covering rapid and automatable genetic strain enhancement, selection of improved variants in conjunction with a low cost, miniaturized yeast oil centered performance monitoring assay.

2. Materials and methods

2.1 Yeast strain and culture conditions

C. oleaginosus ATCC 20509 (from the culture collection of Werner Siemens Chair of Synthetic Biotechnology – WSSB, TU, Munich) was maintained on YPD (yeast extract peptone dextrose) agar plates (20 g L^{-1} peptone, 20 g L^{-1} agar, 20 g L^{-1} glucose, 10 g L^{-1} yeast extract). A single colony was initially cultured in 125 mL Erlenmeyer flask holding 50 mL YPD liquid medium at 28 °C and in a rotary incubator at 120 rpm for 24 h. Lipid accumulation was induced by subsequent inoculation in 125 mL Erlenmeyer flask holding 50 mL of minimal-mitrogen media MNM (40 g L^{-1} glucose, 0.75 g L^{-1} yeast extract, 1.5 g L^{-1} $MgSO_4 \cdot 7H_2O$, 0.4 g L^{-1} KH_2PO_4, 0.22 g L^{-1} $CaCl_2 \cdot 2H_2O$ and trace elements: 1.2 mg L^{-1} $(NH_4)_2SO_4$, 0.55 μg L^{-1} $ZnSO_4 \cdot 7H_2O$, 24.2 μg L^{-1} $MnCl_2 \cdot 4H_2O$, 25 μg L^{-1} $CuSO_4 \cdot 5H_2O$) prepared according to.[1] With a starting optical density of 0.1, measured at 600 nm, cultivation was sustained for 96 h at 28 °C in a rotary incubator at 120 rpm.

2.2 Experimental design

2.2.1 Fast neutron irradiation. FN mutagenesis was conducted at the Research Neutron Source Heinz Maier-Leibnitz (FRM II) facility of the Technical University of Munich in Garching, Germany. The nuclear research reactor produces free neutrons through uranium fission that is utilized for numerous scientific experiments (tumor treatment and physical and biological dosimetry). A secondary source, consisting of two uranium plates, stands one meter from the reactor core. This source produces fast fission neutrons that are guided through beam tube number 10 (SR-10) to the MEDAPP (medical

applications) instrument.[56] The MEDAPP set up displays a neutron flux density of approximately 3.2×10^8 cm^{-2}. s^{-1}. The experimental setup parameters are displayed in Table 1. Triplicate samples of exponentially grown cells of *C. oleaginosus* were set to 10^7 cells per mL^{-1} *via* fluorescence-activated cell sorting (FACS) counting in a KCl-media (27 g L^{-1} NaCl, 6.6 g L^{-1} $MgSO_4 \cdot 7H_2O$, 1.5 g L^{-1} $CaCl_2 \cdot 2H_2O$, 5 g L^{-1} KNO_3, 0.07 g L^{-1} KH_2PO_4, 0.014 g L^{-1} $FeCl_3 \cdot 6H_2O$ and 0.021 g L^{-1} Na_2-EDTA$\cdot 2H_2O$). A total of 56 Eppendorf tubes (2 mL), which were completely filled with cell suspension, were placed horizontally within the beam area in a custom-made rack (3D-printed from polylactic acid (PLA)). Following radiation clearance, treated samples were stored in the dark at room temperature to prevent photorepair events. Aliquots of the mutant library were stored at −80 °C in 10% glycerol.

2.2.2 Cerulenin screening

A cerulenin stock solution (1 mg mL^{-1}) was prepared in DMSO (dimethyl sulfoxide). To estimate the proper working concentration of cerulenin for the selection of *C. oleaginosus* mutants, non-irradiated cells were plated on YPD agar, supplemented with cerulenin (Applichem, Germany) at a concentration gradient of 2, 4, 6, 8, 10 and 12 μg μL^{-1}. Based on the survival fraction, cerulenin selection took effect at a concentration of 10 μg μL^{-1}. Approximately 2×10^6 *C. oleaginosus* irradiated (mutants pool U) and non-irradiated (pool A) cells were plated on cerulenin-supplemented YPD agar plates. Following incubation for 7 days, large colonies were transferred to fresh cerulenin-free MNM agar plates, and sub-cultured over a period of 4 weeks. Subsequently, the individual colonies were cultivated in liquid MNM for 96 h to assess growth and lipid production (see section 2.1).

2.3 Analytical methods

2.3.1 High-throughput and absolute quantitation *via* Nile red analysis. Lipid titers of wild-type *C. oleaginosus* and its mutants were calculated based on a calibration curve generated using purified microbial oil (ML) extracted from wild-type *C. oleaginosus.* Additionally, an analytical grade TO (Sigma-Aldrich, Germany) standard curve was prepared. Also, a third standard curve was based on analytical grade OA (Applichem, Germany). All three standard curves were constructed following a modified protocol of Priscu *et al.*[54] Briefly, chloroform was chosen as a carrier for all standards (1 : 1 standard : chloroform) into anhydrous ethanol to make intermediate dilutions of 2.0, 4.0, 8.0 and 10.0 mg mL^{-1}. Additionally, another OA acid standard was prepared following the exact protocol, save for the initial chloroform dilution step. Following vigorous vortexing, the final dilution step was prepared in deionized (DI) water, specifically to realize an intermediate stock:final diluent (v/v) that is consistent across all prepared dilutions (20, 40, 80 and 100 μg mL^{-1}). This procedure resulted in hydrophobic micelles of uniform size that mimic the nature of the *C. oleaginosus* samples' final solvent system. In that respect, Nile red analysis of wild-type *C. oleaginosus*, mutants and prepared standards (ML, TO and ML) followed a modified protocol of Sitepu *et al.*[50] Briefly, triplicates of wild-type and mutant yeast cells were diluted with DI water to OD600 < 1 in black Nunc™ F96 MicroWell™ Polystyrene Plate (Thermo Scientific Waltham, MA, USA). These plates ensure minimal fluorescence background and stray light. Following the addition of 50 μL DMSO, initial readings were recorded for growth and background fluorescence. A Nile red (9-diethylamino-5H-benzo [alpha] phenoxazine-5-one) (Sigma-Aldrich, Germany) stock solution (60 μg mL^{-1}) was prepared freshly in DMSO. Additionally, the stock and staining solutions were protected from light to avoid photo-bleaching. Nile red was then added to a working concentration (WC) of 5 μg per mL per well. Kinetic reading of fluorescence emission was measured at 590/35 nm with an excitation wavelength of 530/25 nm for 5 min with 30 s intervals using an EnSpire 2 microplate reader from Perkin Elmer (Waltham, MA, USA). Maximal fluorescence emission (MFE) values were recorded to calculate lipid yields (g L^{-1}) and maximal lipid productivity (mg L^{-1} h^{-1}). MFE values were further corrected for cell density variations by norming with optical density measurements at 600 nm to obtain normalized fluorescence and subsequently calculate the lipid content (%, g g^{-1}) of DCW.

2.3.2 Fatty acid profile analysis. Fatty acid methyl esters (FAMEs) were obtained by methanol transesterification of lyophilized yeast biomass. The transesterification protocol was originally adopted from Griffiths *et al.* and modified in our lab by Gorner *et al.*[10,57] Briefly, pre-weighed lyophilized cells were loosened in toluene and sodium methoxide in methanol and incubated at 80 °C and 600 rpm for 20 min. Following a sequential incubation step at room temperature, HCl/methanol was added and the incubation was repeated. FAME extraction followed shaking of samples in hexane and water and a quick centrifugation at 4000 rpm. The upper phase was aspired and transferred into GC vials. FAME profiles were analyzed on a GC-2010 Plus gas chromatograph from Shimadzu (Nakagyo-ku, Kyōto, Japan) equipped with a flame ionization detector. A sample of 1 μL was applied by AOC-20i auto injector (Shimadzu) onto a ZB-WAX column (30 m, 0.32 mm ID; 0.25 μm df; phenomenex (Torrance, CA, USA). The initial column temperature was 150 °C (maintained for 1 min). A temperature gradient was applied from 150 °C–240 °C (5 °C min^{-1}), followed by 6 min maintenance at 240 °C. Fatty acids were identified according to retention times of the authentic standard: Marine

Table 1 Experimental setup for FN irradiation of *C. oleaginosus*

Parameters	Setup
Distance to converter plate	5.33 m
Lead filter thickness	6 cm
D_n [Gy min^{-1}]	0.4028
D_γ [Gy min^{-1}]	0.1840
Cumulative dose [Gy min^{-1}]	0.5868
Dosage steps [Gy]	0–1000, increment of 50[a]
Ratio $D_n D_\gamma^{-1}$	2.189
Strain	*C. oleaginosus*

[a] Pools of *C. oleaginosus* subjected to increasing irradiation dosage based on 50 Gy increments were labeled A–U (Pool A: non-irradiated cells).

Oil FAME Mix (Restek, USA). Individual FAME concentrations were based on peak areas relative to Methyl Nonadecaanoate C19 (Sigma-Aldrich, Germany), which was incorporated in all samples as an internal standard. Biological triplicate measurements were recorded for each of the screened yeast mutants.

2.4 Statistical analysis

2.4.1 Survival rate. To estimate cellular concentration and viability, a volume of 50 μL of each of the irradiated and non-irradiated suspensions (Samples A–U) was plated on YPD agar plates in triplicates. Following incubation for 96 h at 28 °C, triplicate colony counts were recorded and an exponential regression trend was fitted.

2.4.2 Calculations of biofuel properties. Various physiochemical properties of biofuels based on FAMEs profiles of the wild-type and improved mutants of *C. oleaginosus* were determined using predictive models and mathematical equations for the transesterified SCOs.[58] These properties include iodine value (IV), cetane number (CN), higher heating value (HHV), kinematic viscosity (KV) and density.

3. Results and discussion

3.1 Accelerated *C. oleaginosus* evolution by fast neutron irradiation

In this study, our efforts to rapidly generate improved *C. oleaginosus* variants are based on random mutagenesis by FN irradiation. This is the first report on the application of FN irradiation to generate improved OY mutants.[33,43] The experimental set up for the nuclear research reactor of this study is displayed in Fig. 1A. The high source strength allowed for high irradiation dosage of 0.5868 Gy min^{-1} by maintaining high neutron fluxes. The lead filter was used to reduce gamma radiation and obtain a neutron-to-gamma ratio of 2–2.7. This ratio was dependent on the installed converter plate and collimator that were changed between reactor cycles. Exponentially grown cells of *C. oleaginosus* were irradiated in KCl media to reduce the formation of longer-lasting radioactive isotopes such as sodium isotopes (half-life: $t_{1/2}$ $^{24}Na = 14.96$ h).[59] Accordingly, decay times of 24 hours were sufficient to obtain non-critical residual activation levels as the decay of radioactive isotopes was ensured. A dose/response assay was performed to determine the optimal irradiation exposure period required to realize the highest accumulation of DNA mutations in *C. oleaginosus* cells, as indicated by low survival rates.[44] The relationship between the irradiation dose and survival rate was fitted by least squares to an exponential equation ($y = 73.098e^{-0.003x}$) with a correlation coefficient of 0.9366 (Fig. 1B). Determination of the survival fraction was based on the colony formation assay. *C. oleaginosus* mutant pool U, which was subjected to highest irradiation dosage (1000 Gy), had a 4.17% survival rate. The resulting mutants underwent subsequent high-throughput selective cultivation using a cerulenin-containing screening medium to identify *C. oleaginosus* variants with improved growth and/or lipid yield (Fig. 1C).

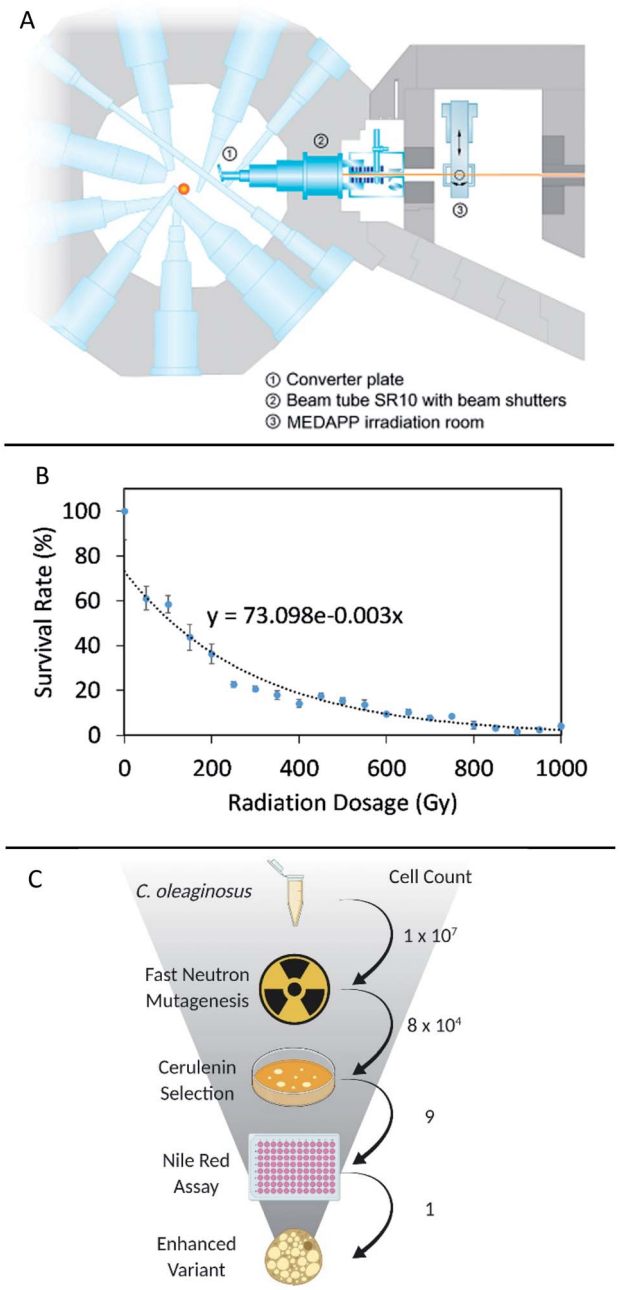

Fig. 1 (A) Experimental set up for the nuclear research reactor of this study. (B) Survival rate of FN-irradiated *C. oleaginosus* cells subjected to increasing irradiation dosage based on 50 Gy increments. The data were fitted to an exponential regression function with a coefficient of determination of 0.9366. (C) Schematic of strain development design and methods employed in this study.

3.2 Cerulenin screening

Cerulenin screening has been successfully employed for the generation of high lipid-producing mutants of *R. glutinis*, *R. toruloides*, *L. starkeyi* and *Y. lipolytica*.[18,44,60–62] According to the original work presenting this methodology, the optimal working concentration (WC) of cerulenin was measured at 10 $\mu g.\mu L^{-1}$ for *R. glutinis*.[18] This concentration was also determined to be optimal in the screening of *R. toruloides* and *L.*

starkeyi mutants.[44,61] Screening of wild-type *C. oleaginosus* on a concentration gradient ranging from 2 to 12 μg μL^{-1} revealed an equivalent WC (10 μg μL^{-1}). Screening of approximately 2×10^6 *C. oleaginosus* mutants on cerulenin resulted in the isolation of 9 mutants with potentially enhanced lipid biosynthesis capacity. The reduction in mutant library complexity is displayed in Fig. 1C. These isolated variants, which displayed visibly large colonies on cerulenin-containing YPD media, were termed *C. oleaginosus* Fast Neutron Mutants (FNM) 1–9.

Previous studies have shown that FN irradiation results in a higher number of non-repairable DNA damage compared to other physical or chemical mutagenesis methods.[32,33,36,37] The inherent stability of the mutations caused by this specific type of IR was further corroborated in our study. Cerulenin-selected FN mutants were initially sub-cultured on cerulenin-free YPD media over a period of 4 weeks. Subsequently, the fermentative potential of the mutants was evaluated following a 96 h batch cultivation without cerulenin selection pressure. For this purpose, a high-throughput spectrofluorimetric method was developed.

3.3 High-throughput variant qualification *via* Nile red spectrofluorimetry

3.3.1 Method development: absolute Nile red quantitation. The traditional gravimetric analysis of neutral lipids is laborious, requires the use of toxic organic solvents and necessitates considerable amounts of biological material. In the search for high-lipid producers, this method is not suitable for large-scale screening of randomly genetically modified yeast strains.[51] Accordingly, evaluation of the fermentative performance of *C. oleaginosus* mutants was carried out by spectrofluorimetry. In that context, a Nile red-based analysis was developed in the last decade into a reliable quantitative method. This method has been extensively employed for the relative quantitation (%, g g^{-1}) of lipids from several OYs.[53,62–64] The major drawback of high-throughput fluorescent techniques (*e.g.* Nile red) for microbial triglycerides (TAGs) assessment is the difficulty in absolute quantification. In that regard, relative quantitative measurements are conventionally conducted by correlating normalized Nile red fluorescence readings to gravimetric measurements.[48–50] This, however, only allows for an estimation of lipid content (%, g g^{-1}). To circumvent this issue, various researchers opted for the utilization of the model triglyceride, TO as a standard to generate a calibration curve, referring to the absolute measurements as TO-equivalents.[53,65–67] TO was also chosen in this study given the prominence of OA (C18 : 1) in the native fatty acid profile of *C. oleaginosus* at about 43–57% lipids (g g^{-1} of DCW).[1] Nevertheless, the use of this particular standard results in various inaccuracies as the Nile red assay depends on the even distribution of lipids within the solution. Exceeding a concentration threshold, the TO emulsion becomes heterogeneous and lipid droplets form, consequently leading to erratic and erroneous fluorescence measurements. Therefore, the droplets would float in or out of the spectrophotometer detector range, resulting in non-reproducible measurements. Hence, the use of TO leads to over or underestimation of the actual neutral lipid content in the cells. This is due to differences in the relative fluorescence of Nile red among the various lipid classes.[52,54,68]

In our study, purified ML extracted from *C. oleaginosus* has been favored for absolute lipid quantification, as it is the most authentic control of *C. oleaginosus* lipids formed. Linear regression of ML was calculated with an R^2 of 0.9921 over a concentration range of 20–100 μg mL^{-1} (Fig. 2). Based on our experimental setup, TO lead to an insignificant overestimation of wild-type *C. oleaginosus* lipid yields (0.67 g L^{-1}) compared to ML. The linear correlation between ML and TO trend-lines, depicted in Fig. 2, is represented by function (1) as:

$$y = 84.72x - 1096.70\ . \quad (1)$$

The spectrofluorimetry method utilized in this study was originally developed in 1990 by Priscu *et al.* and later utilized by Massart *et al.* in 2010 for lipid estimation from microalgae strains.[54,66] These studies all reported the use of large volumes (10 mL) for standard preparation. In this study, miniaturization of sample volume (300 μL) allowed the use of a 96-well plate, which is a crucial step for high-throughput sample handling, automation and the development of an absolute lipid quantitation method, especially in industrial settings. In an attempt to further reduce cost and develop this analytical method, OA was tested for its potential as a standard for absolute quantitation of *C. oleaginosus* lipid titers. Both ML from *C. oleaginosus* and TO have OA as the most prominent fatty acid and basic component, respectively. Compared to TO, OA is inexpensive, easy to handle and does not require a toxic organic solvent carrier, such as chloroform, to deliver the hydrophobic molecules into aqueous solution (Fig. S1 in ESI†). Additionally, OA was found to maintain a stable emulsion in water at higher lipid concentrations than TO (data not shown). In our study, OA resulted in a significant overestimation of wild-type *C. oleaginosus* lipid yields (3.70×) compared to ML, as depicted in a linear correlation with a function (2) represented by:

$$y = 652.56x - 2354.58. \quad (2)$$

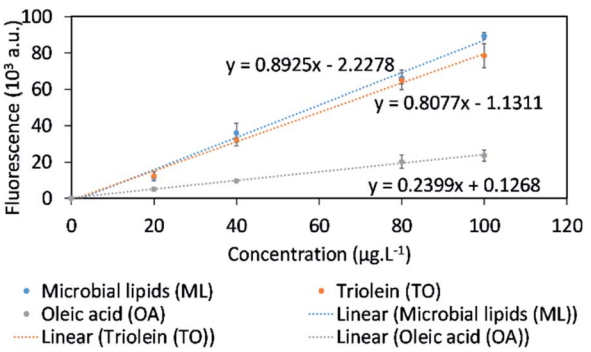

Fig. 2 Nile red spectrofluorimetry standard curves generated from purified microbial lipids from *C. oleaginosus* ($R^2 = 0.9921$), TO ($R^2 = 0.9965$) and OA ($R^2 = 0.9974$).

Yet, in the absence of purified ML from *C. oleaginosus*, OA can be used as a standard for absolute lipid quantitation by correcting the fluorescence readings of the samples by the function displayed above (2). For other OYs, OA can also be utilized as a standard in high-throughput lipid quantitation, following a similar correlation between OA and the respective purified ML. This general lipid assay can therefore be utilized for screening of other OYs, including *R. glutanis*, *Y. lipolytica* and *L. starkeyi*.

3.3.2 Absolute and relative quantitation of *C. oleaginosus* lipids *via* Nile red. By applying the quantitative Nile red method coupled with the ML standard detailed above (Fig. 2), lipid yields (g L^{-1}) of wild-type *C. oleaginosus* and mutants were calculated from their respective detected fluorescence readings (Fig. 3). Total fluorescence measurements and their respective calculated lipid yields (g L^{-1}) are displayed in Fig. 2 and Table 2. In one of our recent studies, maximal lipid productivity for *C. oleaginosus* was determined at 96 h of cultivation. Accordingly, this time point was used in the calculation of lipid productivity (mg L^{-1}. h^{-1}) in this study (Table 2). Additionally, biomass estimation was based on a linear correlation (R^2 = 0.9237) between DCW (g L^{-1}) and optical density (OD_{600}; a.u.), which were both previously determined for the wild-type *C. oleaginosus* strain under various culture conditions (Fig. S2 in ESI†).[1] The calculated biomass yields (g L^{-1}) were employed, along with lipid yields (g L^{-1}) to calculate the intracellular lipid content (%, g g^{-1}) (Table 2). In parallel, the relative quantitation of lipid content (%, g g^{-1}) is also reflected in the normalized fluorescence measurements displayed in Fig. 2.

Notably, *C. oleaginosus* FN M2 recorded a higher total fluorescence measurement than the wild-type *C. oleaginosus* strain, corresponding to lipid yields of 8.05 g L^{-1} and 6.56 g L^{-1}, respectively. This 22.58% (g L^{-1}) increase in lipid yield was due to enhanced growth and biomass yield (13.42 g L^{-1}) rather than an improved intracellular lipid content (%, g g^{-1}). The increase in lipid yield of *C. oleaginosus* FN M2 resulted in a maximal lipid productivity of 83.81 mg L^{-1} h^{-1}. This enhanced variant was attained following the strain development design shown in Fig. 1C, which was aimed at greatly reducing the complexity of the mutant library. By contrast, *C. oleaginosus* FN M8 displayed a higher normalized fluorescence reading compared to the wild-type control. Consequently, this strain had a calculated lipid content of 73.16% (g g^{-1} of DCW). In comparison, under the same conditions, the intracellular lipid content of the wild-type *C. oleaginosus* strain was determined to be 59.45% (g g^{-1} DCW). Quantitation of the lipid content (%, g g^{-1}) of wild-type *C. oleaginosus* in this study was found to be consistent with the gravimetric quantitation of the lipid fraction previously reported by our group.[1] However, the increase in lipid content of *C. oleaginosus* FN M8 was concurrent with a 37.90% (g L^{-1}) decrease in DCW (6.85 *versus* 11.03 g $L^{-1}$for the wild-type control). These data translates to a 16.70% (g L^{-1}) decrease in total lipid yield and maximal lipid productivity of this mutant.

The high-throughput random mutagenesis technique employed in this study, coupled with rapid cerulenin-selection singled out *C. oleaginosus* FN M2 as a candidate strain for industrial applications due to its enhanced overall lipid yields, fast growth rate and maximal productivity. Further, the enhanced intracellular lipid content of *C. oleaginosus* FN M8 renders it a candidate for studying the tight regulatory controls of lipogenesis, specifically with respect to comparative proteomics. Similar strain improvements *via* random mutagenesis for other OY strains have been reported in the last decade. To that end, UV mutagenesis triggered a 43.2% increase in lipid productivity of a mutant strain of *R. toruloides*.[6] Similarly, a 20% (g L^{-1}) increase in lipid production was observed for the green microalgae *Chlorella sp.* following FN irradiation.[69] Further, a lipid yield increase of 55% (g L^{-1}) for *Y. lipolytica* following EMS mutagenesis were reported in an extensive bioreactor optimization study,[70] and in another controlled fermentation a 30.7% increase in lipid productivity by *L. starkeyi* was achieved by random mutagenesis coupled to cerulenin screening.[5]

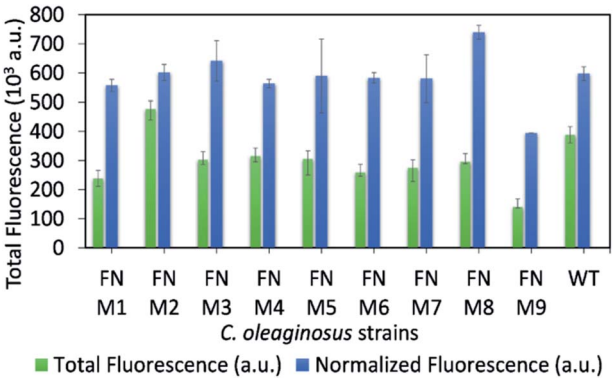

Fig. 3 Total and normalized fluorescence (a.u.) measured for wild-type *C. oleaginosus* and its FN mutants, which were selected on cerulenin.

3.4 Fatty acid profile and biofuel properties

Although the lipid profiles of the *C. oleaginosus* FN mutants diverged slightly from the wild-type strain, the main fatty acid components remained OA (C18 : 1), palmitic acid (C16 : 0) and stearic acid (C18 : 0). The effect of our strain improvement on the fatty acid profile of *C. oleaginosus* is most apparent in the increased degree of the fatty acids saturation (Fig. 4). This shift in saturation level is observed as an increase in stearic acid (C18 : 0) concurrent with a decrease in OA (C18 : 1) and linoleic acid (C18 : 2). This effect was most evident for *C. oleaginosus* FN M2, M5, M7 and M9. Except for *C. oleaginosus* FN M3, M4 and M8, a minor, yet significant decrease in palmitic acid was also recorded for all mutants. Notably, several FN mutants have an up to two-fold increase in long-chain fatty acids concentrations (Table S1 in ESI†), *i.e.* FN M1 (C20 : 2), FN M2, FN M5 and FN M9 (C22 : 0 and C24 : 0), FN M7 (C20 : 3) and FN M10 (C22 : 0).

From a biofuel production perspective, these fatty acid profiles are interesting. In fact, their degree of saturation determines the physiochemical properties of biofuels such as iodine value (IV), cetane number (CN), higher heating value (HHV), kinematic viscosity (KV) and density.[44] These biofuel properties were estimated for several OYs based on rigid

Table 2 Fermentative performance of wild-type *C. oleaginosus* and its FN mutants. Yeast DCW (g L^{-1}) and lipid yield (g L^{-1}) are calculated based on a correlation between optical density measure at 600 nm and the DCW and ML standard curves, respectively

C. oleaginosus strains	DCW (g L^{-1})	Lipid yield (g L^{-1})	Lipid content (%, g g^{-1} DCW)	Maximal lipid productivity (mg L^{-1} h^{-1})
FN M1	7.3 ± 0.76	4.04 ± 0.45	55.29 ± 2.08	42.06 ± 4.7
FN M2	13.42 ± 0.55	8.05 ± 0.63	59.92 ± 2.77	83.81 ± 6.56
FN M3	8.07 ± 0.45	5.11 ± 0.26	63.63 ± 6.80	53.27 ± 2.72
FN M4	9.51 ± 0.68	5.33 ± 0.33	56.04 ± 1.42	55.49 ± 3.39
FN M5	8.86 ± 0.35	5.16 ± 0.92	58.61 ± 12.45	53.78 ± 9.62
FN M6	7.59 ± 0.56	4.39 ± 0.22	57.83 ± 1.71	45.69 ± 2.29
FN M7	8.05 ± 0.57	4.64 ± 0.78	57.64 ± 8.05	48.36 ± 8.12
FN M8	6.85 ± 0.32	5.01 ± 0.11	73.16 ± 2.30	52.16 ± 1.15
FN M9	6.1 ± 0.13	2.39 ± 0.05	39.23 ± 0.06	24.91 ± 0.53
WT	11.03 ± 0.45	6.56 ± 0.47	59.45 ± 2.38	68.37 ± 4.91

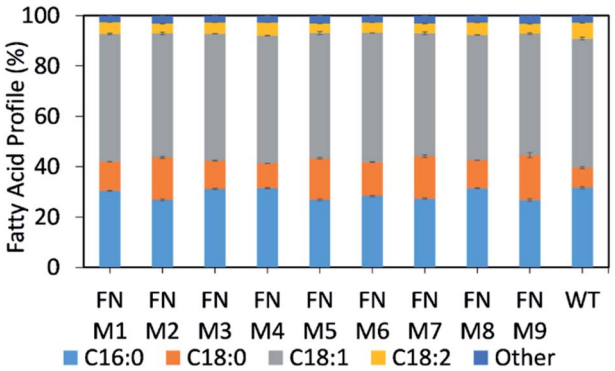

Fig. 4 Fatty acid profiles of wild-type *C. oleaginosus* and its FN mutants, which were selected on cerulenin. "Other" constitutes fatty acids with a presentation below 1%, including C12 : 0, C14 : 0, C16 : 1, C18 : 3, C20 : 0, C20 : 1, C20 : 2, C20 : 4, C20 : 3, C20 : 5, C22 : 0, C22 : 1 and C24 : 0.

calculations by Sergeeva *et al.*[58] These calculations were adopted in this study for wild-type *C. oleaginosus* and its FN M2 mutant, given the high lipid titers of the latter (Table 3).[61] The determined properties were found to be positioned within the limits specified by internationally accepted biofuel standards (US biodiesel ASTM D6751 and EU biodiesel standard EN 14214). A comparison with other prominent OY lipid profiles, including those of *Y. lipolytica, L. starkeyi and R. toruloides,* is presented in Table 3. Interestingly, the *C. oleaginosus* lipid profile shows significant similarities to that of palm oil with respect to the prominence of oleic and palmitic acids in its fatty acid distribution. Hence, he biofuel properties of palm oil were also listed in Table 3.[58] The calculated density values were applied in this study to deliver appropriate concentrations in the preparation of ML standard. The degree of saturation indicated by IV was lower in *C. oleaginosus* FN M2, in comparison to the wild-type strain, yet remained within the limits of the internationally accepted IV range. Notably, lipids derived from the *C. oleaginosus* FN M2 variant demonstrated an improved CN compared to the wild-type strain. Higher CN values are associated with improved cold-start properties and reduced smoke formation.[62] Similar improvements in biofuel properties were also reported for *Y. lipolytica* following chemical mutagenesis coupled with cerulenin selection.[62]

4. Conclusion

Microbial-derived high-energy biofuels, *i.e.* microbial biodiesel, enjoy a worldwide research focus as an alternative energy source for personal mobility concepts. However, commercialization has been hampered by the relatively high production cost. A major challenge for SCOs in achieving economic feasibility for large-scale industrial applications lies in the isolation of microbial strains displaying high lipid titers.[51] In this study, FN irradiation was employed for the first time in the mutagenesis of an OY strain. The application of cerulenin selection pressure

Table 3 Calculated and reported biodiesel characteristics obtained from prospective OYs, palm oil and corresponding requirements of biodiesel standards according to United Stated and European regulations

Biodiesel Source	Iodine value	Cetane number	Higher heat value (MJ kg^{-1})	Kinematic viscosity (mm^2 s^{-1})	Density (g cm^{-3})	Reference
C. oleaginosus wt	57.56	60.06	38.38	3.85	0.91	This study
C. oleaginosus FN M2	51.39	61.62	38.30	3.93	0.90	This study
Y. lipolytica	80.95	60.11	39.13	3.25	0.86	58
L. starkeyi	77.07	59.80	38.83	3.20	0.85	58
R. toruloides	74.13	62.19	39.14	3.43	0.86	58
Palm oil	57.95	65.19	39.46		0.87	58
US biodiesel ASTM D6751	≤120	≥47	—	1.9–6.0	0.86–0.91	58 and 61
EU biodiesel standard EN 14214	≤120	≥51	—	3.5–5.0	0.86–0.90	58 and 61

on mutated *C. oleaginosus* cells (subjected to 1000 Gy) allowed for the isolation of two strains with improved growth and lipid characteristics. High-throughput Nile red analysis revealed one mutant (FN M2) displaying a 21.67% increase in biomass formation (g L^{-1}), which in turn resulted in a 22.58% increase in total lipid yield (g L^{-1}) compared to the wild-type strain. Further characterization of this mutant showed a higher degree of fatty acid saturation, with biofuels properties that meet international standards. Another mutant (FN M8) displayed an improved lipid content (73.16%, g g^{-1}). However, as biomass formation of this *C. oleaginosus* mutant was substantially lower than that of the wild-type strain, total lipid yield (g L^{-1}) was not enhanced. This work demonstrates that the FN mutagenesis technique can be successfully applied to manipulate biomass formation, lipid productivity and fatty acid composition of OYs. Furthermore, our study clearly indicates that the enhanced phenotypes (improved lipid and biomass accumulation) of mutants - FN M2 and M8-were stable over the observed growth cycles/generations, even in the absence of selection pressure. Specifically, these enhanced mutants did not require the continuous presence of cerulenin pressure to deliver higher lipid titers. Hence, this approach has subsequent industrial applications (*e.g.* biodiesel) without the need for targeted genetic engineering.

Adopting "zero-concepts" with respect to emissions and excess resources in bioprocess engineering is expected to drive industrial biotechnology to become highly integrated into sustainable technology systems.[71] *C. oleaginosus* has been previously adapted to various cost-effective fermentative conditions (*e.g.* lignocellulose and hemicelluloses hydrolysates, waste materials) while maintaining elevated lipid titers. Specifically, brown algae and seagrass have been applied as feed-stock in a well-designed waste-free cyclic bio-refinery approach for biofuels and the oleochemical industry.[4] The fermentative growth of *C. oleaginosus* FN M2 should be assessed under these conditions. Most interestingly, growth and lipid production capabilities of this mutant should be assessed, when cultivated in a nitrogen-rich medium with glucose and acetic acid as carbon sources, which allows concomitant growth and lipid formation without the need for N-limiting cultivation conditions. In a recent study performed by our group, wild-type *C. oleaginosus* was capable of accumulating 85% (g g^{-1} DCW) lipids when grown under these specific conditions.[16] Following high-yield fermentation in aerated stirred tanks, techno-economic analyses estimated that oil from this wild-type yeast strain (US$1.6 kg^{-1}) would be cheaper than eco-certified palm oil (US$ 2.1 kg^{-1}) and would also result in lower CO_2 emissions.[16] *C. oleaginosus* FN M2 with its inherent enhanced growth and lipid yields, and FN M8, with its inherent higher lipid content, can potentially achieve even greater biomass and lipid productivity under these desirable high-monoauxic growth conditions, thereby significantly lowering the cost of *C. oleaginosus* oil production.

The analytical approach established in this study links current efforts in SCO advancements to an accelerated process development by implementing high-throughput selection. In fact, cost-efficient, rapid and automatable Nile red analysis coupled to our high-fidelity correlation system alleviated the need for time-consuming laborious analytical techniques (*e.g.* gravimetric analysis, growth rate analysis, biomass analysis). The use of purified ML from *C. oleaginosus* delivered a more accurate representation of intracellular lipid concentrations than the previously reported TO standard. Additionally, our correlation study demonstrates that OA is a low-cost, easy to handle and accurate standard for absolute lipid quantification, when harmonized with the determined correlation factor in this study.

The high-throughput technologies for genetic yeast strain enhancement, production variant selection and performance monitoring presented in this study are each amenable to be transferred into a consolidated, miniaturized and automatable processing format. These consolidated processes have the capacity to provide a technology platform for a completely automated yeast lipid and biofuel production optimization process, where artificial intelligence-based software solutions guide and accelerate developments with a minimized need for human intervention. This scenario allows for accelerated and more cost efficient process optimization that ultimately allow fast track industrial deployment of oleaginous yeast-based high-energy biofuel production processes. Realizing such a scenario requires consequent miniaturization and validation of all processes presented in this study and their integration in a consecutive work flow on an automated robotic workstation. To that end, integrated robotic systems have been previously employed for high-throughput screening in various cell culture conditions.[72,73] Moreover, several strategies have successfully shortened process development timelines from large to micro-scale processes by employing high-throughput technology platforms such as microtiter plate (MTP) culture, micro-scale bioreactors, and parallel fermentation systems.[74,75] Accordingly, the synergistically integrated high-throughput methods for strain mutagenesis, selection and characterization developed in this study can also be coupled with FACS sorting using 96 deep well MTP formats for quantitative evaluation of the fermentative potential of all generated mutants, even in the absence of cerulenin. Hence, future studies in our group will employ an automated high-throughput process development (HTPD) approach, which employs robotic platforms. This would incorporate necessary tools for MTP culture studies, automated fast screening, as well as advanced artificial intelligence (AI)-guided analytical capabilities (assessment of cell growth, lipid content) without operator intervention.[76,77] With the advantage of high sensitivity and reproducibility, correlating batch data would reliably predict culture performance. Additionally, benchtop parallel bioreactor systems can establish robust scalable processes and enable reliable Design of Experiment (DoE) studies for mutants with metabolic altered pathways. Employing this HTPD approach will lead to an accelerated manufacturing process, with significantly reduced risk of project failure, decreased costs and higher market penetration capability. Finally, investigation of the metabolic alterations using genomic and proteomic tools (sequencing, transcriptomic analysis) should be performed to identify key genes/enzymes that were modified during mutagenesis.[78] These

identified genes can be target of genetic engineering of this yeast in future studies for elevated lipid titers.

Author contributions

Conceptualization of the study was conducted jointly by DA and TB. The methodological approach was designed and carried out by DA and SY. Data validation was jointly carried out by all authors. DA and SY prepared the original draft of the manuscript. The manuscript was jointly finalized by all authors.

Funding

The authors gratefully acknowledge funding of the Werner Siemens foundation for establishing the research field of Synthetic Biotechnology at the Technical University of Munich. SY, DA and NM gratefully acknowledge funding by the Bavarian State Ministry for Environmental and Consumer affairs for funding of the project Resource efficient PHB production processes within the project consortium BayBioTech (TP7, TLK01U-69045, http://www.baybiotech.de/startseite/).

Conflict of interest

The authors declare that the research was conducted in the absence of any commercial or financial relationships that could be construed as a potential conflict of interest.

List of Abbreviations

AGMT	Agrobacterium tumefaciens-mediated gene transfer
CN	Cetane number
CRISPR	Clustered regularly interspaced short palindromic repeats
DI	Deionized
DCW	Dry cell weight
DMSO	Dimethyl sulfoxide
EMS	Ethyl methane sulfonate
FAME	Fatty acid methyl esters
FAS	Fatty acid synthase
FN	Fast neutron
GMO	Genetically modified organism
HHV	Higher heating value
IR	Ionizing radiation
IV	Iodine value
KPI	Key Performance Indicator
KV	Kinematic viscosity
LET	Linear energy transfer
MEDAPP	Medical applications
MFE	Maximal fluorescence emission
ML	Microbial lipid
MNM	Minimal-nitrogen media
NTG	Nitrosomethyl guanidine
OA	Oleic acid
OM	Oleaginous microorganism
OY	Oleaginous yeast
PLA	Polylactic acid
SCO	Single-cell Oil
TAG	Triglycerides
TO	Triolein
YPD	Yeast peptone dextrose

Acknowledgements

The authors gratefully acknowledge the valuable input offered by Elias Kassab with regard to GC-MS sample analysis. The authors also acknowledge Mahmoud Masri for providing a purified extract of ML.

References

1 D. Awad, F. Bohnen, N. Mehlmer and T. Brueck, *Frontiers in bioengineering and biotechnology*, 2019, **7**, 54.
2 S. Bruder, S. Hackenschmidt, E. J. Moldenhauer and J. Kabisch, in *Lipid Modification by Enzymes and Engineered Microbes*, Elsevier, 2018, pp. 257–292.
3 C. Huang, X.-f. Chen, L. Xiong, L.-l. Ma and Y. Chen, *Biotechnol. Adv.*, 2013, **31**, 129–139.
4 M. A. Masri, S. Younes, M. Haack, F. Qoura, N. Mehlmer and T. Brück, *Energy Technol.*, 2018, **6**, 1026–1038.
5 E. Tapia, A. Anschau, A. L. Coradini, T. T. Franco and A. C. Deckmann, *AMB Express*, 2012, **2**, 64.
6 M. Guo, S. Cheng, G. Chen and J. Chen, *Eng. Life Sci.*, 2019, **19**, 548–556.
7 K. W. Chew, S. R. Chia, P. L. Show, T. C. Ling and J.-s. Chang, in *Bioreactors for Microbial Biomass and Energy Conversion*, ed. Q. Liao, J.-s. Chang, C. Herrmann and A. Xia, Springer Singapore, Singapore, 2018, pp. 359–388, DOI: 10.1007/978-981-10-7677-0_9.
8 X. Meng, J. Yang, X. Xu, L. Zhang, Q. Nie and M. Xian, *Renewable energy*, 2009, **34**, 1–5.
9 S. Papanikolaou and G. Aggelis, *Eur. J. Lipid Sci. Technol.*, 2011, **113**, 1052–1073.
10 C. Gorner, V. Redai, F. Bracharz, P. Schrepfer, D. Garbe and T. Bruck, *Green Chem.*, 2016, **18**, 2037–2046.
11 P. Gujjari, S.-O. Suh, K. Coumes and J. J. Zhou, *Mycologia*, 2011, **103**, 1110–1118.
12 A. Yaguchi, D. Rives and M. Blenner, *AIMS Microbiol.*, 2017, **3**, 227–247.
13 S. Younes, F. Bracharz, D. Awad, F. Qoura, N. Mehlmer and T. Brueck, *Bioprocess Biosyst. Eng.*, 2020, DOI: 10.1007/s00449-020-02354-0.
14 F. Bracharz, T. Beukhout, N. Mehlmer and T. Bruck, *Microb. Cell Fact.*, 2017, **16**, 178.
15 M. A. Masri, W. Jurkowski, P. Shaigani, M. Haack, N. Mehlmer and T. Brück, *Appl. Energy*, 2018, **224**, 1–12.
16 M. A. Masri, D. Garbe, N. Mehlmer and T. B. Brück, *Energy Environ. Sci.*, 2019, **12**, 2717–2732.
17 Y. Zhang, M. He, S. Zou, C. Fei, Y. Yan, S. Zheng, A. A. Rajper and C. Wang, *Bioresour. Technol.*, 2016, **207**, 268–275.
18 J. Wang, R. Li, D. Lu, S. Ma, Y. Yan and W. Li, *World J. Microbiol. Biotechnol.*, 2009, **25**, 921–925.

19 S. Ochoa, G. Wozny and J.-U. Repke, *J. Process Control*, 2010, **20**, 983–998.
20 E. G. Kana, J. Oloke, A. Lateef and M. Adesiyan, *Renewable energy*, 2012, **46**, 276–281.
21 E. C. Rivera, S. C. Rabelo, D. dos Reis Garcia, R. M. Filho and A. C. da Costa, *J. Chem. Technol. Biotechnol.*, 2010, **85**, 983–992.
22 S. Hansen and A. Mirkouei, 2018.
23 S. Y. Lee and H. U. Kim, *Nat. Biotechnol.*, 2015, **33**, 1061–1072.
24 S. d'Oelsnitz and A. Ellington, *Curr. Opin. Biotechnol.*, 2018, **53**, 158–163.
25 G. Katre, N. Ajmera, S. Zinjarde and A. RaviKumar, *Microb. Cell Fact.*, 2017, **16**, 176.
26 R. Kourist, F. Bracharz, J. Lorenzen, O. N. Kracht, M. Chovatia, C. Daum, S. Deshpande, A. Lipzen, M. Nolan and R. A. Ohm, *mBio*, 2015, **6**, e00918-00915.
27 P. B. Otoupal, M. Ito, A. P. Arkin, J. K. Magnuson, J. M. Gladden and J. M. Skerker, *mSphere*, 2019, **4**(2), DOI: 10.1128/msphere.00099-19.
28 Y. K. Park, J. M. Nicaud and R. Ledesma-Amaro, *Trends Biotechnol.*, 2018, **36**, 304–317.
29 T. Beacham, V. M. Macia, P. Rooks, D. White and S. Ali, *J. Appl. Biotechnol. Rep.*, 2015, **7**, 87–94.
30 T. T. Y. Doan and J. P. Obbard, *Algal Res.*, 2012, **1**, 17–21.
31 D. R. Ort, X. Zhu and A. Melis, *Plant Physiol.*, 2011, **155**, 79–85.
32 Y.-r. Cheng, Z.-j. Sun, G.-z. Cui, X. Song and Q. Cui, *Enzyme Microb. Technol.*, 2016, **93**, 182–190.
33 S. Kumawat, N. Rana, R. Bansal, G. Vishwakarma, S. T. Mehetre, B. K. Das, M. Kumar, S. Kumar Yadav, H. Sonah and T. R. Sharma, *Plants*, 2019, **8**, 164.
34 J. I. Lucas-Lledó and M. Lynch, *Mol. Biol. Evol.*, 2009, **26**, 1143–1153.
35 U. M. Tillich, S. Lehmann, K. Schulze, U. Dühring and M. Frohme, *PLoS One*, 2012, **7**, e49467.
36 C. B. Bennett, L. K. Lewis, G. Karthikeyan, K. S. Lobachev, Y. H. Jin, J. F. Sterling, J. R. Snipe and M. A. Resnick, *Nat. Genet.*, 2001, **29**, 426.
37 J. H. Hendry, *Radiat. Res.*, 1991, **128**, S111–S113.
38 M. Frankenberg-Schwager, D. Frankenberg, R. Harbich and C. Adamczyk, *Int. J. Radiat. Biol.*, 1990, **57**, 1151–1168.
39 E. Schmid, F. Wagner, H. Romm, L. Walsh and H. Roos, *Radiat. Environ. Biophys.*, 2009, **48**(1), 67–75.
40 J. M. Al-Khayri, S. M. Jain and D. V. Johnson, *Advances in plant breeding strategies: Breeding, biotechnology and molecular tools*, Springer, 2015.
41 N. Gajendiran, K. Tanaka, T. S. Kumaravel and N. Kamada, *J. Radiat. Res.*, 2001, **42**, 91–101.
42 K. Sakai, S. Suzuki, N. Nakamura and S. Okada, *Radiat. Res.*, 1987, **110**, 311–320.
43 P. Unrau, *Radiat. Res.*, 1986, **107**, 39–48.
44 V. E. Tapia, A. Anschau, A. L. Coradini, T. F. T and A. C. Deckmann, *AMB Express*, 2012, **2**, 64.
45 R. Yamada, T. Kashihara and H. Ogino, *World J. Microbiol. Biotechnol.*, 2017, **33**, 99.
46 E. G. Bligh and W. J. Dyer, *Can. J. Biochem. Physiol.*, 1959, **37**, 911–917.
47 E. Marcellin and L. K. Nielsen, *Curr. Opin. Biotechnol.*, 2018, **54**, 33–40.
48 H. Morschett, W. Wiechert and M. Oldiges, *Microb. Cell Fact.*, 2016, **15**, 34.
49 L. Balduyck, C. Veryser, K. Goiris, C. Bruneel, K. Muylaert and I. Foubert, *J. Microbiol. Methods*, 2015, **118**, 152–158.
50 I. Sitepu, L. Ignatia, A. Franz, D. Wong, S. Faulina, M. Tsui, A. Kanti and K. Boundy-Mills, *J. Microbiol. Methods*, 2012, **91**, 321–328.
51 W. Chen, C. Zhang, L. Song, M. Sommerfeld and Q. Hu, *J. Microbiol. Methods*, 2009, **77**, 41–47.
52 H. De la Hoz Siegler, W. Ayidzoe, A. Ben-Zvi, R. Burrell and W. McCaffrey, *Algal Res.*, 2012, **1**, 176–184.
53 Y. Liang, T. Tang, A. L. Umagiliyage, T. Siddaramu, M. McCarroll and R. Choudhary, *Appl. Energy*, 2012, **91**, 451–458.
54 J. C. Priscu, L. R. Priscu, A. C. Palmisano and C. W. Sullivan, *Antarct. Sci.*, 1990, **2**, 149–155.
55 V. Orr and L. Rehmann, *J. Appl. Phycol.*, 2015, **27**, 2181–2189.
56 F. M. Wagner, P. Kneschaurek, A. Kastenmüller, B. Loeper-Kabasakal, S. Kampfer, H. Breitkreutz, W. Waschkowski, M. Molls and W. Petry, *Strahlenther. Onkol.*, 2008, **184**(12), 643–646.
57 R. Morales-Rayas, P. F. Wolffs and M. W. Griffiths, *Int. J. Food Microbiol.*, 2010, **139**, 48–55.
58 Y. E. Sergeeva, E. B. Mostova, K. V. Gorin, A. V. Komova, I. A. Konova, V. M. Pojidaev, P. M. Gotovtsev, R. G. Vasilov and S. P. Sineoky, *Appl. Biochem. Microbiol.*, 2017, **53**, 807–813.
59 D. Ekendahl, P. Rubovic, P. Zlebcik, O. Huml and H. Mala, *Radiat. Prot. Dosim.*, 2018, **178**, 329–332.
60 Y. Liu, C. M. J. Koh, S. A. Yap, M. Du, M. M. Hlaing and L. Ji, *BMC Microbiol.*, 2018, **18**, 14.
61 R. Yamada, T. Kashihara and H. Ogino, *World J. Microbiol. Biotechnol.*, 2017, **33**, 99.
62 G. Katre, N. Ajmera, S. Zinjarde and A. RaviKumar, *Microb. Cell Fact.*, 2017, **16**, 176.
63 I. R. Sitepu, L. Ignatia, A. K. Franz, D. M. Wong, S. A. Faulina, M. Tsui, A. Kanti and K. Boundy-Mills, *J. Microbiol. Methods*, 2012, **91**, 321–328.
64 I. R. Sitepu, M. Jin, J. E. Fernandez, L. da Costa Sousa, V. Balan and K. L. Boundy-Mills, *Appl. Microbiol. Biotechnol.*, 2014, **98**, 7645–7657.
65 M. Isleten-Hosoglu, I. Gultepe and M. Elibol, *Biochem. Eng. J.*, 2012, **61**, 11–19.
66 A. Massart, E. Aubry and A.-L. Hantson, *Biotechnol., Agron., Soc. Environ.*, 2010, **14**, 567–572.
67 E. Bertozzini, L. Galluzzi, A. Penna and M. Magnani, *J. Microbiol. Methods*, 2011, **87**, 17–23.
68 W. Chen, M. Sommerfeld and Q. Hu, *Bioresour. Technol.*, 2011, **102**, 135–141.
69 S. Liu, J. Xu, W. Chen, H. Fu, L. Y. Ma, H. Xu, L. Xinnian, M. Wu and F. Ma, *Biomass Bioenergy*, 2016, **91**, 196–203.
70 L. Liu, A. Pan, C. Spofford, N. Zhou and H. S. Alper, *Metab. Eng.*, 2015, **29**, 36–45.

71 A. J. J. Straathof, S. A. Wahl, K. R. Benjamin, R. Takors, N. Wierckx and H. J. Noorman, *Trends Biotechnol.*, 2019, **37**, 1042–1050.
72 C. Daniels, J. Rodriguez, E. Lim and M. Wenger, *Eng. Life Sci.*, 2016, **16**, 202–209.
73 S. R. Decker, R. Brunecky, M. P. Tucker, M. E. Himmel and M. J. Selig, *BioEnergy Res.*, 2009, **2**, 179.
74 Q. Long, X. Liu, Y. Yang, L. Li, L. Harvey, B. McNeil and Z. Bai, *J. Biotechnol.*, 2014, **192**, 323–338.
75 F. L. Gonzalez, S. R. Wisniewski, K. Katipally, J. M. Stevens, V. Rosso, B. Mack and T. M. Razler, *Org. Process Res. Dev.*, 2019, **23**, 1143–1151.
76 L. A. d. C. Meleiro, F. J. V. Zuben and R. M. Filho, *Eng. Appl. Artif. Intell.*, 2009, **22**, 201–215.
77 A. L. Oliveira, *Biotechnol. J.*, 2019, **14**, e1800613.
78 D. Awad and T. Brueck, *Anal. Bioanal. Chem.*, 2020, **412**, 449–462.

View Article Online
DOI: 10.1039/D0SE00540A

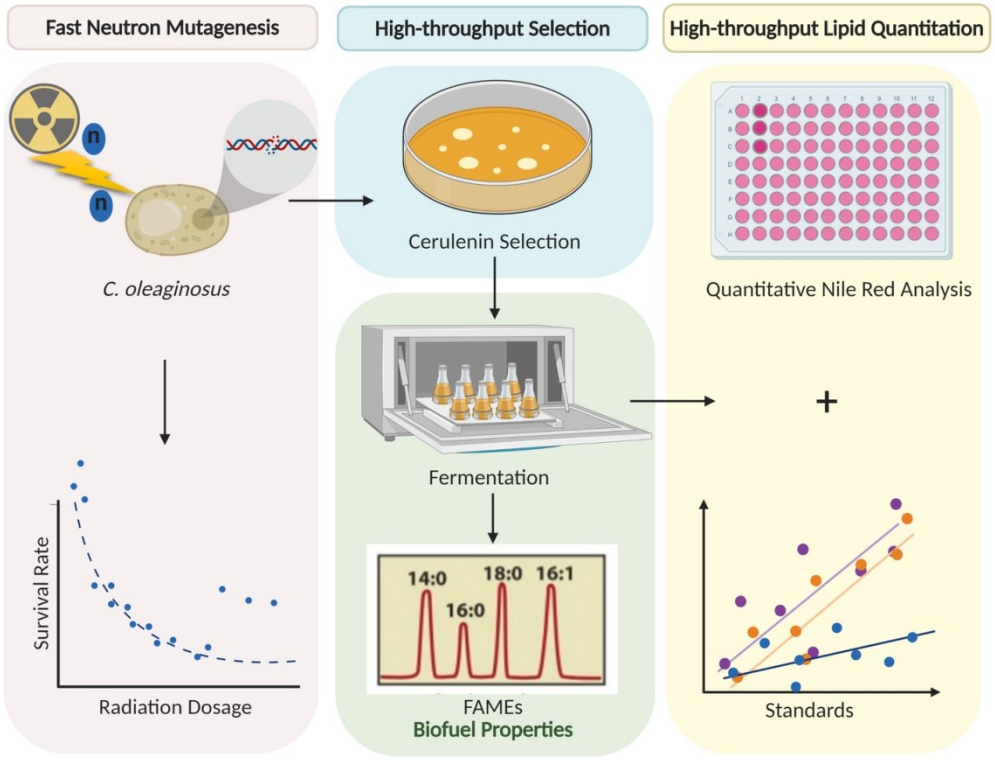

120x95mm (300 x 300 DPI)